KWAME NKRUMAH UNIVERSITY OF SCIENCE AND TECHNOLOGY, KUMASI

College of Engineering

Department of Civil Engineering

Agricultural Land Use Change in the Lowlands of Southern Mali under Climate Variability

DOCTOR OF PHILOSOPHY

in

Climate Change and Land Use

By

ALOU TRAORE

(BSc. Geography; MSc. Geomatic Engineering)

July 2023

DECLARATION

I hereby declare that this submission is my own work towards the Ph.D. in Climate Change and Land Use and to the best of my knowledge, it contains no material previously published by another person, nor material which has been accepted for the award of any other degree or diploma at Kwame Nkrumah University of Science and Technology (KNUST), Kumasi or any educational institution, except where due acknowledgement has been made in the thesis.

Alou TRAORE   …………………….....   ……………..............

(PG9990519)   Signature   Date

Certified by:

Ing. Prof. Nicholas Kyei-Baffour   …………………….....   ……………..............

(Supervisor)   Signature   Date

Prof. Jonathan Arthur Quaye-Ballard   …………………….....   ……………..............

(Supervisor)   Signature   Date

Prof. Romain Lucas Glele Kakaï   …………………….....   ……………..............

(Supervisor)   Signature   Date

Prof. Sampson Oduro-Kwarteng   …………………….....   ……………..............

(Head of Department)   Signature   Date

DEDICATION

This work is dedicated to God, my wife, Mrs Aminata Coulibaly Traore, and my children Cheick Bougadaly, Fatoumata, Mohamed Lamine and Oumou Kouthoum

ABSTRACT

This research investigated agricultural land use change in the lowlands of Southern Mali under climate variability. Four supervised classification techniques, Classification and Regression Tree (CART), Support Vector Machine (SVM), Random Forest (RF) and Gradient Tree Boosting (GTB) in Google Earth Engine (GEE), were used for the image classification. An integrated Cellular Automata-Artificial Neural-Network (CA-ANN) within the MOLUSCE plugin of QGIS was used for future Land Use and Land Cover prediction. The Mann-Kendall test, Sen's slope, Pettit-test and change-point detection analyse were applied for climate variability assessment. Monthly rainfall and mean temperature extending over a period of 61 years (1960–2020) recorded at Sikasso District were analysed. Annual rainfall varied between 800 mm to 1600 mm and annual mean temperature ranged between 25 ^{o}C to 28 ^{o}C. Seasonal rainfall ranged between 37-387 mm, March-April-May (MAM), 400-1030 mm, June-July-August (JJA), 77-577 mm September-October-November (SON) and 0-45 mm for December-January-February (DJF). Mean seasonal temperature ranged from 29 ^{o}C to 32 ^{o}C (MAM), 26.5 ^{o}C to 28.5 (JJA) ^{o}C and 26 ^{o}C to 28 ^{o}C (SON). Annual and seasonal rainfall trends increased slightly. Temperature showed a significant increase in both annual and seasonal trends. Out of 395 respondents, 79 % were of the view that annual rainfall decreased while 83 % reported mean temperature increased. Again, respondents perceived late onset rainfall (97 %), early cessation of rainfall (96 %), increased in drought (83 %) and flooding (96 %). Also, 43 % of respondents adopted new varieties to cope with climate variability. The findings showed that physical and socioeconomic driving forces had impact on terrain patterns. Over the past three decades, the study revealed that apart from cropland area which increased from 43.81 % to 52.75 %, the size of the other land uses decreased, forest cover (19.93 % - 13.93 %) shrubs (16 % - 14 %), and streams (6 % - 4 %). However, the forecast for the 2020 to 2030 predicted an increasing trend in forest cover and decreasing trend in agricultural land in the study area due to the ongoing afforestation projects. The study demonstrates the need to reinforce regional land management policies and programmes.

TABLE OF CONTENTS

LIST OF TABLES

LIST OF FIGURES

LIST OF ABRBREVIATIONS

CA-ANN	Cellar Automate-Artificial Neural network
CART	Classification and Regression Tree
CPD	Change Point Detection
DEM	Digital Elevation Model
ETM	Enhanced Thematic Mapper
GEE	Google Earth Engine
GIS	Geographical Information System
GPS	Global Position System
GTB	Gradient Tree Boosting
IPCC	Intergovernmental Panel on Climate Change
JJA	June-July-August
LRB	Lotio River Basin
LULC	Land Use Land Cover
MAM	March-April-May
NDVI	Normalised Difference Vegetation Index
OLI	Operational land image
PNPI	Percentage Normal Precipitation Index
QGIS	Quantum Geographical Information System
RAI	Rainfall Anomaly Index
RF	Random Forest
SAVI	Soil Adjusted Vegetation index
SD	Sikasso District
SON	September-October-November
SPEI	Standardised Precipitation Evapotranspiration Index
SPI	Standardized Precipitation Index
SRTM	Shuttle Radar Topography Mission
SVM	Support Vector Machine
USGS	United State Geological Survey
UTM	Universal Transverse Mercator

ACKNOWLEDGEMENTS

CHAPTER 1: GENERAL INTRODUCTION

1.1 Background

Climate change is the term used to describe notable alterations in global temperature, precipitation, wind patterns, and various other climate indicators that transpire over extended periods, typically spanning decades or more (IPCC, 2011). From the pre-industrial era to 2008, there was a notable rise in the atmospheric concentration of carbon dioxide, which increased from 278 to 387 parts per million. Throughout this period, there were annual variations in carbon dioxide concentration, with a general upward trend (Manning & Keeling, 2006). Over the past two decades, there has been a resurgence in greenhouse gas emissions. Specifically, between the 1990s and 2000-2006, the rate of greenhouse gas emissions escalated from 1.3% annually to 3.3% annually (Canadell et al., 2007). These greenhouse gas emissions have led to global warming as well as the temperature of the earth's surface through radiation in the atmosphere, which has multiple consequences on human activities in general and agriculture in particular (Ciesla, 1995; FAO, 2013; US Environnemental Protection Agency, 2015).

Projections indicate that climate change will have an impact on food security across the globe, as well as at regional and local scales (Unite State Environmental Protection Agency, 2015). The impacts of climate change can lead to disruptions in food availability, limitations in accessing food, and alterations in food quality (Brown *et al*., 2015). As an illustration, the anticipated rise in temperature, alterations in precipitation patterns, shifts in extreme weather occurrences, and decreased water resources can collectively result in a decline in agricultural productivity. The heightened frequency and intensity of extreme weather events can further disrupt the distribution of food, leading to more frequent instances of price spikes in the aftermath of such events. Additionally, elevated temperatures can contribute to the spoilage and contamination of food products. (Unite State Environmental Protection Agency, 2015).

Mali, situated in the heart of West Africa, spans an extensive land area of 1,241,238 square kilometers. Approximately half of the nation is encompassed by the Sahara Desert, with an annual precipitation average of not more than 200 mm. Mali has experienced a population growth rate of approximately 3% annually since 2009. (UN,

2014) with a total population of 14 million inhabitants in 2009 (RGPH, 2009). In 2025, it was estimated that 25 million inhabitants, nearly half of whom are under 15 years old, will face doubling need of food in the medium term (United Nations, 2013). The country's economy is mainly based on agriculture, accounting for 36% of Gross Domestic Product (GDP), which provides a livelihood for nearly 80% of the population (World Bank, 2021). However, this agriculture is vulnerable to climatic hazards, such as droughts which occurred in the 1970s and 1980s. Despite the increase in cereal production, Mali is still facing food and nutritional crises (CSA, 1990). Thus, the Government of Mali, with the support of its partners, has implemented vast programmes and projects to develop irrigable land to improve yields, such as Malibya with 25,000 hectares in 2014 and impact of Rice Policies and Technologies on Food Security and Poverty Reduction (Commod Africa, 2018; Kindjinou, 2013). Despite these efforts, irrigable land is underutilised. For instance, only 25% of the 2.2 million hectares of irrigable land under total or partial control (FAO, 2020).

Faced with these various constraints, recourse to irrigated farming in the South of the country seems to be an alternative with a potential of 2,200,000 irrigable hectares, where only 371,000 hectares benefit from water control (Samake *et al*., 2007). The government as well as private initiatives have sought to develop all the surfaces favourable for irrigation (Sudre, 2015). Among these high-potential areas are the lowlands, which are being increasingly developed, and the extreme south of the country (Sikasso region) has a concentration of the larger share of lowlands (Sudre, 2015). It is in this context that several studies have been carried out to characterize the lowlands and highlight the potential of these areas (CBF, 1997; Albergel *et al*., 1993; Chabi *et al*., 2010; Oloukoi, 2016). However, the aspects of land-use change in these lowlands and the role of climate change in these changes have not been projected in order to assess the impact of climate change on land-use changes and possible scenarios in the short, medium and long term in the lowlands of the south of the country.

1.2 Problem Statement

Lowlands are areas of flat or concave bottomed lowlands (Ahouandjinou, 2004). They are considered to be small floodable valleys that collect runoff from the slopes

constituting the basic drainage axes (Ahouandjinou, 2004). These are axes of preferential convergence of surface waters, hypodermic flows and aquifers (Albergel et *al.*, 1993). In sub-Saharan Africa, it is estimated that more than 200 million hectares of lowlands remain unexploited (Sonia and Joel, 2010). The lowlands present privileged geomorphological and agronomic conditions for increased agricultural production. They are places where there are better land and water conditions, making it possible to secure and increase the agricultural and animal production (Ahouandjinou, 2004). They are also in favour of the introduction of new speculations (arboriculture, market gardening, fodder crops, etc.), the diversification and development of fish farming, bee keeping, rural entrepreneurship (agricultural mechanization, processing, etc.), harvesting, handicrafts (Chabi *et al.*, 2010; Kindjinou, 2013). Thus, the lowlands make it possible to ensure security and increased agrosylvopastoral production, while contributing to the diversification of the incomes of West African rural populations, due to the fertility of their soils and their hydromorphic characteristics (Kindjinou, 2013; Oloukoi, 2016). Under the combined effect of climate change with drastic consequences on projected agricultural productivity (Unite State Environmental Protection Agency, 2015), the strong demographic pressure leading to a doubling of food needs in general and for West Africa in particular, a shift in agricultural activities more and more towards the lowlands is witnessed (Oloukoi, 2016). It is in this context that we are witnessing a new change in the system of land use and occupation in the lowlands of West Africa in general and in Mali in particular.

In Mali, this new change began with the projects and programmes for the development and reclamation of flood-prone and lowland lands between 1970 and 1980 (Ahmadi *et al.*, 1994). This dynamic was followed by other public actors (rural engineering, communities, the Malian company for textile development, and national and international organizations) and private actors (NGOs and other private initiatives) with more or less large areas; and since then it has continued to increase because of the relative cost of development and knowledge compared to other hydro-agricultural developments (Neville *et al.*, 1998). For example, the cost of development for the beneficiary farmers represents an investment in labour. For one hectare, 140 to 280 men are needed per hectare for a period of between twenty and forty days, that is, five months of work for a team of five farmers (accompanied by a

planner) for two working days per week (Neville *et al*., 1998). It is in this sense that research and development studies of the lowlands have been developed and carried out (Africa-Rice, CORAF-R3S, RAP, etc.). However, rare studies on this new change in land use and cover in these lowlands have been conducted as a result of climate change.

1.3 Research Aim and Objectives

The aim of the study is to model the change in agricultural land use in the lowlands of southern Mali under the effect of climate change.

The specific objectives are to:

1. Map the distribution of the lowland areas of southern Mali;
2. Assess variability and trends of temperature, relative humidity and rainfall between 1960 to 2020 in the study area;
3. Assess the dynamics of agricultural land use change for the period of 2000 to 2020; and
4. Model the changes of Land Use Land Cover (LULC) in these lowlands.

1.4 Research Questions

To address the above specific objectives, four research questions were raised as follows:

1. What are the spatial distribution of lowlands of southern Mali?
2. What is the variability and trends of temperature, relative humidity, and rainfall from 1960 to 2020?
3. What are the dynamics of agriculture land use from 2015 to 2020?
4. How will the change of land use in the lowlands be like over the next few years?

To find solutions to the above mention research questions, the following techniques were deployed:

a) **Empirical Method for Field Measurements, GIS and Remote Sensing Analysis**

    This involved GPS observations on the selected point of the various land cover and GIS and remote sensing analysis of images. This was deployed to answer research questions one, two and three.

b) **Statistical Approach**

This was deployed to assess meteorological time series data and identify variability and trend of temperature and rainfall.

This approach which involves Mann-Kendall test, Pettit test, slope Sen's estimation and survey were utilised to:

- o Assess variability and trend of rainfall and temperature in LRB
- o Analyse the trend of change
- o Identifying change points
- o Assess farmer's perception and adaptation strategies

The above approach was used to answer research question two.

c) **Land Use Land Cover Modelling**

Cellar Automate-Artificial Natural Network (CA-ANN) were adopted to predict land use land cover change in Lotio River Basin (LRB). This includes

- o Support Vector Machine classification was used to analyse LULCC dynamics
- o Setting up, calibrating and validating the model
- o Using Artificial Neural Network (ANN) method to predict land use land cover change.

The above was adopted to answer research questions three and four.

1.5 Justification of study

The LRB support livelihood of 725,494 of people. It offers food (crop and fish), water for domestic agricultural and industrial use, wastewater disposal, recreation natural resources, employment etc. Several activities such as urbanisation, agricultural expansion have immensely affected the land use and land cover dynamic of the LRB. Various hypotheses related to the problem encountered in this basin have been put forward as follows:

- o LRB has the high lowland potential;
- o Climate variability is increasing and farmers are understood the, adopt lot of techniques to face uses;
- o LULCC has a rapid dynamic and generate most consequences on water availability and degradations.

However, extensive research has not been carried out in LRB to holistically to understand the interaction within the basin in the analysis of the climate variability. This study is significant since it seeks to enhance the knowledge of the climate variability and trend which subsequently, show a capacity for measuring changes in the driving forces that control climate changes. The study additionally gives statistics significant on climate variability, trend of rainfall and temperature, especially in link to farmers perception and adaptation strategies. The study can valuable in addressing challenges affecting environmental development and sustainability of the naturel resources within the basin. In perspective of the above, this study assessed the historical LULCC and forecast the future LULCC.

1.6 Structure of the thesis
This thesis is organised five chapters, which are briefly outlined below.

Chapter 1: Introduction
This chapter deliberates the background information, objectives and justification of the study. It portrays the issues persisting in this study area as a result of land use and land cover change due to anthropogenic disturbances and climate change. Its looks at the probable results and their significance in the area.

Chapter 2: Literature review
A description of the LRB in totality is captured in this chapter. This includes literature concerning land use and land cover change modelling for future dynamics. The issue of climate change and climate variability as well as their trend and how the farmers perceive it also what are the adaptation strategies to face in the basin. It deliberates on the development achieved in the modelling and classification of LULC.

Chapter 3.1: Determine the spatial distribution of lowlands in southern Mali
This part first looks at the potential and spatial distribution of lowland in southern Mali. Then, the methodological approaches adapted for the selection of indices and parameters for the identification of lowlands is presented in this chapter. Furthermore, validation method employed, which is based on a comparison of field data and results obtained from various treatments.

Chapter 3.2 Assessment of Temperature and Rainfall Variability, Trends, Farmers' Perceptions and Adaptation Strategies in Southern Mali between 1960-2020

This chapter discusses temperature and rainfall variability, trends, farmer's perceptions and adaptation strategies. The approach used for temperature, rainfall variability assessment, trends, farmer's perception is captured as well adaptation strategies are discussed.

Chapter 3.3 Assessment of Seasonal and Annual Rainfall Anomaly Index (RAI) Trends and Variability in Southern Mali

The seasonal and annual rainfall anomaly index trends and variability are described in this chapter. It discusses the approach to compute and the criteria to class RAI. The results of RAI classification are presented. The maximum intensity droughts with durations for the rainfall are presented.

Chapter 3.4 Modelling past and future land use and land cover dynamics in the Lotio River Basin, West Africa

This chapter discusses statistics on historical and future LULC change. The approach adopted for LULC classification, change detection, future prediction of LULC and accuracy assessment is captured as well trend, rate caver changes discussed.

Chapter 4: General Discussion

The general discussion of all the results of the thesis has been presented in this chapter. The aim is to confirm or compare the key results of each specific objective in light of previous research and studies in the world in general and Africa in particular.

Chapter 5: Conclusions and Recommendations

This chapter consolidates the conclusions from the whole thesis. It contains the significant findings and summarizes the limitations of the study. Recommendations aiming at achieving forest and water transformations to preservation, availability, sustainable and efficient management in *Lotio* River Basin are presented in this chapter. In additional future recommendations for researches and policy are also stated in this last part of the work.

CHAPTER 2: LITERATURE REVIEW

2.1 Lowlands

The lowlands are areas of low landscape with flat or concave bottoms. They are considered to be small floodable valleys that collect runoff from the slopes and constitute the basic drainage axes (Ahouandjinou, 2004). These are areas where surface water, underground flows, and groundwater converge preferentially (Albergel and Claude, 1994).

Lowlands are small flat- or concave-bottomed valleys located in the upstream parts of drainage systems (Raunet, 1985). According to him, the lowlands of the Sudano-Sahelian zone are composed of three (3) parts from the geomorphological point of view:

- o The head of the lowland: devoid of a hydrographic network and widened in the shape of a "spatula" or "amphitheatre". The watershed has a surface area ranging from a few hectares to 1 or 2 km². It is often made up of small gullies which are only fed by rainwater flowing down the slopes and draining towards the upstream part of the lowland. The soils are sandy.

- o The upstream part: The flanks become clearly concave and the surface of the catchment area widens further (from 5 to 20 km²). The high concentration of surface runoff in the centre of the lowland creates water erosion and leads to the creation of gullies. This part of the lowland is characterized by the presence of a poorly developed hydrographic network. The soils become clayey-sandy.

- o The swallowing part: The hydrographic network becomes more developed. The shallows widen and its transverse profile flattens. The surface of the watershed ranges from a few dozen km² to 200 km². It is in this part of the lowland that crops are most frequently found (Albergel and Claude, 1994). These induce particular surface organizations and variations in the hydrodynamic parameters of the soils. It has a soil with a clayey-1imonous texture. The part that follows the downstream part of the lowland constitutes the alluvial valley or alluvial plain. After a certain number of lowland confluences, when the watershed becomes large enough and river flows become sufficiently competent (sorting of materials, construction of levees,

formation of basins, etc.), the lowland gives way to the alluvial plain (Raunet, 1985).

2.2 Modelling

Modelling is the simplified representation of a complex reality. On this basis, any modelling is a simplification. It goes through the design of a model, therefore an abstraction allowing to better understand a complex object or system. Kouassi (2014) defines the model as an ideal or a given prototype, which can either serve as a reference or be reproduced.

Indeed, modelling differs in particular from simulation. Modelling consists in identifying and formulating problems, then building models that contribute to problem solving through simulations. As for simulation, it comes after modelling. Simulation consists in predicting the state of a phenomenon using a model. A model used to make predictions (simulations) is called predictive. There are modelling tools to simulate the state of land use such as the CA Markov and Land Change Modeler (LCM), and so on.

2.3 Digital Elevation Model

The Digital Elevation Model (DEM) is the representation of the topographic surface while considering the altitude of the objects on it. In its wider acceptation, it is an image containing the values of the altitude (Z) of a given terrain and its overground. The term DEM is most often used to refer to the DTM or DEM. However, it is important to remember that there is a nuance between a DEM and a DTM even if the two terms are used several times in place of each other.

Kindjinou (2013) provides a succinct definition of the term DTM. According to him, the Digital Terrain Model refers to the representation of the topographic surface without taking into account buildings or vegetation. The sample of points X, Y, Z constituting the initial data can be a raster image of the relief, with Z the altitude of the point of planimetric coordinates (X, Y) in a defined projection. Doungmo (2017) proposes different definitions for the terms DEM, DTM and DEM. According to him, DEM represents a set of points where the value of the elevation data (Z) takes precedence over the two other horizontal components (X and Y). By default, aerial or

satellite imagery results in the production of a DEM by photo-interpretation. Further processing is required to extract a DEM. It defines the DTM as the set of points corresponding solely to the elevation of the terrain itself. The DEM (Digital Elevation Model) is defined in turn as the set of points representing the relief (elements of the natural terrain), but also what is called the "canopy" (tops of trees) or the overground (elevation of buildings). The most commonly used types of DEM and DTM are SRTM and ASTER GDEM images.

2.4 State of the art

Numerous studies have previously focused on the identification of areas with agricultural potential, particularly the lowlands in West Africa. These studies have shown that there is a huge area of untapped potential lowland areas in sub-Saharan Africa and the need to develop these areas for agriculture in the current context of population growth and adverse climatic conditions. The authors only proposed methods to identify and map the lowlands. Some of them focused on agricultural intensification and the need to increase cultivated land, especially in the lowlands, to meet the growing demand for food. However, a few fundamental issues deserve deep reflection. Are the potentials in the lowlands inexhaustible? With the annual increase in cultivated areas, what will be the situation of the reserves in the lowlands in the future?

2.5 Lowlands identification and mapping

The theme of identification of the lowlands is problematic. The authors who have addressed it have all validated their results with field data. In addition, the methods adopted differed greatly from one author to another, each with weaknesses and points of clarification. As part of this study, a field visit will be carried out to validate the lowlands detected. Fieldwork is indeed essential for all studies using remote sensing techniques because the results can have a large margin of error if not verified and confirmed. Ouattara (2009) classifies the slope of the Bani watershed using Topographic Position Index (TPI) extension in ArcView, to determine toposequence classes. His method did not require more advanced image processing. The goal was to identify the shallows based on the toposequence. He then distinguished 5 classes of toposequence: high plateau, high slope, mid-slope, lowland, thalwegs and shallows. Kindjinou (2013) used ASTER images to identify the lowlands in Togo. The author

did not limit himself to the simple use of the DTM. His second detection approach was a field inventory of the lowlands using the GPS receiver. Validation methods consisted in visualizing the inventoried shallows and the shallows derived from the DTM in Google Earth software, and then calculating the compliance rate between the two groups of shallows.

Sudre (2015) initiated a deeply distinct topographic method to identify the lowlands of the communes of *Kokofata* and *Gadougou* in Mali using an SRTM image. His method consisted of extracting a hydrographic network from the DEM. The hydrographic network is then multiplied by the DEM to obtain the altitude of each pixel. The author then generated the sub-watersheds from the drainage network with the elevations. He then highlighted the difference between the sub-watersheds and the DEM to obtain the height of the surfaces in relation to the hydrographic network. This height in meters is then multiplied by the slope to create a potential lowland area index. The closer the index is to 0, the more likely the area is to have lowlands. To validate his result, the author has developed a land use analysis method that has made it possible to identify, from GPS points taken in the field and unsupervised Iso data classifications, the different geographical entities within the potential lowland areas and to reduce the over-evaluation obtained by the topographical method. Souberou *et al.* (2016) introduced a new approach to detect lowlands in the commune of Matéri in Benin. Their method consisted in generating NDVI from a Landsat OLI image, slope and water accumulation from an ASTER DEM. The high NDVI values, the low values of the slope and the areas of high-water accumulation were then extracted according to criteria, superimposed and intersected to obtain the potential lowland areas. The authors validated their results through field inventory of lowland areas. The same techniques were used by Souberou *et al.* (2017) to identify the lowlands in the Oti watershed (Benin). This time the authors included NDWI and TWI among the parameters for identifying lowlands.

2.6 Land Use Land Cover, and Climate Change and Variability

Land cover is characterized as the physical and biological cover of the Earth's surface, while land use refers to human activities on land cover (Ellis *et al.*, 2010). According to (IPCC, 2000), climate change is any change in the climate system over

time (at least three decades). Whereas climate variability refers to the seasonal changes of the climate.

2.7 Prior works on LULCC dynamics

2.7.1 Image classification Methods

Image classification is the process through which pixels are sorted into different classes focused on their spectral value (Song *et al.*, 2000). It is divided into supervised and unsupervised classification. Unsupervised use the spectral signature of each feature and group into similar pixels called cluster. Cluster identification is performed through the comparison of variance within and between the clusters or spectral classes (Zhu *et al.*, 2012). In this method, the user must determine the number of classes. In supervised classification, the operator is required to create training data by selecting pixel based on his/her own pattern recognition skills and specify the type and the number of land use and land cover class (Forkuor *et al.*, 2017). In supervised method, one sample training is used for the classification and another for accuracy assessment (Galiano-Rodriguez *et al.*, 2012). There are two types of supervised classification methods: parametric and non-parametric. The parametric method is based on statistical parameters, that are extracted from training datasets such as Maximum Likelihood, parallelepiped, and Minimum Distance Classifier. These methods are focused on the normal distribution of spectral signature or pixels value within classes (Al-doski *et al.*, 2013).

The non-parametric classifiers such as Neutral Network, Decision Tree, Generic Algorithms, Support Vector Machine are currently widely used because they have good predicted power (Sikonja, 2004). One of the most widely used is Random Forest (Kulkarni et al., 2016). Because it can use categorical datasets, robust to noise, not sensitive to over-fitting and easy to parametrise (Sikonja, 2004). The assumption behind this method is its capacity to provide the best classification compared to an individual classifier (Galiano-Rodriguez et al., 2012).

2.7.1.1 Random Forest classification

Random Forest (RF) is a machine learning classifier, which builds many individual decision trees by using a bootstrap aggregated sampling technique (Breiman, 2001). The advantage of Random Forest compared to the other algorithm of classification is

its capacity to handle variables and missing data, not sensitive to noise and over-fitting and easy to parametrise (Sikonja, 2004). It has been applied in numerous studies and in different countries (Senf *et al.*, 2012; Puissant *et al.*, 2014), Random Forest is currently considered as one of best algorithms of classification. Jhonnerie et al. (2015) utilized Random Forest and Likelihood classification methods to generate a mangrove land cover map for the Kembung river and Bengkalis Island regions in Indonesia. However, the comparison of Random Forest and Maximum Likelihood was one of the major objectives of their work. In order to accomplish their goal, Jhonnerie et al. (2015) employed Landsat TM, ALOS PALSAR FBD, and vegetation indices such as NDVI, NDWI, and NDBI. Their findings revealed that the Random Forest (RF) algorithm outperformed the Maximum Likelihood (ML) method in generating an accurate mangrove land use and land cover (LULC) map. Specifically, the RF algorithm yielded the best results when all input layers were combined, while the ML approach achieved satisfactory outcomes when Landsat TM and ALOS PALSAR data were combined. In addition, the overall accuracy and Kappa resulting from RF were better compared to Maximum Likelihood. They concluded that RF classification can be improved by adding layers input, contrary to Maximum Likelihood.

In France, (Puissant et al., 2014) combined RF with Object-Oriented to inventory and map the urban trees species from mono-temporal very high resolution (VHR) optical image. The outcome showed that Random Forest algorithm is useful for vegetation identification in the urban area. In Turkey (Ok *et al.*, 2017) assessed the performance of RF with Maximum Likelihood for cropland classification. They underlined that RF is better than Maximum Likelihood. Random Forest is an effective method and flexible technic to assess land cover map. In the South East of Asia, (Senf *et al.*, 2012) noted that RF-enables the optimisation of the cloud cover of MODIS images. In Burkina Faso (Forkuor et al., 2017) mapped the distribution of soil properties by comparing Multiple Linear Regression, Random Forest Regression, Support Vector Machine, and Stochastic Gradient Boosting. They concluded that RF Regression is the best model for soil properties prediction.

2.7.1.2 CART (Classification and Regression Tree) in Machine Learning

CART is a variation of the decision tree algorithm. It can handle both classification and regression tasks. Scikit-Learn uses the Classification and Regression Tree (CART) algorithm to train Decision Trees (also called "growing" trees). CART was first produced by Leo Breiman, Jerome Friedman, Richard Olshen, and Charles Stone in 1984 (Tirumalachandraveni, 2022).

CART Algorithm

CART is a predictive algorithm used in Machine learning and it explains how the target variable's values can be predicted based on other matters. It is a decision tree where each fork is split into a predictor variable and each node has a prediction for the target variable at the end.

In the decision tree, nodes are split into sub-nodes on the basis of a threshold value of an attribute. The root node is taken as the training set and is split into two by considering the best attribute and threshold value. Further, the subsets are also split using the same logic. This continues till the last pure sub-set is found in the tree or the maximum number of leaves possible in that growing tree. The CART algorithm works via the following process (Figure 2.1);

- o The best split point of each input is obtained.
- o Based on the best split points of each input in Step 1, the new "best" split point is identified.
- o Split the chosen input according to the "best" split point.
- o Continue splitting until a stopping rule is satisfied or no further desirable splitting is available

The CART algorithm uses Gini Impurity to split the dataset into a decision tree. It does that by searching for the best homogeneity for the sub nodes, with the help of the Gini index criterion.
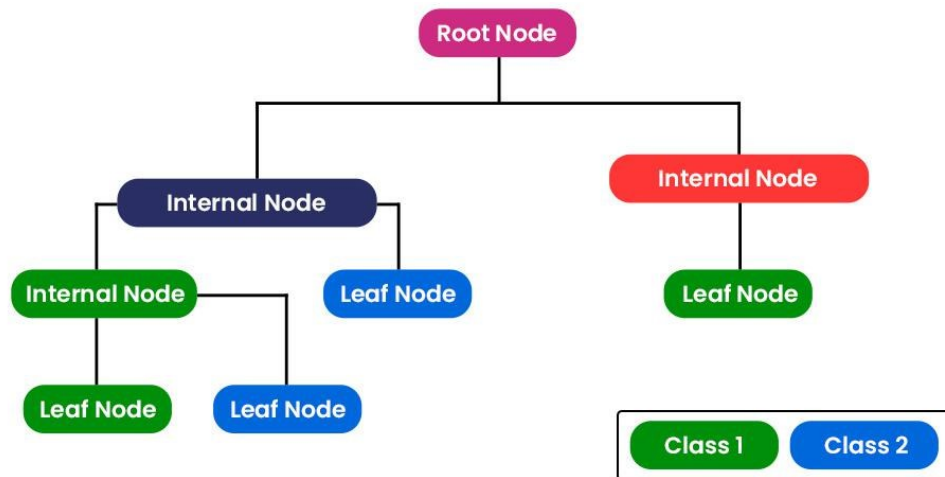
Figure 2.1: The CART algorithm work flow Source: (Tirumalachandraveni, 2022).

Gini index/Gini impurity

The Gini index is a metric for the classification tasks in CART. It stores the sum of squared probabilities of each class. It computes the degree of probability of a specific variable that is wrongly being classified when chosen randomly and a variation of the Gini coefficient. It works on categorical variables, provides outcomes either "successful" or "failure" and hence conducts binary splitting only.

The degree of the Gini index varies from 0 to 1,

- Where 0 depicts that all the elements are allied to a certain class, or only one class exists there.
- The Gini index of value 1 signifies that all the elements are randomly distributed across various classes, and
- A value of 0.5 denotes the elements are uniformly distributed into some classes.

Mathematically, we can write Gini Impurity as follows:

$$Gini = 1 - \sum_{i=1}^{n}(pi)^2$$

where pi is the probability of an object being classified to a particular class.

Classification tree

A classification tree is an algorithm where the target variable is categorical. The algorithm is then used to identify the "Class" within which the target variable is most

likely to fall. Classification trees are used when the dataset needs to be split into classes that belong to the response variable (like yes or no).

Regression tree

A Regression tree is an algorithm where the target variable is continuous and the tree is used to predict its value. Regression trees are used when the response variable is continuous. For example, if the response variable is the temperature of the day.

CART model representation

CART models are formed by picking input variables and evaluating split points on those variables until an appropriate tree is produced.

Steps to create a Decision Tree using the CART algorithm:

- *Greedy algorithm*: In this the input space is divided using the Greedy method which is known as a recursive binary spitting. This is a numerical method within which all of the values are aligned and several other split points are tried and assessed using a cost function.

- *Stopping Criterion:* As it works its way down the tree with the training data, the recursive binary splitting method described above must know when to stop splitting. The most frequent halting method is to utilize a minimum amount of training data allocated to every leaf node. If the count is smaller than the specified threshold, the split is rejected and also the node is considered the last leaf node.

- *Tree pruning:* Decision tree's complexity is defined as the number of splits in the tree. Trees with fewer branches are recommended as they are simple to grasp and less prone to cluster the data. Working through each leaf node in the tree and evaluating the effect of deleting it using a hold-out test set is the quickest and simplest pruning approach.

- *Data preparation for the CART*: No special data preparation is required for the CART algorithm.

Classification and regression trees are nonparametric and nonlinear, and results are basic, among other benefits of CART. Feature selection is automatically performed via classification and regression trees, CART is unaffected by outliers in a significant way, needs little oversight, and generates models that are simple to comprehend.

Overfitting, High Variance, Low Bias, and an Unstable Tree Structure are some of CART's drawbacks.

2.7.1.3 Gradient Tree Boosting (GTB) classification

The approach achieves its classification accuracy via stepwise lowering of the loss function based on gradient descent optimization and iteratively combining weak learner ensembles into stronger ensembles of trees (Friedman, 2002). Like RF, GTB combines a group of decision trees (Figure 2.2). However, GTB limits the complexity of the decision trees by limiting each tree to a weaker prediction model. Figure 5 illustrates how adding a new tree (Fm+1) can strengthen the model created by the weaker prediction Fm. A new model, Fm+1, is built using m+1 trees in the following iteration, and it corrects the previous model, Fm. In the following cycle, Fm+1 is then upgraded to model Fm+2, and the subsequent error correction ultimately results in a model that provides the most accurate categorisation (Ouma et al., 2022).
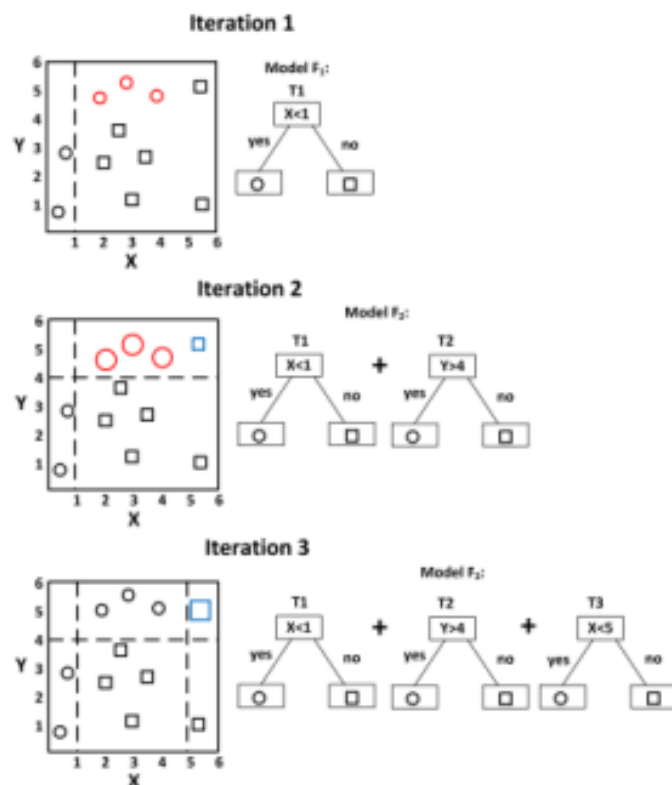
Figure 2.2: Visualization of gradient tree decision boosting Source: (Ouma et al., 2022).

According to (Ouma et al., 2022) the key distinction between GTB and other ensemble learning algorithms is that GTB fits the residual of the regression tree at each iteration using negative gradient values of loss. GTB complements the weak learning DTs, improving the ability of representation, optimization, and generalization. GTB can capture higher-order information, is invariant to scaling of sample data, and can effectively avoid overfitting by weighting combination scheme.

2.7.1.4 Support vector machine (SVM) classification

The SVM algorithm initially maps the n-feature data items into an n-dimensional feature space before categorizing linear and non-linear data (Figure 2.3). The marginal distance between classes is maximized and classification mistakes are minimized by establishing an ideal decision hyperplane that divides the data points into two classes. The classification is carried out when the decision hyperplane differentiates any two classes by the maximum margin (Ouma et al., 2022). The class marginal distance is the distance between the decision hyperplane and its nearest instance that is a member of that class. If x is the input feature vector, w is the weight vector and b is the bias, the aim of training in SVM model is to determine the w and b so that the hyperplane separates the data and maximizes the margin 2 1/ w. Vectors i x for which i y ( ) 1 T wx b i + = will be termed support vector. The main advantage of the SVM is in the ability to overcome the high dimensionality problem, with a high discriminative power for classification (Ouma et al., 2022).
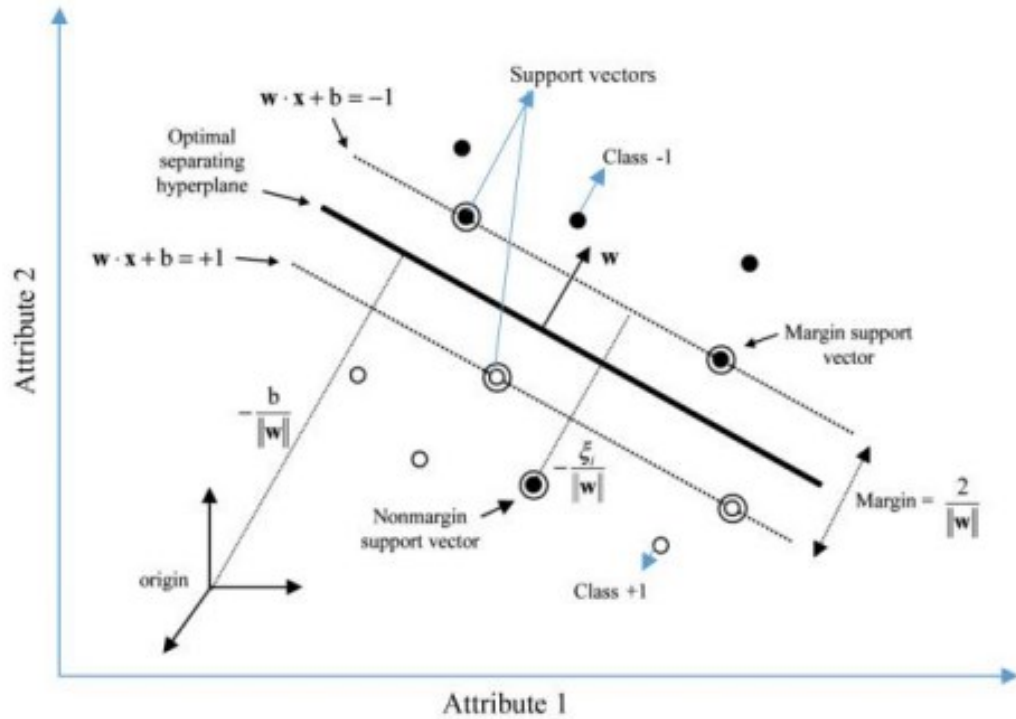
Figure 2.3: The SMV classification algorithm   Source:(Ouma et al., 2022)

2.8 Overview of change detection techniques

Change detection (CD) involves identifying the state of an object or phenomenon by observing it at multiple time points (Nori *et al*., 2006; Singh *et al*., 2013). The change of Earth's surface is a matter of great concern for researchers to develop methods for identifying changes on Earth's surface at different scales (Ross and Bhadauria, 2015). Change detection enables us to understand the correlation and interactions between human and the environment. The primary goal of change detection is to address the following inquiries: (i) What has changed? (ii) When was the change? (iii) How much has changed? (vi) What has changed to what (v) and how will be the change in the future? (Lu et al., 2004). Change detection (CD) finds applications in diverse domains including environmental monitoring, forestry management, urban development, geospatial data updates, and military operations (Singh, 2017). The objective of change detection (CD) is to generate information regarding alterations in area, rate of change, spatial distribution of different types of changes, and the trajectories of land cover transformations (Lu et al., 2004), and accuracy assessment of the results (Timothy et al., 2016). According to certain authors (Lu *et al*., 2004; Singh, 2017); CD methods encompass a range of techniques, including image differencing, image

regression, image rationing, vegetation index differencing, change vector analysis (CVA), principal component analysis (PCA), and tasselled cap (KT) analysis.

2.9 Techniques in Image Processing

Some of the techniques the research adopted in processing and analysing the Remote Sensing data are as follows:

- **Image differencing** is a CD method that involves subtracting the pixel values of the first date image from those of the second date image. This approach is simple, direct, and provides easily interpretable results. However, it does not offer a comprehensive change matrix that captures detailed changes (Singh, 2017).

- **Image regression** method establishes relationships between bitemporal images and estimates the pixel values of the second image using a regression function. This approach helps mitigate the effects of atmospheric, sensor, and environmental differences between the two dates. However, it necessitates the development of precise regression functions for the selected bands prior to implementing change detection (Lu *et al.*, 2004).

- **Image rationing** technique calculates the ratio of two images captured on different dates, considering each band separately. This method helps minimize the effects of factors like sun angle, shadows, and topography. However, it's important to note that the resulting data from this approach often exhibit non-normal distribution (Lu *et al.*, 2004).

- **Vegetation index differencing** technique generates vegetation indices for each date separately and subtracts the second date's vegetation index from the first date's. This method highlights variations in the spectral response of different features and helps mitigate the influence of topographic effects and illumination. However, it may amplify random noise or coherence noise in the results (Lu *et al.*,2004).

- **Change vector analysis** generates two outputs: (i) the spectral change vector describes the direction and magnitude of change from the first to the second date and (ii) the total change magnitude per pixel is computed by determining the Euclidian distance between endpoints through n-dimensional change space. It can process any number of spectral bands and produce detailed change

detection information but difficult to identify land cover change trajectories (Singh, 2017).

- **Principal component analysis (PCA)** There are two approaches to utilizing PCA for change detection. The first approach involves combining the images into a single file and applying PCA to analyse the minor component images for detecting changes. The second approach applies PCA separately. Principal component analysis helps reduce data redundancy among bands. However, since PCA is scene-specific, interpreting change information across different dates can be challenging, and it may not provide a complete change matrix (Alqurashi and Kumar, 2013).

- **The Tasselled cap** method, similar to PCA, differs in that it is not dependent on the visual scene. Change detection using the Tasselled Cap approach focuses on brightness, greenness, and wetness. While the Tasselled Cap method reduces data redundancy between bands and highlights different information in the derived components, it can be challenging to interpret and may lead to labelling changes (Lu *et al*., 2004).

However, the most common approach is post-classification (Areendran *et al*., 2013; Timothy *et al*., 2016). The post-classification approach involves classifying multi-temporal images into thematic maps separately and then comparing the classified images pixel by pixel. This method minimizes the impact of radiometric, atmospheric, and geometric differences between the multi-date images (Alqurashi and Kumar, 2013). By employing post-classification, a comprehensive matrix of change information can be obtained.

2.10 Modelling of land Use and land Cover

Land use modelling is very important for monitoring environmental phenomena, land management and territorial development. Knowing the phenomena, their past and present, the related factors, it is interesting to simulate their situation in the future. Several studies have addressed this issue.

The FAO (1996) has monitored the evolution of tropical forests using Landsat satellite images. It emerged from this study that the reduction of forests is explained by timber exploitation and destructive practices such as bush fires. According to the

results, this worrying trend will have to continue in the future as long as bad practices are not stopped.

Maestripieri (2012), following a diachronic analysis of the spatial-temporal dynamics of land use in southern Chile (Chile), adopted a comparative method of the CA-Markov and LCM models to make a prospective simulation of plantation dynamics. The result of CA-Markov gave less errors and more accuracy in prediction than that of LCM. Both also reported an increase in plantations.

Behera et al (2012) used criteria in the CA-Markov model to simulate land use dynamics in the Choudwar catchment (India). After a calibration made for 2004, the authors made a simulation for the year 2014. Their result indicated a spectacular growth of cultivated areas in the basin.

Kouassi (2014) used Landsat images to monitor the spatial-temporal dynamics of land use in the Yamoussoukro Regional Directorate (Cote d'Ivoire) from 1987 to 2012. The author used the CA-Markov model to simulate land use in 2020. His results showed a decrease in forest cover.

CHAPTER 3.1: DETERMINATION OF THE POTENTIAL AND SPATIAL DISTRIBUTION OF LOWLANDS IN SOUTHERN MALI

3.1.1 Introduction

In the past few decades, there has been a significant increase in the utilisation of lowland areas, both in terms of quantity and extent. This can be attributed to the fertile nature of the soils and their hydromorphic characteristics. These lowlands are therefore of great interest in an environment marked by climatic variability and changes in agricultural use patterns (Souberou *et al*., 2017). In developing countries, a shift in the front of agricultural activities is noted more and more towards hydromorphic environments (floodplains, lowlands, valleys), according to Mahaman and Windmeijer (1995). Thus, lowlands ecosystems have emerged as a set of resources whose development is becoming an imperative for the development, intensification and diversification of agricultural production (Oloukoi, 2016). They are therefore a challenge for the sustainable development of agriculture, especially for a country like Mali. The development of lowlands is of capital interest and has become a major issue in agricultural development in order to reduce water constraints (Souberou *et al*., 2017). In this context, in Mali, important research and development studies, both government and private initiatives, have been undertaken and carried out, such as the projects to develop irrigable land to improve yields, such as *Malibya* with 25,000 hectares in 2014 and impact of Rice Policies and Technologies on Food Security and Poverty Reduction (Commod Africa, 2018; Kindjinou, 2013). These studies focused on the characterization, management and development of the lowlands in general (CBF, 1997; Albertgel *et al*., 1993; Chabi *et al*., 2010; Oloukoi, 2016). However, in order to coordinate efforts in these areas (lowlands), which have particular geomorphological conditions for rainfed and dry season agricultural activities on the one hand, and in a context of high climatic variability in the Sahel on the other hand, mastery of the total potential and spatial distribution over the entire territory is a crucial requirement.

3.1.2 Approach and Methods

3.1.2.1 Study Area

The study was conducted at the Lotio River catchment area, situated within the Sikasso district, is a tributary of the Bafing River. It is positioned between 5°20' and 5°50' W longitudes and 11°50' and 11°10' N latitudes. It is the only river that waters

several communes in the circle with an area of 4,414.83 km² and a length of 121.9 km. Its outlet is located in the commune of *Kouoro,* and it flows from south to north (Figure 3.1.1). The Lotio River basin experiences a tropical *Sudanian* climate, characterized by distinct dry and rainy seasons that occur in alternating patterns.
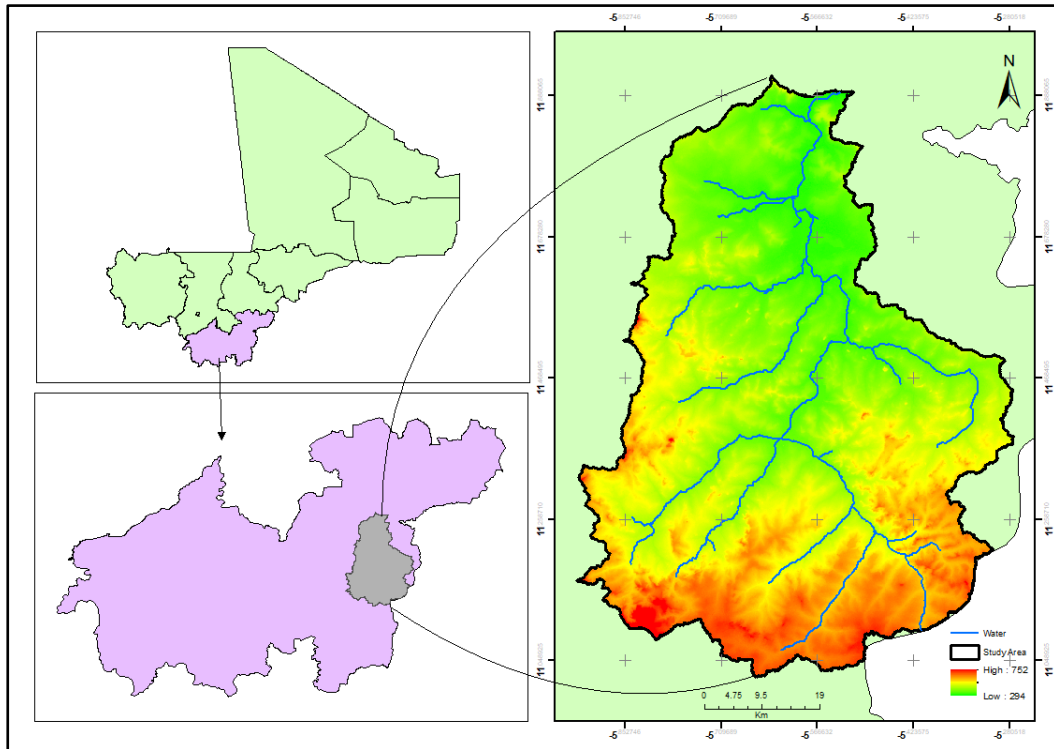
Figure 3.1: Study Area

Climate

The Lotio basin experiences a tropical Sudanian climate with abundant rainfall ranging from 754 to 1687 mm per year between 1980 and 2020. The region has a distinct rainy season that lasts for about 5 to 6 months and is accompanied by over 90 days of rainfall per year. During this season, the prevailing wind is the moisture-laden monsoon blowing from the southwest to the northeast. Conversely, the dry season is characterized by the hot and dry harmattan wind blowing from the North-East. In December, which is the coldest month, the average temperature is around 24°C. In the rainy season, the average maximum temperature reaches approximately 29°C. The months of July, August, and September receive the highest rainfall, with August recording the highest amount exceeding 307 mm. This heavy rainfall leads to significant runoff and groundwater recharge. From December to April, the study area experiences little rainfall, corresponding to the dry season. The average extreme

temperatures range from 17°C (minimum) to 38°C (maximum). The hottest months in the Lotio basin are March, April, and May, with April being the peak period. Conversely, December and January have the lowest temperatures, representing the cooler period between 1980 and 2020.

Relief

The geological matrix of Sikasso is made up of a metamorphic basement, folds and Eburnian orogenic granitization, sedimentary layers, Taoudéni syclenite, including Sikasso sandstone, basaltic intrusions outcropping in the form of rubble mountains and rare plateaus. The soil in this area consists of red laterite, lateritic clay and yellow or red clay on the surface. These formations are located on micro-sandstone or weathered shale. In addition to this, we also found stratified or diabase sandstone, but with fractures (Konaté, 2018).

Forest

The District of Sikasso has a total area of 33,149 hectares, of which 18,017 hectares are managed by the Water and Forestry Service; 18,132 hectares are managed by the Rural Wood Management Structures (SRGB). According to *Konaté*, 2018, the vegetation of the Sikasso District is made up of open forest and wooded savannah. This vegetation is dense especially in the southern part and is degrading in the north. According to him in the valleys, they are forest galleries.

Population

The Sikasso region is composed of seven circles with an unevenly distributed population and a fairly high density in the circle (29.3 inhabitants/km²). The surface area of the Sikasso circle is 15375km² with an estimated population of 725494 inhabitants (RGPH-2009). Since before independence to the present day, Sikasso has been a place of welcome and passage for populations from many corners. More recently, however, populations from the north of Mali have arrived. The *Sénoufos*, who are recognized as the native inhabitants, form the predominant ethnic group in the region. Between 1997 and 2020, the rural population exhibited an average annual growth rate of 1.9 percent, while the urban population experienced a higher average annual growth rate of 4.2 percent (Coulibaly et al, 1998). The different ethnic groups are: the *Senoufos*, the *Gana*, the *Samogos*, the *Bambaras*, the *Malinkés*, the

Minyankas, the *Bobos*, the *Peuls*, and even the Sonrhaïs, *Touaregs. Dogons or Kassonkés* (Djiguiba *et al*, 2009).

Economy

The main economic activity in this district is agriculture, forestry and livestock. In terms of agriculture, the main cash crop is cotton (*Gossypium hirsutum*), to which should be added potatoes (*Solanum tuberosum*), yams (*Dioscorea sp.*), sweet peas (*Lathyrus odoratus*), fruits and vegetables. Livestock plays an important role in rural development, particularly through animal traction and the income generated by this activity. The forested domain encompasses over 80% of the entire land area within the circular region and boasts abundant resources. In the area of trade, due to its status as a crossroads, the Sikasso District is an important centre for interaction with the country and beyond. Industrial activity dominated by cotton gins, supported by CMDT and other development support organizations (Djiguiba *et al*, 2009).

3.1.2.2 Data Collection

Several data from various sources were used in this study. However, they can be grouped into two (2) very distinct typologies according to their characteristics.

Satellite Images

The satellite data mobilised were of two types: Sentinel image and the Shuttle Radar Topography Mission (SRTM) images.

Sentinel-2, part of the Copernicus Programme, is a mission dedicated to Earth observation, capturing optical imagery with a high spatial resolution of 10 meters. It provides systematic coverage over both land and coastal waters. It has been downloaded on the website of EAS. Also, the most recent 12-meter resolution SRTM image covering the area were uploaded via the USA National Aeronautics and Space Administration (NASA) portal.

Digital Data

Digital data are necessary for thematic maps. They were collected in vector format for better manipulation in GIS and remote sensing software. These are mainly the digital layers of Mali with the smallest entities (the boundaries of the communes, districts, and regions) that were extracted from the database of the Mission of Decentralization and Institutional Reforms of the Republic of Mali.

Socio-economic database

The socio-economic data are data from the socio-economic survey conducted between June and July 2022 in the study area. They are composed of qualitative and quantitative variables on the socio-demographic and economic characteristics of households; perceptions of climate dynamics and land use, and strategies for adaptation to climate variability.

Field data

A field campaign was conducted in 2021 (September and October) for the formation/ground truth data for classification and validation using Global Positioning System (GPS) with Universal Transverse Mercator (UTM WGS84 zone 30 North) as the projection system. Reference points were overlaid on Landsat images (1990, 2000, 2010, 2020) and unchanged areas were selected. The unchanged areas were identified by focusing on field data, local community knowledge, and input from elders and community leaders. Google Earth was used to validate the unchanged areas.

3.1.2.3 Methods

Pre-processing

In this study, a DEM from SRTM with a spatial resolution of 30 m is used. Knowing the limitation of DEMs (images with empty cells and noise, i.e. cells with values much higher or lower than those of neighbour cells), a low-pass filter with a 3×3 neighbour window was applied to the SRTM image in order to correct the noise and assign a value to the empty cells. This filter greatly improved the image by scanning over each noise, each empty cell and their eight (8) immediate neighbours.

Lowlands Detection

This study adopts a multi-criteria approach to identify the lowlands. The method used was based on the combination, superposition and intersection of criteria established from the calculation of certain parameters, namely: the normalized difference vegetation index (NDVI), the adjusted ground vegetation index (SAVI), the slope, the water accumulation area and the height of the surfaces with the drainage network (Dembele, 2019; Oloukoi, 2016).

Selection and justification of indices and parameters

These indices were chosen due to their importance in the detection of lowlands because of their ability to clearly distinguish between uplands and lowlands (slope, surface height), vegetated and non-vegetated areas such as rock outcrops and water surfaces (SAVI, NDVI), wetlands likely to have lowlands (water accumulation zone, etc.), and wetlands likely to have lowlands (water accumulation zone, etc.)(Dembele, 2019). SAVI and NDVI were generated from the Landsat OLI image. Slope, flow accumulation, and surface height relative to the river network were obtained from the SRTM 30 image.

Index and parameter generation

o **Normalized Difference Vegetation Index**

The normalized difference vegetation index, developed by Rouse and Haas in 1973 (Rouse et al., 1974 and Tucker 1979), is an index that distinguishes vegetated areas from unvegetated or moderately vegetated areas. It is determined using the formula below:

$$NDVI = \frac{PIR-R}{PIR+R} \qquad (3.1.1)$$

Where, PIR = Near-Infrared and R = Red

High NDVI values will be used to identify lowlands. The extraction of the high values is based on the results of recent studies in Benin (Oloukoi, 2016; Souberou *et al.*, 2017).

o **Soil Adjusted Vegetation Index (SAVI)**

The SAVI is a vegetation index initiated by Huete (1988). It is of interest for detecting lowlands (Sudre, 2015). It introduces an adjustment parameter, denoted L, which characterizes the soil and its rate of cover by the plant cover. It makes it possible to clearly distinguish vegetation zones from armoured soils. It will be calculated by the following formula:

$$SAVI = \frac{[(1+L)(PIR-R)]}{(PIR+R+L)} \qquad (3.1.2)$$

where, PIR = Near Infrared; R = Red; 1 = Constant and L = Recovery rate to reduce ground effect with 0.25 (low recovery); 0.50 (medium recovery) and 0.75 (high recovery).

o **Slope**

Slope values less than or equal to 2 or 3% have been retained in this study (Dembele, 2019; Kindjinou, 2013; Oloukoi, 2016). This threshold was proposed by (Albereel & Claude, 1988) and then in other more recent studies such as (Dembele, 2019; Kindjinou, 2013; Oloukoi, 2016) to distinguish the lowlands from the alluvial plains.

o **Water storage area**

The accumulation of flow streams highlights areas of high and low water accumulation, important for the identification of lowlands (Oloukoi, 2016; Souberou *et al.*, 2017).The interest is to extract drainage networks and surfaces with a high concentration of water. Areas of high-water accumulation are areas where surface water is concentrated and stagnates for a long time. They include rivers and their tributaries, all drainage surfaces (lowlands, valleys, plains). On the other hand, areas of low water accumulation are upland areas that most often constitute ridges. These areas with low values have been excluded in the identification of the lowlands.

o **Height of surfaces to drainage systems**

This parameter is very important for identifying lowlands (Kindjinou, 2013; Sudre, 2015). The aim is to determine the low areas in the vicinity of the hydrographic network. To do this, the difference between the elevations of the hydrographic network and those of the surrounding surfaces (sub-watersheds) were calculated. The lower the height, the more the area is a flooded environment likely to have low areas.

Determination of potential lowland areas

Suitable values of the parameters selected according to criteria allowed the detection of inland valleys in this study (Table 3.1.1**Error! Reference source not found.**). The ap of potential lowland areas was obtained from the intersection of these resulting data.

Table 3.1: Values of indices and parameters retained for lowlands identification

S/N	Indices	Range of values	Sources
1	NDVI	0.10 to 0.56	Oloukoi, (2016)
2	SAVI	0.10 to 0.83	Sudre, (2015)
3	Slope	0 to 3%	Oloukoi,(2016); Souberou et al., (2017)
4	Water storage area	5083 to 20326	Oloukoi, (2016); Souberou et al., (2017)
5	Height of surfaces	0 to 2 meters	Kindjinou, (2013); Sudre, (2015)

Like other image processing, the detection of lowlands from image processing requires validation in the field. Therefore, we geo-referenced a few areas of lowlands during the field trip. These points were then superimposed on the detected shallows to assess the conformity between the two areas.

Validation of the results of lowland inventory and mapping work

A total of 100 points were geo-referenced in lowlands in the field. These were GPS geolocation points of the lowlands in the study area. For each inventoried lowland, the geographic coordinates are taken. The inventoried lowlands and the lowlands derived from the DEM are then overlaid to observe compliance. The calculation of the conformity rate and the omission error (Kindjinou, 2013), carried out following the superposition of the two (2) groups of lowlands allowed the validation of the lowland identification approach in this study. It is calculated using the following formula:

$$T = \frac{n \times 100}{N} \tag{3.1}$$

where **T**= Compliance rate between detected shallows and inventoried shallows. It is a positive real number varying between 0 and 100. The closer its value is to 100, the more the rate is compliant and vice versa; **n**= Number of lowland points inventoried in the field superimposed on the lowlands detected from image processing; and **N**= Total number of lowland points inventoried.

The omission error was determined from the non-overlapping points on the detected lowlands. In addition to this validation method, the lowlands were visualized in Google Earth software for comparison with the shape of the terrain.

3.1.3 Results and interpretation

3.1.3.1 Lowland

The observation of the map of the lowlands indicates that the study area is an area with a high density of lowlands (Figure 3.1). The surface of the detected lowlands amounts to 71479 ha, which represents a proportion of 17% of the study area.

Based on the intersection between the two (2) groups of lowlands, the compliance rate is 58.48% with an error of omission of 41.52%. The compliance rate from the validation shows us that the result is statistically acceptable
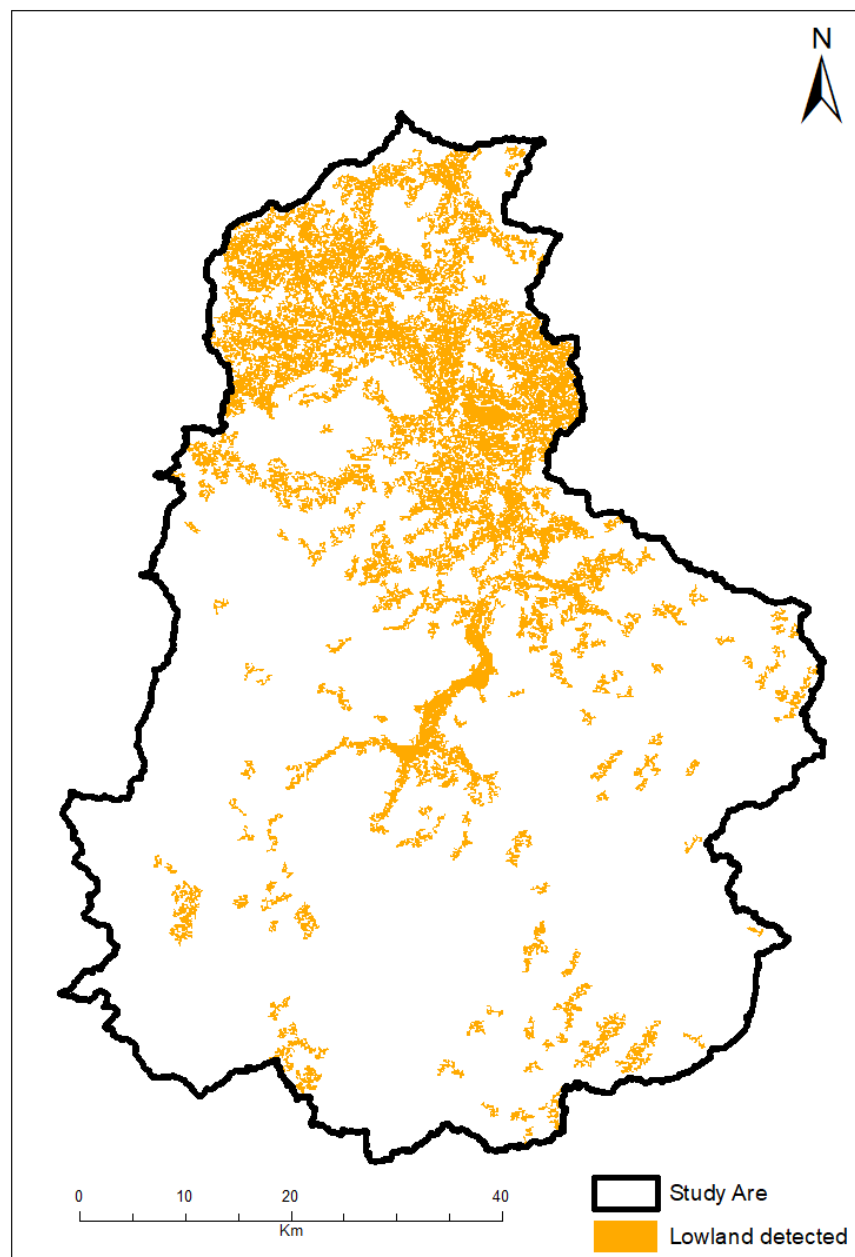
Figure 3.1: Lowland detected

3.1.4 Discussion

The study estimated the area of the lowlands at 71479 ha with a compliance rate of 58.48%. This means that the area has a significant potential in lowlands. The same result was found on a national scale by (Dembele, 2019) in his master's thesis on the detection of areas with agricultural potential in the rural commune of *Bougaribaya*. At the international level, in Benin, within the framework of the implementation of the Atlas of the lowlands of the North-West of the country in 2015-2016, the total area of the lowlands surveyed is estimated at 46.264 ha for the department of *Atacora-Donga* (Souberou *et al.*, 2017).

The multi-criteria approach adopted showed the importance of GIS and remote sensing and the degree of reliability of the results in the identification, estimation and mapping of the lowlands as it had been highlighted by several previous studies (Chabi *et al.*, 2010; Dembele, 2019; Kindjinou, 2013; Oloukoi, 2016; Souberou *et al.*, 2017).

3.1.5 Conclusion

The southern zone of Mali has 71 479 ha of lowland, which constitute a rich potential in lowlands with a good spatial distribution. The multi-criteria approach is a recognized and recommendable method for the identification, area estimation, geophysical and geomorphological characterization of lowlands.

CHAPTER 3.2: ASSESSMENT OF TEMPERATURE AND RAINFALL VARIABILITY, TRENDS, FARMERS' PERCEPTIONS AND ADAPTATION STRATEGIES IN SOUTHERN MALI BETWEEN 1960-2020

3.2.1 Introduction

The variability in the hydrological cycle and weather extremes has been amplified due to the ongoing global climate change. Consequently, there is a necessity to examine the subsequent modifications in hydroclimatic variables to comprehend the localized impacts of climate change (Easterling *et al*., 2012; Lelieveld *et al*., 2016). As stated in the 6th assessment report of the Intergovernmental Panel on Climate Change (IPCC), West Africa has already suffered considerable loss and damage due to climate change (IPCC, 2013). The same report states that the climate is changing significantly and unprecedentedly for at least 2,000 years due to human activity and most African countries are among those that contribute the least to global greenhouse gas emissions. Yet, African countries are experiencing considerable loss and damage from the resulting climate change. West Africa is also affected and is already experiencing loss of life, human health impacts, reduced economic growth, water shortages, reduced food production, loss of biodiversity, and impacts on human habitation and infrastructure. Several authors, for example (Bichet & Diedhiou (2018a, , 2018b), Dosio (2017), ; Gutiérrez *et al*. (, 2021),; Ranasinghe et al. (, 2021),; Sanogo *et al*. (, 2015), Sylla *et al*. (2016) and ; Thomas & Nigam (, 2018), assert that the situation in the southern African region, particularly changes in annual and seasonal temperatures and precipitation, is likely to reach unprecedented levels under projected regional climate change scenarios.

While climate change is widely acknowledged as a reality, the level of uncertainty surrounding the specific projections for the region remains high. Currently, there is limited understanding of the magnitude and variability of hydroclimatic trends in most West African countries. Various studies have attempted to evaluate the reliability of climate models by comparing simulated climate data with observed data, aiming to assess the uncertainties associated with these models (Malmgren *et al*., 2003; Meehl *et al*., 2007). The findings of these studies indicated that current climate models face challenges in accurately reproducing extreme climate events, which introduces additional uncertainties when predicting future changes. As a result, it is

crucial to consistently evaluate the long-term and short-term fluctuations of climate variables, particularly those pertaining to the availability of freshwater, by relying on in situ climate data. This underscores the significance of ongoing assessments to better understand the variability of climate factors and ensure reliable information (Benestad, 2013; Malmgren *et al*., 2003; Sillmann & Roeckner, 2008). Globally, numerous research studies are actively involved in analyzing patterns and fluctuations in hydrometeorological data, primarily focusing on precipitation and temperature, on an international scale (Donat *et al*., 2014; Manton *et al*., 2007) to mention only a few contributions. On the other hand, for many African countries, mainly the Sahelian and Saharan regions such as Mali, research coverage is still insufficient despite recent work (Doukoro *et al*., 2022). Studies on desertification (Olivry *et al*., 1994) have shown a clear positive trend over the last 3 decades. In the southern region of Mali, although extensive research has been conducted, there is currently no documented quantitative evidence regarding long-term rainfall records that can attribute trends and temporal variability to climate change.

The objective of this study was to examine the long-term patterns and fluctuations in rainfall in the city of Sikasso, located in southern Mali. Climate variability is typically defined as the deviation of seasonal and annual climate parameters, such as rainfall and temperature, from the long-term average. However, this study specifically aimed to identify and analyse continuous temporal changes and trends in annual, seasonal, and monthly rainfall, as these indicators can provide insights into potential impacts of climate change (Jones *et al*., 2015). According to previous research, changes in precipitation and temperature over a long-term period of 30 years or more are regarded as valuable indicators for evaluating the potential effects of climate change in a specific region (Cooper *et al*., 2002; Donat *et al*., 2014; Easterling *et al*., 2012; Liebmann *et al*., 2010). The processed dataset includes annual and seasonal precipitation and temperature data spanning a period of 61 years (1960-2020) in the Sikasso district. Following an assessment of data quality, various analyses such as the Mann Kendall test, Sen's slope, Pettit-test, and change point detection were employed to investigate and quantify the long-term and short-term trends and variability of annual and seasonal rainfall and temperature. Additionally, the study examined the variability of extreme events and changes in frequency (such as return period) to evaluate potential alterations in the wet and dry seasons.

3.2.2 Approach and Methods

3.2.2.1 Data collection

Climate Data

Monthly precipitation and temperature data spanning from 1960 to 2020 (61 years) were gathered from the Agence Nationale de la Météorologie du Mali.

3.2.2.2 Methods

Mann-Kendall Statistical Test

The Mann-Kendall statistical test, which is a non-parametric test for trend, is employed to evaluate the statistical significance of whether a set of data values exhibits an increasing or decreasing trend over time. (Praveen, *et al*., 2020; Merabtene *et al*., 2016). The MK test was calculated using :

$$S = \sum_{i=1}^{n-1} \sum_{j=i+1}^{n} \mathbf{sgn}(X_j - X_i) \tag{3.2.1}$$

where Xi and Xj are the values of sequence i, j; n is the length of the time series and

$$sgn(\theta) = \begin{cases} 1 \ if \ \theta > 0 \\ 0 \ if \ \theta = 0 \ -1 \\ -1 \ if \ \theta < 0 \end{cases} \tag{3.2.2}$$

The statistic S is approximately normally distributed when $n \geq 8$, with the mean and the variance of statistics S as follows:

$$E(S) = 0 \tag{3.2.3}$$

$$V(S) = \left[\frac{n(n-1)(2n+5) - \sum_{i=1}^{m} T_i i(i-1)(2i+5)}{18} \right] \tag{3.2.4}$$

where T_i is the number of data in the tied group and m is the number of groups of tied ranks. The standardized test statistic Z is computed by:

$$Z = \begin{cases} \frac{S-1}{\sqrt{V(S)}} \\ 0 \\ \frac{S+1}{\sqrt{V(S)}} \end{cases} \tag{3.2.5}$$

Where **S > 0, S = 0 and S < 0.** The standardized MK statistic Z follows the standard normal distribution with $E(Z) = 0$ and $V(Z) = 1$, and the null hypothesis is rejected if the absolute value of Z is larger than the theoretical value $Z_{1-\alpha/2}$ (for two-tailed test) or $Z_{1-\alpha}$ (for one-tailed test), where α is the statistical significance level concerned.

Sen's Slope Estimator

Several hydrologic variables exhibit a notable right skewness, primarily due to natural phenomena, and they do not conform to a normal distribution. Climate data demonstrates fluctuations and deviations from a normal distribution (Nasher, 2021). Therefore, the study utilized Sen's slope estimator, a nonparametric approach, to construct the linear models. Sen's slope estimator is a commonly employed nonparametric method for estimating the actual slope of an existing linear trend. When a time series exhibits a linear trend, the true slope (rate of change per unit of time) can be estimated using Sen's straightforward nonparametric procedure, originally introduced by Sen in 1986. This allows the linear model (t) to be expressed as follows:

$$f(t) = Qt + B \tag{3.2.6}$$

where Q is the slope, B is a constant and t is time.

To derive an estimate of the slope Q, the slopes of all data pairs are calculated using the equation:

$$Qt = \frac{x_j - x_k}{j - k} \tag{3.2.7}$$

where i = 1,2, 3,.... N, j > k

If there are n values x_j in the time series there will be as many as n(n-1)/2 slope estimates Q_i . To obtain estimates of B in the equation the **n** value of differences $x_i - Qt_i$ are calculated. The median of these values gives an estimate of B. The estimates for the constant B of lines of the 99% and 95% confidence intervals are calculated by a similar procedure. Data were processed using Slope Sen's in R.

Method for Change Point Detection (CPD)

The study applied the Pettit test, introduced by Pettit (1979), to identify abrupt change points in the time series of annual and seasonal rainfall and temperature in the study area. The Pettit test is a nonparametric rank-based test that is utilized to detect significant changes in the mean of a time series. This test is particularly useful in cases where there is no need for hypothesis testing related to changes in location (Praveen et al., 2020).

Farmers' Perception and Adoption Strategies Assessment

A sample of 395 farmers was selected from 25 villages across five municipalities in the study area. The focus of the study was on lowland farmers in the southern region of Mali. The proportional allocation of the sample size (n) for each municipality was determined using the equation proposed by Krejcie and Morgan (1970) as shown in (Table 3.1).

$$n = \frac{x^2 Np(1-p)}{e^2(N-1)+x^2 p(1-p)} \qquad \text{(3.2.1.8)}$$

where n represents the sample size, N represents the population size, e is the acceptable sampling error, X2 represents the chi-square of the degree of freedom 1 at a confidence of 95% (which is 3.841) and p is the proportion of the population (which 0.5 if unknown).

Both quantitative and qualitative data were utilized in the study. Data collection involved the use of a structured questionnaire consisting of closed-ended questions, which was administered to respondents via the "Kobo Collect" application on mobile phones. From June to July 2022, a field survey was conducted, and face-to-face interviews were conducted with farmers in the research area. The interviews aimed to gather information on various aspects, including people's perceptions of recent changes in rainfall patterns such as amount, duration, and the onset and cessation of the rainy season. Additionally, socio-demographic characteristics of households, climate change awareness, and farmers' adaptation strategies were also explored during the interviews.

The majority of the questions in the survey were structured with closed-ended items or phrases, requiring respondents to select from multiple-choice answers. However, a few open-ended questions were also included. The closed-ended questionnaire was designed to incorporate various formats, such as dichotomous (requiring a "Yes" or "No" response), multiple-choice, and a five-point Likert scale. The Likert scale provided respondents with five options to indicate their level of agreement with a statement: Strongly Disagree, Disagree, Neither Agree nor Disagree, Agree, and Strongly Agree. These question formats were chosen to streamline the response process and generate data that could be easily analyzed statistically. Moreover, the use of a Likert scale questionnaire enabled the evaluation of the reliability and validity of

the main constructs examined in the study. (Koné *et al.*, 2022). Individual farmers' judgments of comparable socioeconomic situations, belonging to the same social network, or owning farms within a certain landscape unit were measured throughout the survey. This form of perception assessment considers previous experiences or future predictions and is associated with the following elements: the farmer's objectives, interests, and demands.

Before conducting the actual survey, the questionnaires underwent a pre-testing phase involving 60 individuals who shared similar socio-economic backgrounds with the study respondents. The aim was to assess the validity and reliability of the data collection instrument. Based on the feedback received during the pre-testing, minor adjustments were made to the questionnaire to enhance clarity and ensure that perceptions not initially included in the original questionnaire were captured.

Table 3.1: Distribution of respondents in the different department of the study area

Municipality	Number of Villages total	Number of villages surveyed	Number of producers
Danderesso	*Bakoronidougou*	*8*	14
	Bambougou		14
	Bandieresso		14
	Lerasso		14
	Nazanadougou		14
	N'golodougou-Deni		12
	Touleasso		12
	Zanton-Zanso		12
Kaboila	*Coulibalibougou*	*6*	16
	Dadoumabougou		16
	Diassadie		16
	Doniena		16
	Kogodoni		16
	Niankorobougou		16
Klela	*Djirigolola*	*5*	16
	Dougoumousso		16
	Kong-Kala		16
	Yaban		16
	Zerelani		16
Pimperna	*Togotan-Diassa*	*2*	16
	Zerilaba		16
Sikasso	*Fama*	*4*	20
	Mankourani		20
	Sanoubougou		20
	Wayerema		21
Total	25	395	

Analysis of survey data

The valid responses obtained at the conclusion of data collection were extracted and subjected to quantitative analysis based on the research objectives. Statistical software (SPSS) was utilized for descriptive analysis of the data. The socioeconomic characteristics, farmers' perceptions of climate change, and their adaptation strategies were examined using descriptive statistics. This approach facilitated an evaluation of local perspectives on climate change and adaptation measures by generating cross-tabulations and calculating means and standard deviations.

3.2.3 Results and interpretation

3.2.3.1 Variation of Annual and seasonal of Rainfall

By analyzing the yearly precipitation records of the Sikasso district spanning from 1960 to 2020, significant differences in precipitation variability between the annual and seasonal patterns in southern Mali are observed. Specifically, the average seasonal precipitation exhibits notable variations across different periods. For the March-April-May (MAM) period, the average ranges from 50 to 350 mm, for the June-July-August (JJA) period it varies from 400 to 1000 mm, and for the September-October-November (SON) period, it ranges from 100 to 500 mm. In terms of the average annual precipitation over the entire period from 1960 to 2020, it fluctuates between 800 and 1600 mm, with an average value of 1200 mm per year (Figure 3.3).
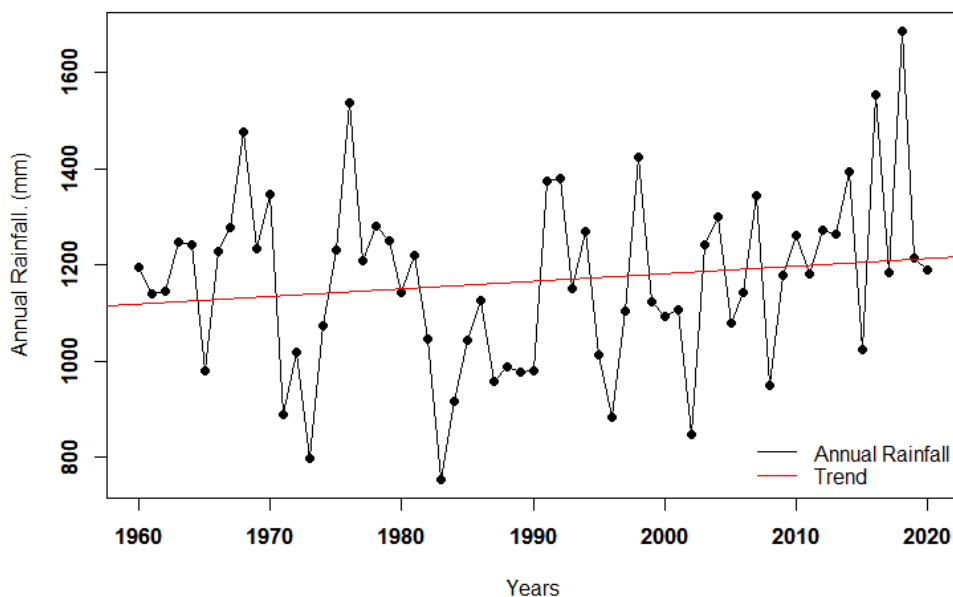
Figure 3.3: Variation of Annual Rainfall for Lotio Basin River
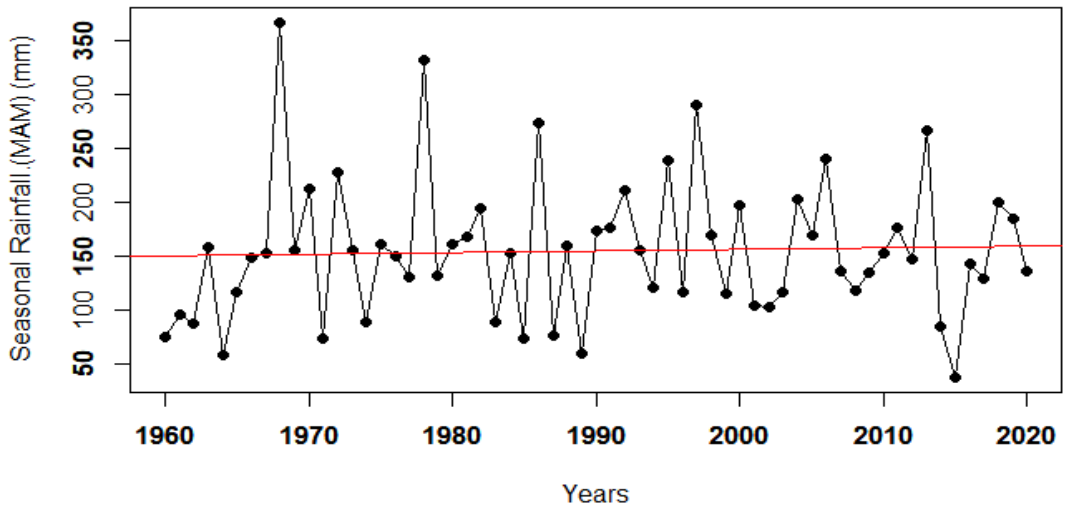
Figure 3.4: Variation of seasonal (MAM) Rainfall for Lotio Basin River
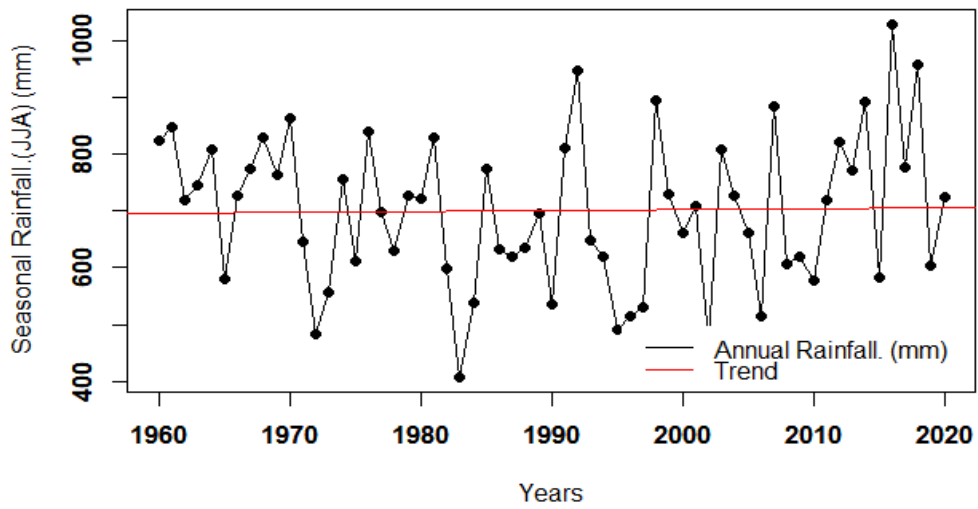
Figure 3.5: Variation of seasonal (JJA) Rainfall for Lotio Basin River
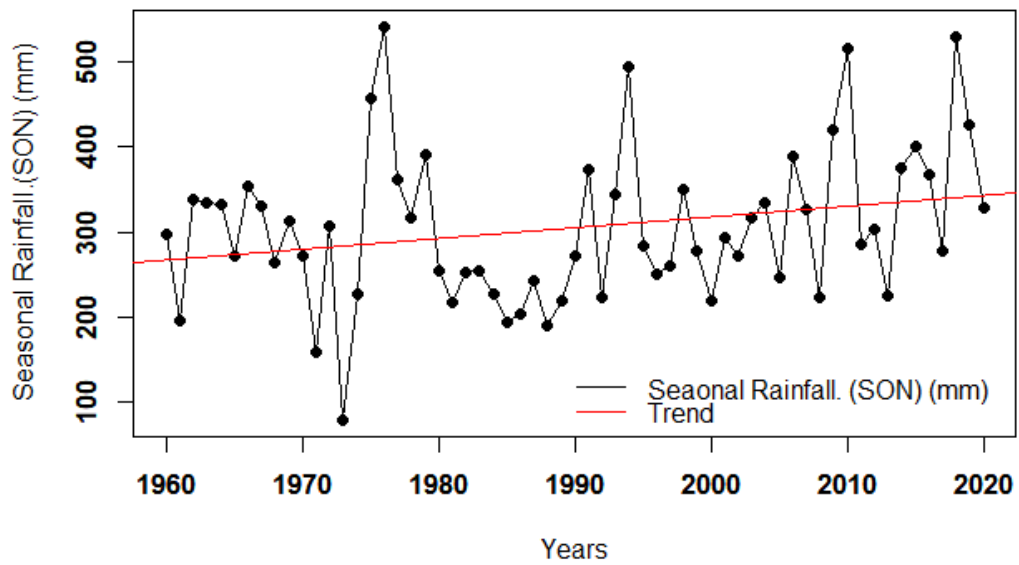
Figure 3.6: Variation of seasonal (SON) Rainfall for Lotio Basin River

3.2.3.2 Variation of Annual and Seasonal and Temperature

The annual and seasonal average temperatures from 1960 to 2020 show that the annual average temperature fluctuates between 26.5 and 28.5 degrees Celsius. Seasonal average temperatures range from 29 to 32 degrees Celsius in MAM, and 26 to 28 degrees Celsius in JJA and SON.
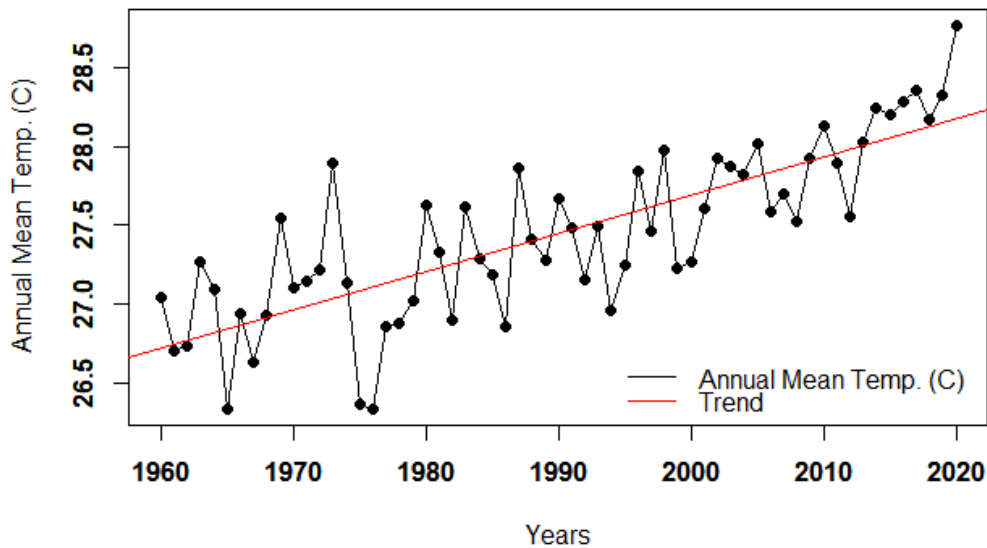
Figure 3.7: Annual Mean Temperature variation for Lotio Basin River
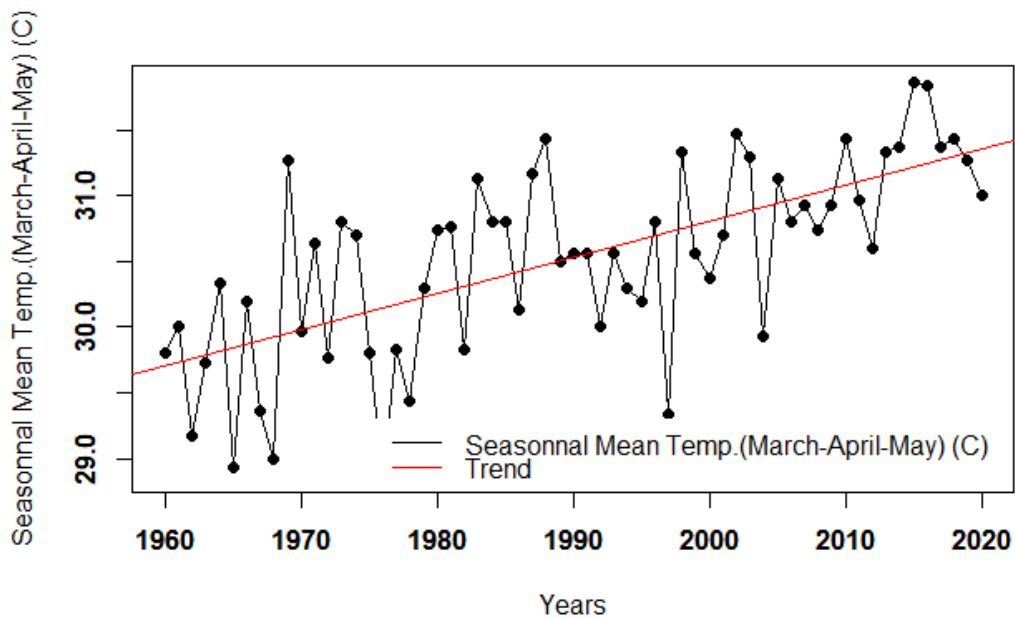
Figure 3.8: Seasonal (MAM) Mean Temperature variation for Lotio Basin River

54
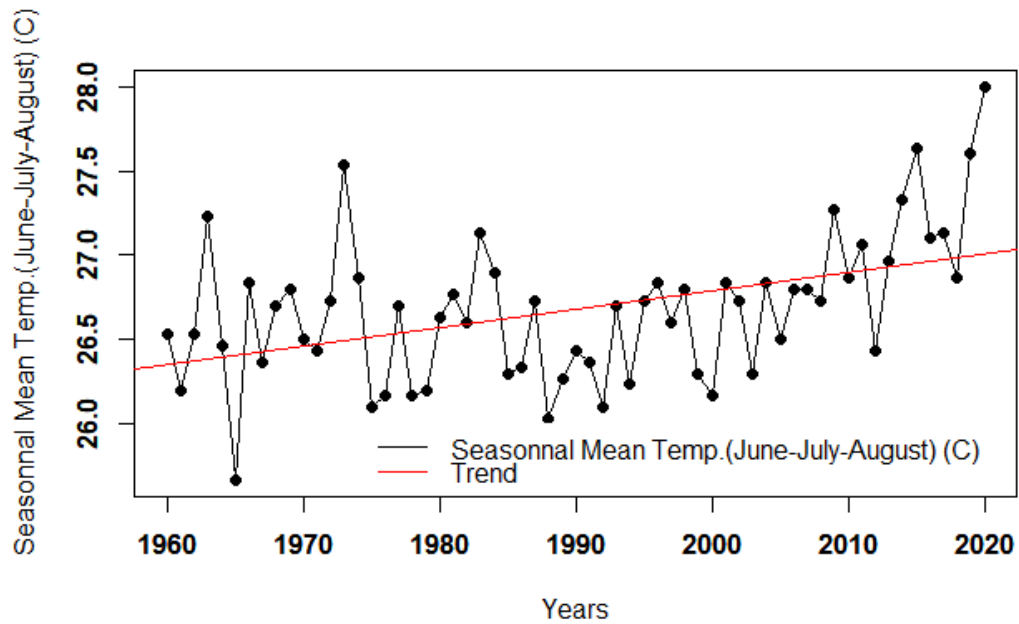
Figure 3.9: Seasonal (JJA) Mean Temperature variation for Lotio Basin River
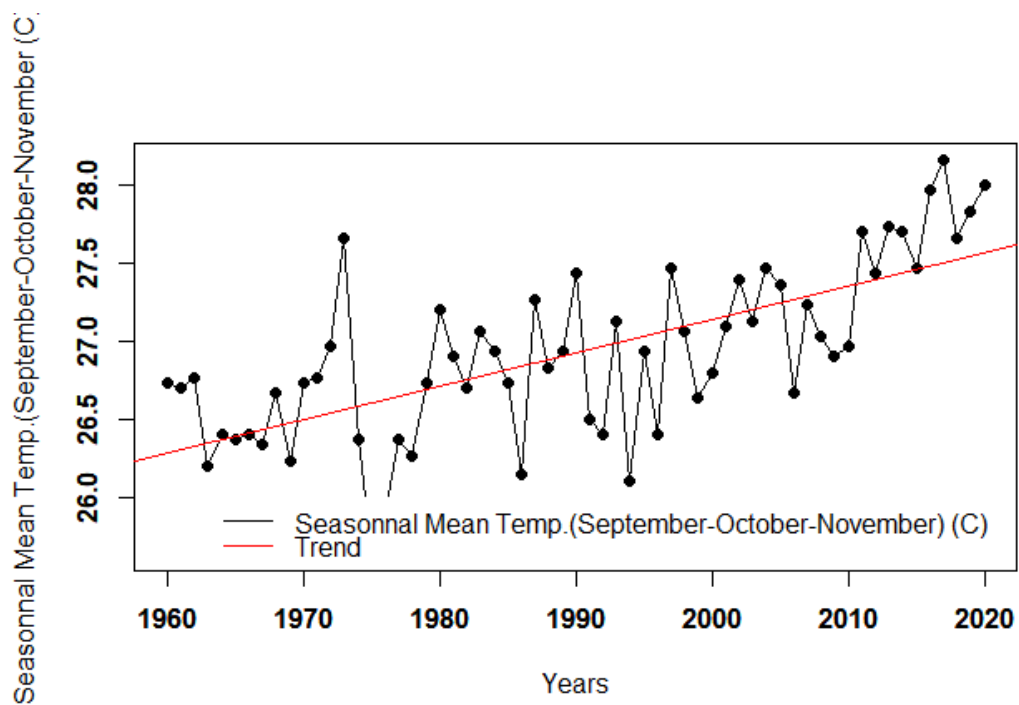
Figure 3.10: Seasonal (SON) Mean Temperature variation for Lotio Basin River

3.2.3.3 Trend of Annual and seasonal Rainfall and Mean Temperature

The trend analysis of rainfall shows that there is a slight increase for all the annual and seasonal with the exception of the period of JJA where we observe a slight decreasing. Any of the increase and the deceasing of annual and seasonal trend of rainfall are statistically significant (p-value < 0,05). The magnitude of trend analysis

(Slope Sen's) indicates the positive trend for annual and all the seasonals periods except June-July-August period. As for the temperature, we observe a general increase in trend for all the periods annual and seasonal over the study period 1960 to 2020 and all the increase trend are statistically significant (Table 3.2).

Table 3.2: Trend of Annual and seasonal Rainfall and Mean Temperature

Time Scale	Rainfall			Temperature		
	Z-value	P-value	Slope	Z-value	P-value	Slope
Annual	**0,989**	0,322	1,255	**7,033**	**0,000**	0,025
MAM	**0,877**	0,380	0,418	**5,593**	**0,000**	0,027
JJA	**-0,305**	0,760	-0,251	**3,595**	**0,000**	0,010
SON	**1,761**	0,078	1,168	**5,792**	**0,000**	0,022

3.2.3.4 First change point detection or break of annual and seasonnal rainfall and temperature

The result of the following (Table 3.3) indicates that the year 2003 was the first year of break or first point of change observed in the annual precipitation between the period 1960 and 2020. For the seasonal precipitation of the periods MAM, JJA, and SON, the following years were observed as the first break point, successively: 1967, 1971, and 2003. In addition, for the annual mean temperature, the period MAM, JJA, and SON, the years 1996, 1998, 2004, and 1997, are considered respectively as the first breakpoint year.

The statistical significance of the observed breaks is examined, and it is discovered that none of the annual and seasonal precipitation breaks are significant, while all of the annual and seasonal mean temperature breaks are significant.

Table 3.3: First change point of rainfall and temperature

Time Scale	Rainfall		Temperature	
	First time change point	P-value	First time change point	P-value
Annual	2003	0.3176	1996	0,000
MAM	1967	0.6214	1998	0,000
JJA	1971	0.4471	2004	0,001
SON	2003	0.1261	1997	0,000

3.2.3.5 Change Point Detection (CPD) of annual and seasonal rainfall

The observation of Change Point Detection (CPD) between 1960 and 2020, revealed that in Sikasso annual and seasonal rainfall they are lot of breaks. For the annual rainfall the break observed matches to years 1971, 1974, 1980, 1991 and 2016. 1976, 1978, 1979, 2014 and 2016 are the change point for the MAM period. For the seasonal periods of JJA and SON, we are noted successively the following years 1971, 1974, 1982, 1985, 2012 and 1975, 1980, 2009, 2011, 2014 as change point.
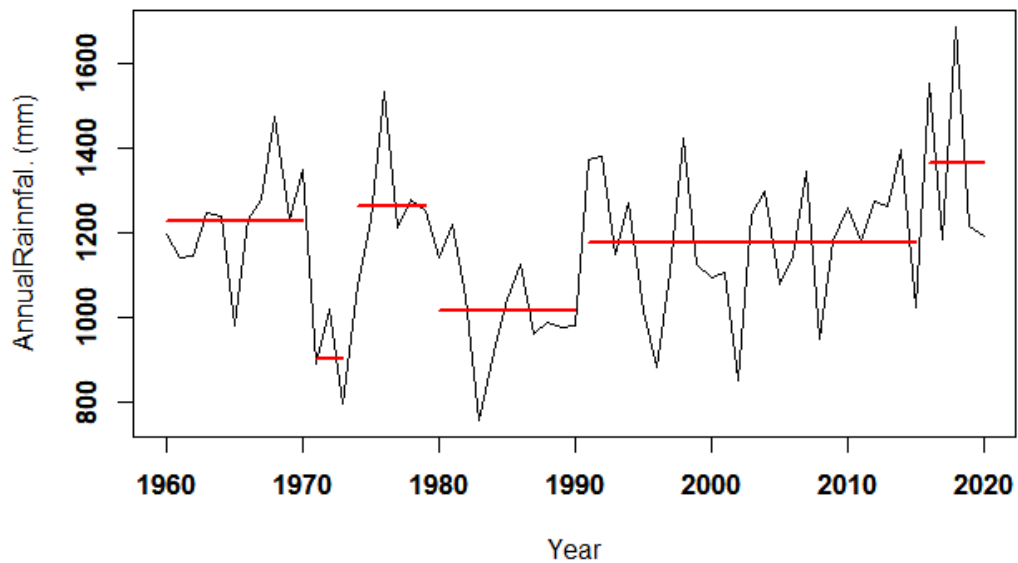
Figure 3.11: Annual Rainfall change point
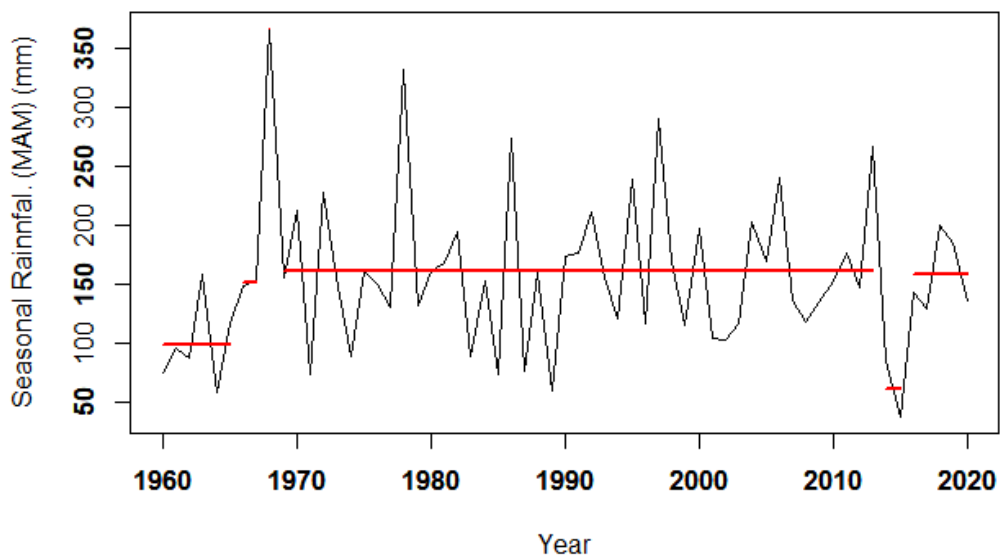
Figure 3.12: Seasonal (MAM) Rainfall change point
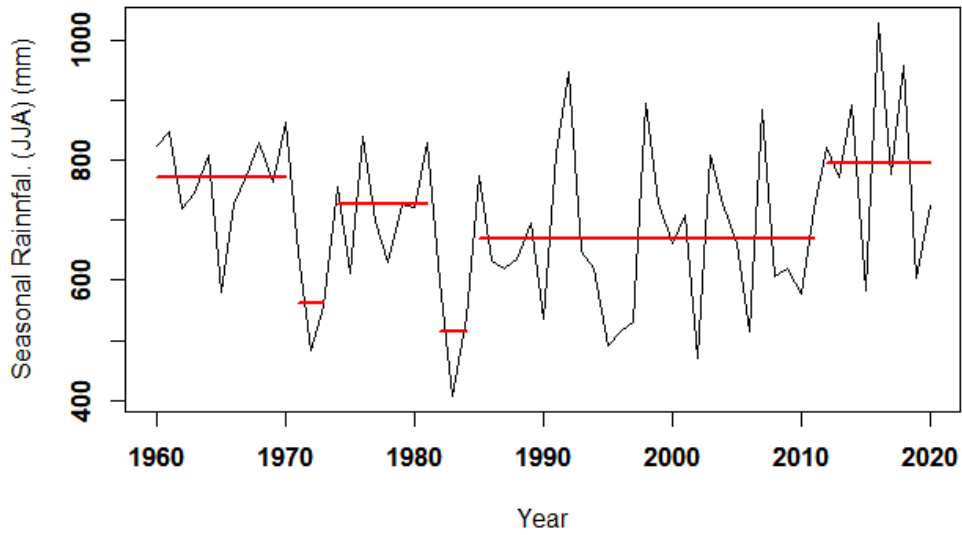
Figure 3.13: Seasonal (JJA) Rainfall change point
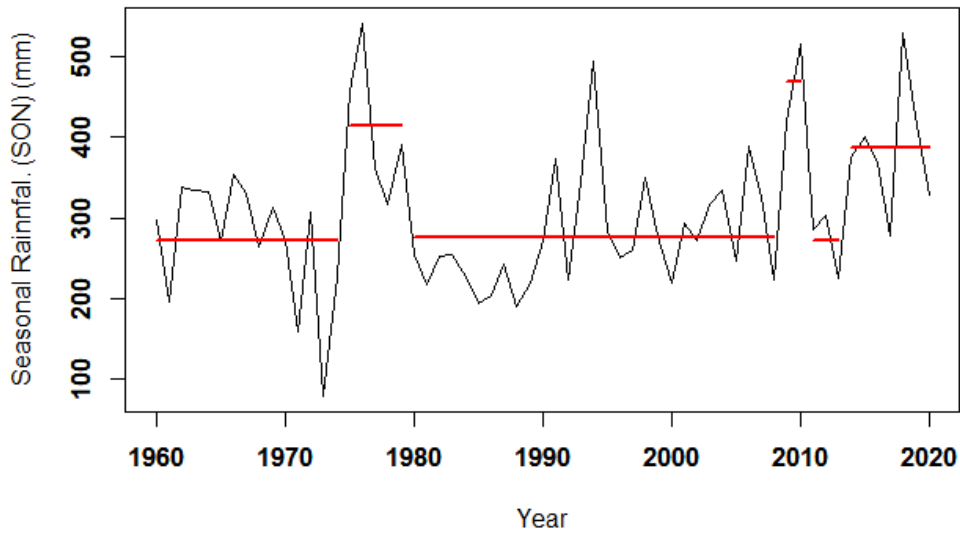
Figure 3.14: Seasonal (SON) Rainfall change point

3.2.3.6 Change Point Detection (CPD) of annual and seasonal Temperature

The results of the change point detection analysis showed any break point in the seasonal periods (MAM, JJA, SON) and the annual mean temperature between 1960 and 2020.
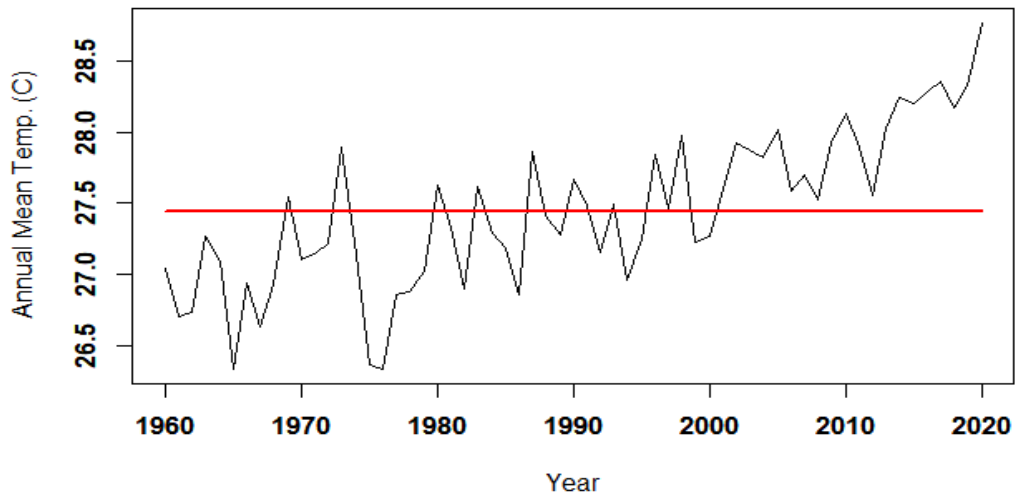
Figure 3.15: Annual Temperature change point
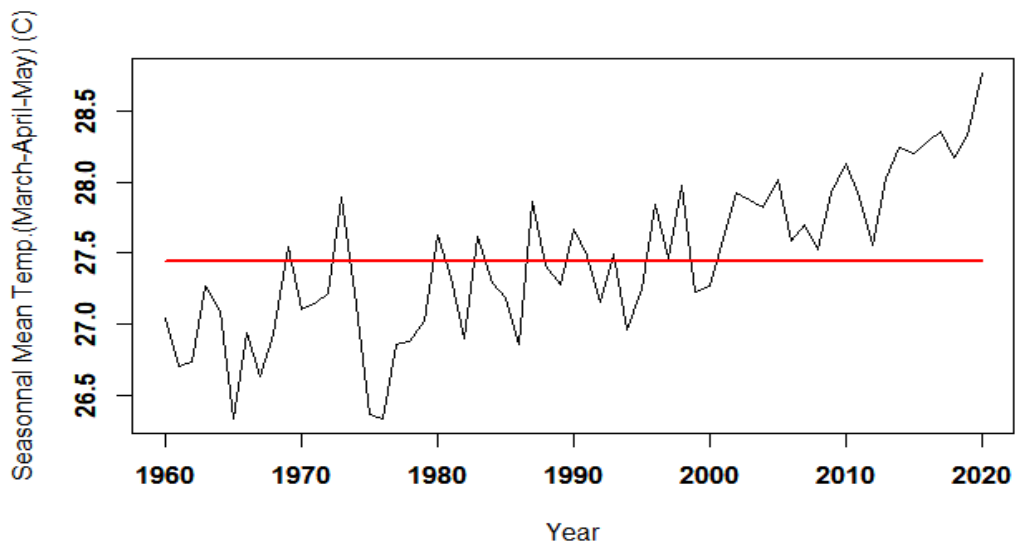
Figure 3.16: Seasonal (MAM) Temperature change point
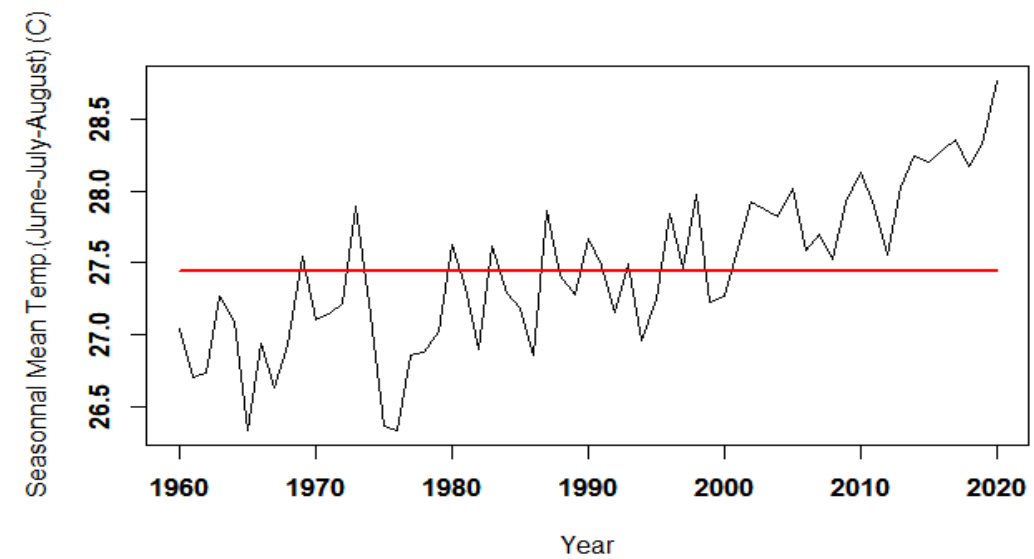
Figure 3.17: Seasonal (JJA) Temperature change point
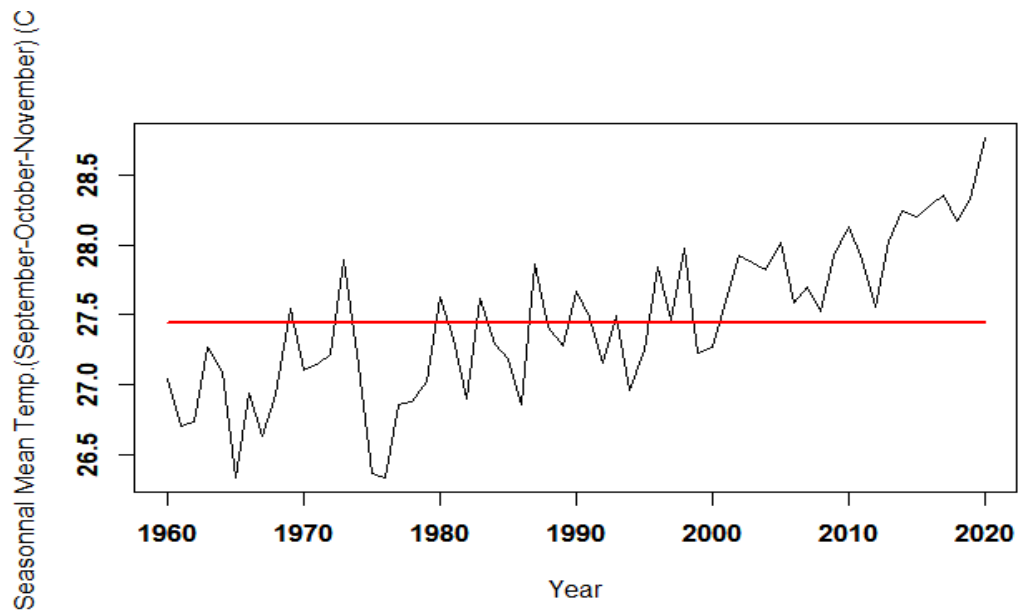
Figure 3.18: Seasonal (SON) Temperature change point

3.2.3.7 Socio-Economic and Demographic Characteristics of Lowland farmers

Table 3.4 displays the findings of an investigation of the socioeconomic and demographic features of lowland farmers. We used the following criteria: gender, sex, marital status, education level, and experience in lowland farming. The findings revealed that lowland farming is primarily performed by men (71.65% vs. 28.35% of women in the examined locations). These manufacturers ranged in age from 20 to 50 years. In this survey, the majority of respondents (48,61%) were between the ages of 20 and 30, and nearly all (88.35%) were married.

Table 3.4: Socio-economic and demographic characteristics of Lowland farmers

Variables	Percentages
Gender	
Male	71.65
Female	28.35
Age	
20-30	48.61
31-50	44.56
> 50	6.84
Marital Status	
Married	88.35
Single	8.61
Widower	3.04
Education	
No Formal Education	45.32
Quranic school	16.46
Primary school	25.57
High school	12.66
Experience	
Less than 10 years	17.72
10 to 20 years	20.76
20 to 30 years	27.09
30 to 40 years	14.68
40 to 50 years	15.19
> 50 years	4.56

3.2.3.8 Farmer's Perception of climate variability changes

Climate variability is a reality in Mali's southern area. Locals recall frequent heavy rains and protracted wet seasons in the past. Rain might fall for several hours during the day. The rainy season is currently being disrupted for lowland farmers. According to lowland farmers, this is evident in a drop in rainfall (79.6%) (Figure 3.19), an increase in temperature (83%) (Figure 3.20), a late start (97%) (Figure 3.21), and a quick conclusion to the season. Respondents noticed a shorter rainy season (97.71%) (Figure 3.22) and a reduction in the number of wet days (97.42%) (Figure 3.23). Lowland producers also perceived that climatic extremes are occurring with increasing frequency, resulting in an increase in periods of drought (83%) and flooding (96%).
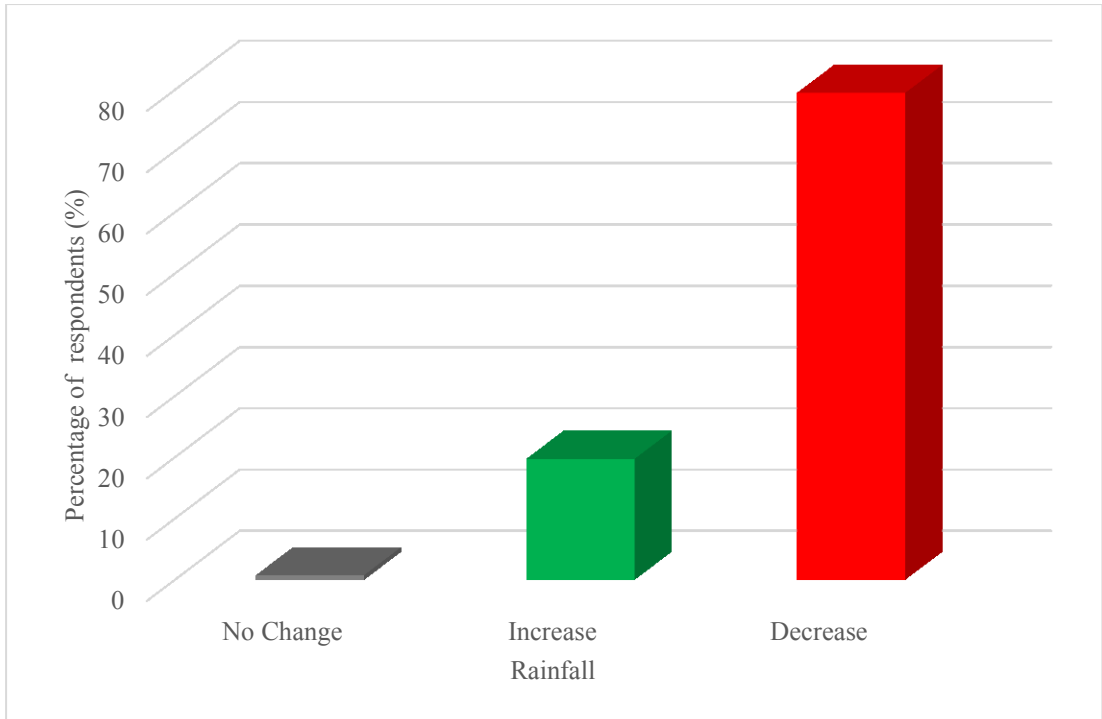
Figure 3.19: Farmers' Perception on Rainfall Variation
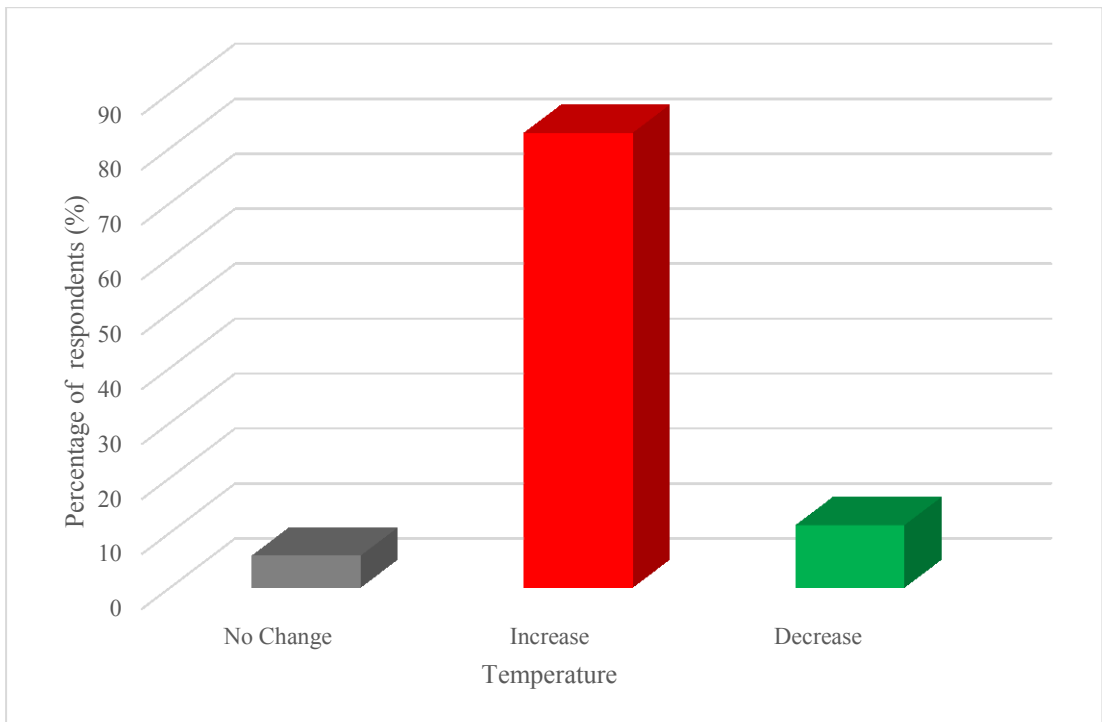
Figure 3.20: Farmers' Perception on Temperature Variation
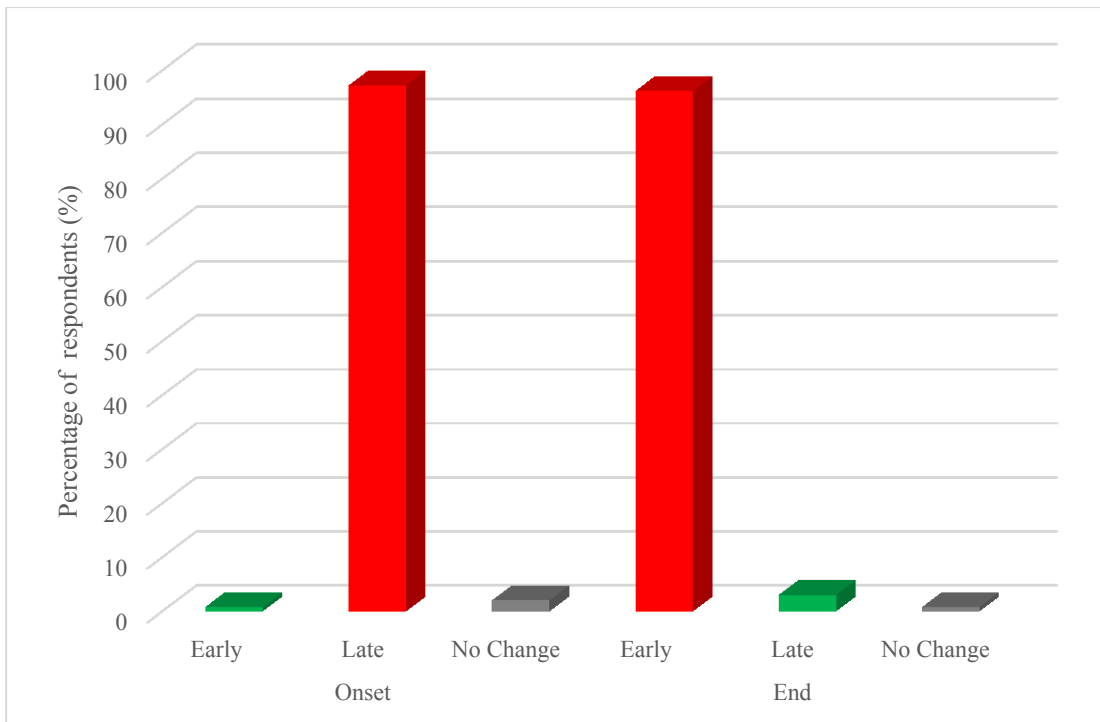
Figure 3.21: Farmers' Perception on Onset-End season Variation
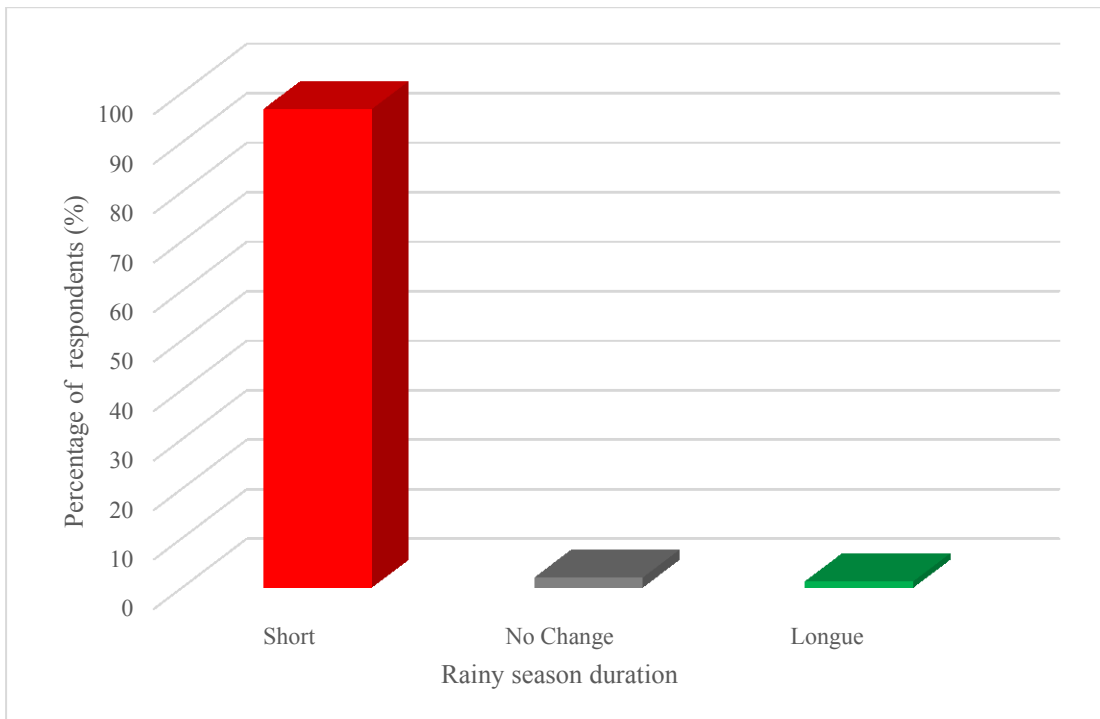
Figure 3.22: Farmers' Perception on Rainy season duration Variation
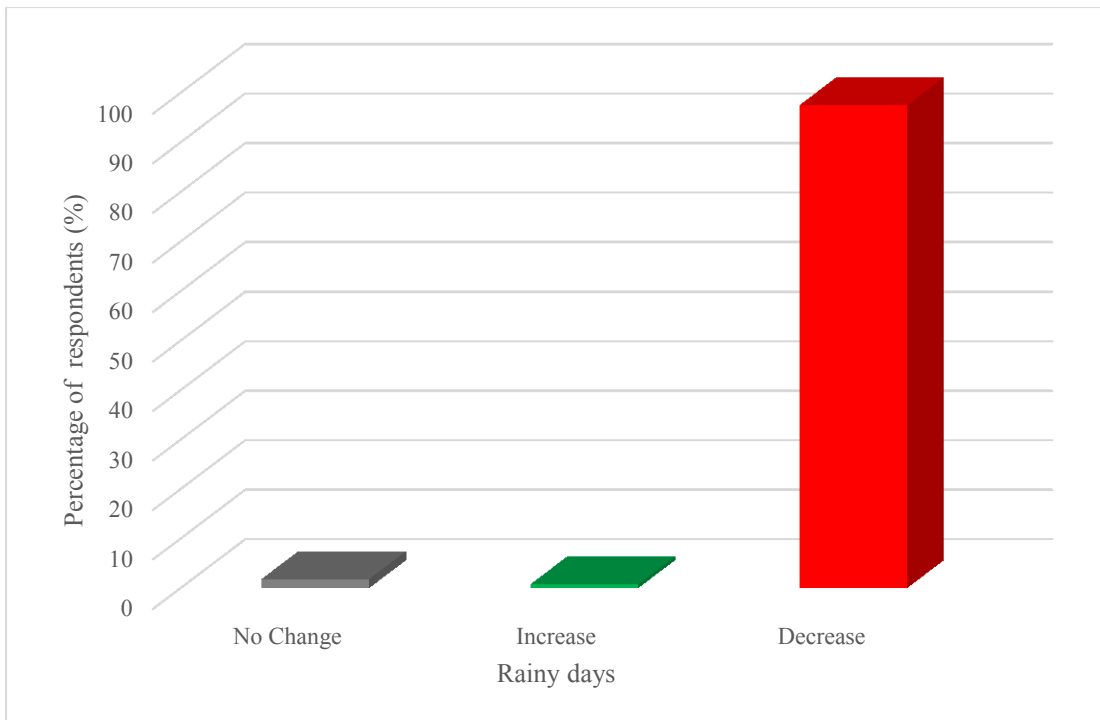
Figure 3.23: Farmers' Perception on Rainy days Variation
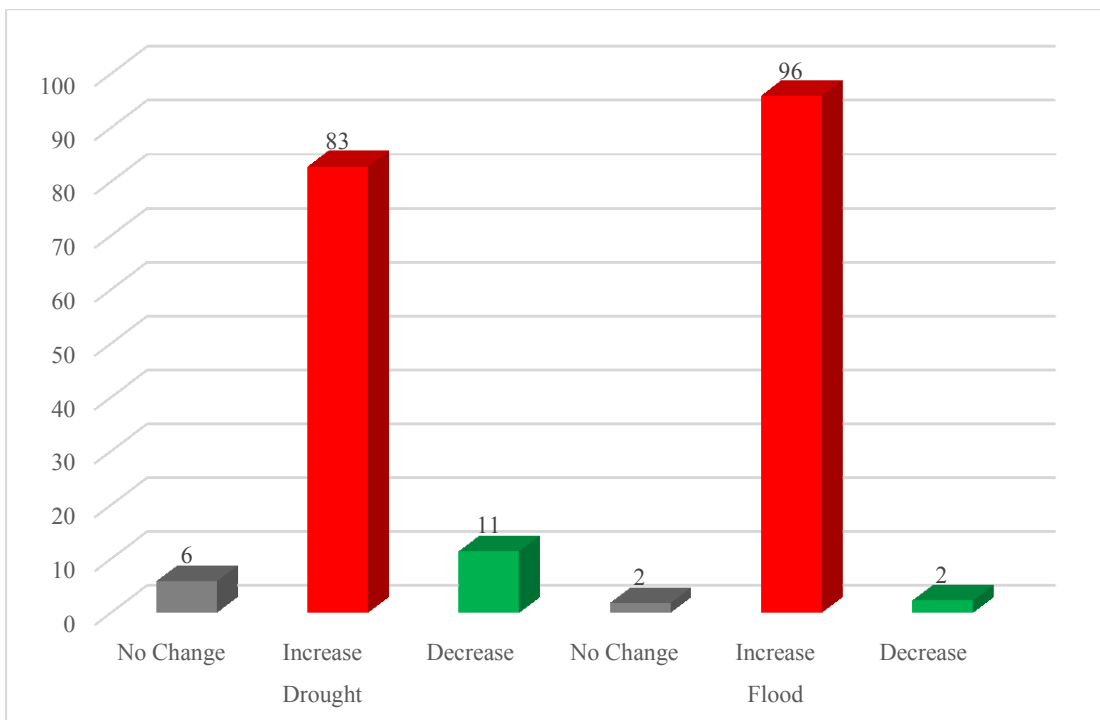
Figure 3.24: Farmers' Perception on Drought and Flood Variation

3.2.3.9 Farmer's Adaptation strategies of climate variability changes

In response to the effects of climate change on their subsistence sources, farmers in southern Mali have devised adaption measures. The figure 3.25 below depicts the

adaptation techniques of people questioned in response to the effects of climate change on their means of sustenance. Lowlands producers have resorted to the use of newer, more adaptable varieties of culture à cycle court. In total, the majority of farmers (43%) have adopted these varieties. Respondents reported other coping strategies such as combining crops and rotating land and crops (17%), changing planting dates (10%), market gardening (5%), and migration (2%). The prevailing climatic conditions have prompted approximately 2% of lowland farmers to adopt various strategies to diversify their agricultural activities. These strategies include engaging in trade/woodcutting, livestock breeding, expanding agricultural land, and implementing soil conservation techniques. By diversifying their activities, these farmers aim to secure alternative sources of income in case of unfavourable harvest seasons. Crop diversification, which involves growing multiple crops together, is one such approaches employed to enhance financial returns and reduce reliance on a single crop for income generation. Moreover, diversifying income sources is considered crucial for local communities as it contributes to the long-term sustainability of their livelihoods and enhances their resilience in the face of climate change impacts.
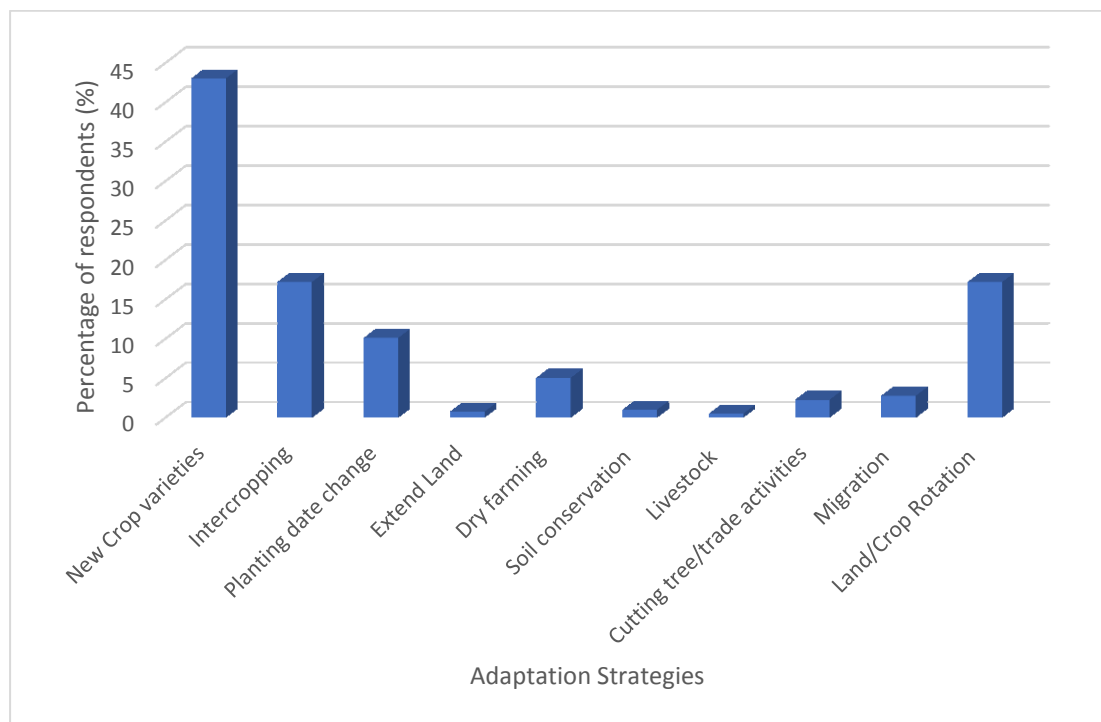
Figure 3.25: Farmer's Adaptation Strategies of climate variability and changes

3.2.4 Discussion

Variation and trend of Annual and seasonal of Rainfall and temperature

The result of the existence of significant variation and positive trend in annual and seasonal rainfall on the one hand and the significant increase with a positive trend in the south of Mali in mean annual and seasonal temperatures on the other hand, confirms previous work (Barry *et al.*, 2018; Bichet & Diedhiou, 2018a, 2018b; Cook & Vizy, 2015; Dosio, 2017; Gutiérrez *et al.*, 2021; Kennedy *et al.*, 2016; Lelieveld *et al.*, 2016; Moron *et al.*, 2016; Nicholson *et al.*, 2018; Nikiema *et al.*, 2017; Ranasinghe *et al.*, 2021; Sanogo *et al.*, 2015; Sylla *et al.*, 2016; Thomas & Nigam, 2018). These studies indicate a favourable pattern characterized by a rise in both precipitation and temperature variability within the Saharan and Sahelian nations of Africa. This trend is attributed to a combination of anthropogenic aerosols and greenhouse gases (GHGs).

Farmer 's Perception and Adaptation strategies of climate variability changes

The survey found that the majority of lowland growers in the research region were above the age of 20. Furthermore, the bulk of them had farming experience ranging from 10 to 50 years. As a result, they must be capable of providing trustworthy information on climate change and its consequences in the study region. Their educational level, however, was quite poor throughout the research region. Farmers' capacity to recognize climatic trends and responses is impacted by their educational level. Lowland farmers with elementary and secondary education are more optimistic about climate change, which is likely owing to their frequent interaction with the outside world through migration and greater access to information sources such as the media. (Kabore *et al.*, 2019; Koné *et al.*, 2022; Sanogo *et al.*, 2016; Toukal Assoumana *et al.*, 2016). Thus, the amount of education of educated farmers enhances the possibility of adaptability to temperature and precipitation seasons. Farmers that are better educated understand how to obtain, interpret, accept, and adapt to climate change knowledge and improved technology, resulting in increased output. Farmers' education levels were shown to have a substantial association with extensive understanding of climate change. (Jha & Gupta, 2021; Sanogo *et al.*, 2016; Asoumana *et al.*, 2016).

3.2.5 Conclusion

In the Sikasso District, the levels of annual and seasonal precipitation and temperature exhibit notable fluctuations. There is a slight upward trend observed in both annual and seasonal rainfall (specifically during the March-April-May and September-October-November periods). However, for the June-July-August season, a decreasing trend in rainfall is observed, although it is not statistically significant.

The average annual temperature in the study area ranges between 26.6 and 28.5 degrees Celsius. The average annual and seasonal temperatures are rising. The increase in mean annual and seasonal temperatures is statistically significant.

There are several breaks in the average for annual and seasonal precipitation in the area but there are no breaks in the temporal variation of annual and seasonal average temperatures.

Producers have a good understanding of climate variations and have devised numerous adaptation strategies; namely: New Crop varieties, Intercropping, Land/Crop Rotation.

CHAPTER 3.3: EVALUATION OF TRENDS AND VARIABILITY IN SEASONAL AND ANNUAL RAINFALL ANOMALY INDEX (RAI) IN SOUTHERN MALI

3.3.1 Introduction

Drought refers to a period characterized by below-average precipitation levels. Insufficient rainfall can lead to reduced runoff, which contributes to hydrological drought. This, in turn, results in declining river levels, decreased water storage, and drying of the soil. A lack of water may jeopardize people's chances of survival. Drought reduces agricultural output, impacts venues, and puts a strain on communities. The impacts of socioeconomic drought are being felt across the community, affecting various aspects of our environment. The vulnerability of the entire ecosystem becomes evident during a drought. In certain situations, it can take several months of increased precipitation for the landscape, waterways, and communities to fully recover.

Mali is situated within the Sahel region of Africa, where the dry seasons are longer (six to eight months of the year, from October-November to May-June). The rainy seasons are shorter (July-August-September) and provide little water. Droughts have a higher probability of occurring throughout any season. Over the past decade, Mali has experienced numerous floods and droughts. Mali is a landlocked country; the droughts of 192-1973, 1982-1983 and the floods of 2013, 2015, 2017, 2and 022 have had significant social, economic, cultural and human consequences. More than 80% of the population in Mali relies on agriculture as their primary source of income and accounts for 42% of the GDP (Bank Word, 2021). Despite significant progress, agricultural activity is rain-fed and remains dependent on climatic conditions. Therefore, drought periods pose a significant threat to both agricultural production and the overall economy of Mali.

The Rainfall Anomaly Index (RAI) has been used in numerous research studies to assess meteorological drought. (Chahal *et al*., 2021) used RAI to study the spatiotemporal drought over the *Sahibi* River basin in Rajasthan, India, at two-time scales: annual and monsoon seasons. The drought characteristics were examined using race theory analysis (magnitude, duration and intensity). (Ndlovu & Demlie, 2020) assessed meteorological drought in KwaZulu-Natal province, South Africa,

using the percentage normal rainfall index (PNPI) and the RAI. The authors conclude that the RAI is more robust for drought assessment than the PNPI. (Goswami, 2018) used RAI to investigate the intensity and frequency of wet and dry years in selected districts in West Bengal's sub-Himalayan region. Between 1901 and 2010, the study area experienced a higher frequency of dry years compared to wet years across all districts. However, a different approach using the standardized precipitation evapotranspiration index (SPEI) was adopted in a separate study to monitor and assess drought variability and climate parameters in the Koutiala and San districts from 1989 to 2019 (Doukoro *et al.*, 2022).

Drought indices are employed by researchers to evaluate the impacts of drought in a specific area, enabling the efficient allocation of water resources among different sectors of water usage. (Khalil, 2022). The main objective of this study was to examine the patterns and fluctuations of the seasonal and annual rainfall anomaly index (RAI) in southern Mali from 1960 to 2020, while also identifying the most severe and prolonged droughts.

3.3.2 Approach and Methods
3.3.2.1 Data Collection
For this research, monthly rainfall data from 1960 to 2020 were utilized. The National Meteorological Agency of Mali supplied the rainfall data from the Sikasso station, which was employed in the computation of the RAI. The temporal distribution and trend are presented in (Figure 3.26).
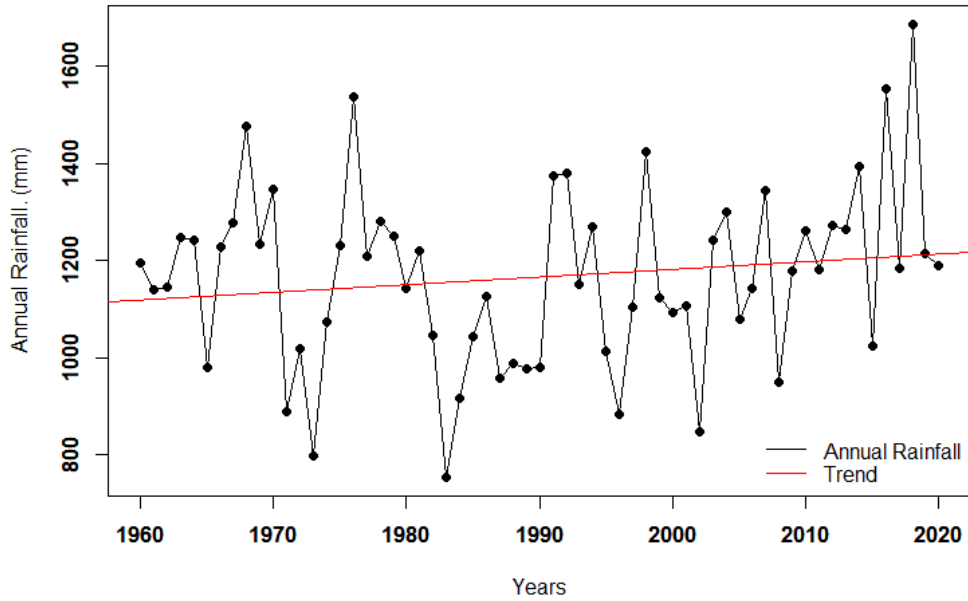
Figure 3.26: Annual Rainfall variation and trend

3.2.2.2 Methods

Rainfall Anomaly Index

The precipitation data was utilized to compute the Annual Rainfall Anomaly Index (RAI) in order to assess the occurrence and severity of dry and rainy years in the study area. The RAI, initially developed by van Rooy (1965), incorporates a ranking method to assign magnitudes to positive and negative anomalies in precipitation. The RAI takes into account two types of anomalies: positive anomalies and negative anomalies. The precipitation data is first arranged in descending order, and the average of the top ten values is used as a threshold for positive anomalies, while the average of the bottom ten values is used as a threshold for negative anomalies. The thresholds are calculated by the following Equations:

The mean of the ten most extreme positive anomalies is assigned a threshold value of +3, while the mean of the ten most extreme negative anomalies is assigned a threshold value of -3. These arbitrary thresholds represent the extreme ends of the scale. The relative rainfall anomaly index is then categorized into nine abnormality classes, which cover a range of conditions from extremely wet to extremely dry. Each class is associated with a specific numerical value on the scale.

$$RAI = 3\left[\frac{N-\bar{N}}{\bar{M}-\bar{N}}\right] \text{ For positive anomalies}$$

$$RAI = -3 \left[\frac{N-\bar{N}}{\bar{X}-\bar{N}} \right] \textit{For negative anomalies}$$

Where: N = current seasonal/yearly rainfall, in order words, of the seasonal/year when RAI will be generated (mm); $\bar{N}$ = seasonal/yearly average rainfall of the historical series (mm); $\bar{M}$ = average of the ten highest seasonal/yearly precipitations of the historical series (mm); $\bar{X}$ = average of the ten lowest monthly/ yearly precipitations of the historical series (mm); and positive anomalies have their values above average and negative anomalies have their values below average. In addition, the seasonal RAI was calculated to analyze the distribution of rainfall in the different seasons.

Mann–Kendall (MK) trend test

The Mann-Kendall test statistic, developed by Mann, (1945) and (endall, (1975), is a non-parametric test used to determine if a dataset exhibits a significant increasing or decreasing trend over time. It assesses the statistical significance of the trend in either direction without making assumptions about the data's underlying distribution. (Praveen, et al., 2020; Merabtene et al., 2016). It is calculated as;

$$S = \sum_{k=1}^{n-1} \sum_{j=k+1}^{n} Sgn(x_j - x_k)$$

where

$$Sgn(x_j - x_k) = \begin{bmatrix} 1 & \text{if } (x_j - x_k) > 0 \\ 0 & \text{if } (x_j - x_k) = 0 \\ -1 & \text{if } (x_j - x_k) < 0 \end{bmatrix}$$

x_j and x_k are sequential values of the time series data, and n is the length of the dataset. A positive value of S indicates an increasing trend, and a negative value indicates a decreasing trend. If the dataset length is more than 10, then the test is done using the normal distribution with expectation (E) and variance (var);

$$var(S) = \frac{1}{18} \left[n(n-1)(2n+5) - \sum_{p=1}^{q} t_p(t_p-1)(2t_p+5) \right]$$

where q is the number of tied groups, and t_p denotes the number of ties of extent p. A tied group is a set of sample data having the same value. The standard test statistic (Z_{MK}) is given by;

$$Z_{MK} = \begin{bmatrix} \dfrac{S-1}{\sqrt{\text{var(S)}}} & \text{if } S > 0 \\ \dfrac{S+1}{\sqrt{\text{var(S)}}} & \text{if } S < 0 \\ 0 & \text{if } S = 0 \end{bmatrix}$$

The value of Z_{MK} is the Mann-Kendall test statistic that follows a normal distribution with mean 0 and variance 1. Testing trend is done at the specific α significance level. When $|Z_{MK}| > Z_{1-\alpha/2}$, the null hypothesis is rejected and a significant trend exists in the time series. $Z_{1-\alpha/2}$ is obtained from the standard normal distribution table. In this analysis, the MK test is applied to detect if a trend in the time series data is statistically significant at significance level, $\alpha=0.05$ (or 95% confidence intervals).

Sen's Slope Estimator

Several hydrologic variables exhibit a notable right skewness, which can be attributed in part to natural phenomena, and as a result, they do not conform to a normal distribution. Climate data demonstrates fluctuations and deviations from the characteristics of a normal distribution (Nasher, 2021). Consequently, the study employed Sen's slope estimator, which is a nonparametric method utilized to construct the linear models. Sen's slope estimator is a nonparametric technique frequently employed to determine the actual slope of an existing linear trend. When a time series exhibits a linear trend, the true slope, representing the rate of change per unit of time, can be estimated using the straightforward nonparametric procedure developed by Sen in 1986. This implies that the linear model (t) can be expressed as follows:

$$f(t) = Qt + B \tag{3}$$

where Q is the slope, B is a constant and t is time.

To derive an estimate of the slope Q, the slopes of all data pairs are calculated using the equation:

$$Qt = \frac{x_j - x_k}{j - k} \tag{4}$$

where i = 1,2, 3,…. N, j > k

If there are n values x_j in the time series there will be as many as n(n-1)/2 slope estimates Q_i . To obtain estimates of B in the equation the n value of differences $x_i - Qt_i$ are calculated. The median of these values gives an estimate of B. The

calculations for the constant B of the 99% and 95% confidence intervals for the lines were performed using a similar approach. The data was processed in R using the Slope Sen's method.

Rainfall Anomaly index intensity classification

All the RAI positives values indicate the wet periods while the negatives values stand for dry periods. The RAI intensity table was utilized to assess the level of wetness or dryness across the study area in southern Mali.

Table 3.5: Classification of Rainfall Anomaly Index Intensity

	RAI Rang	Classification
	Above 4	Extremely Wet
	2 to 4	Very Wet
Rainfall Anomaly Index	0 to 2	Wet
	-2 to 0	Dry
	-4 to -2	Very Dry
	Below -4	Extremely Dry

Source: Freitas (2005) adapted by Araújo *et al*. (2009)

3.2.2.3 Results and interpretation

3.2.2.3.1 Annual variability of Rainfall Anomaly index

The global analysis of annual rainfall anomaly index between 1960 and 2020 shows that the period was dry with an average RAI of -0.037. Over the period of 61 years there are 29 years with a negative RAI and 32 years with a positive RAI. The years 1973 and 1983 were the extremely dry years with an RAI of -4.54 and -4.08 respectively (Figure 3.27).
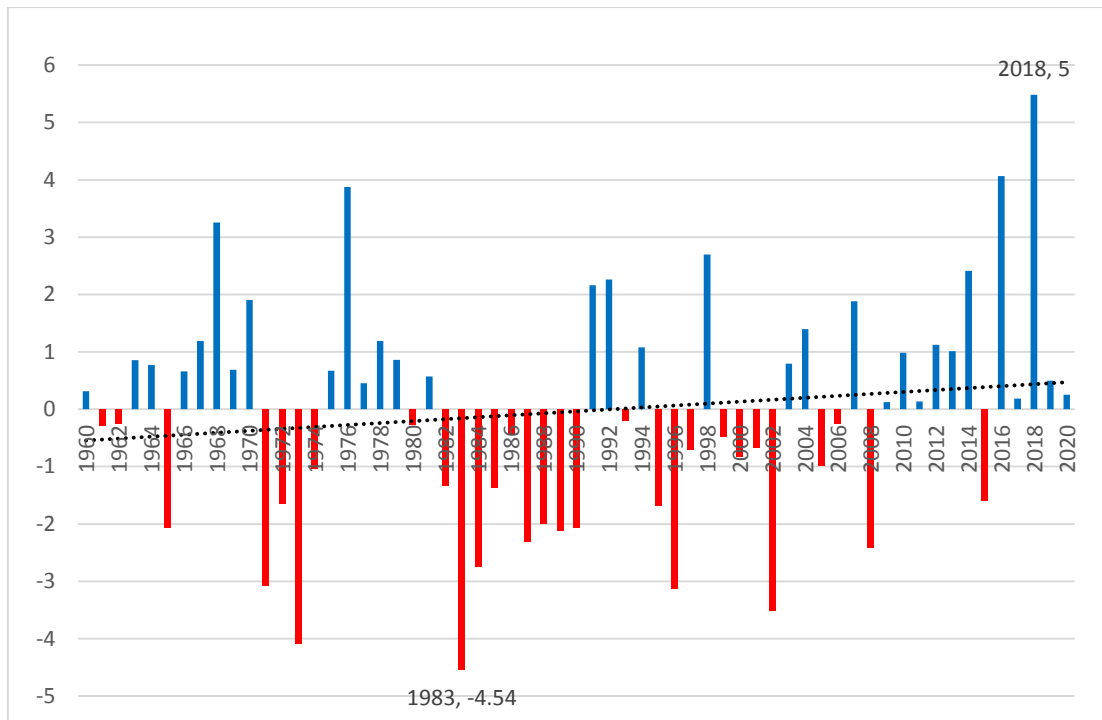
Figure 3.27: Annual Rainfall Anomaly index

The Table 3.6 below represents the annual analysis of RAI by *30-year* climatic period. Interpretation of the table result reveals that during the first climatic period (1960-1990), there were 17 years with a negative RAI value and 14 years with a positive RAI value. The year 1983 was the driest among the years with a negative RAI, classified in the extremely dry category; while 1976 was an extremely wet year with RAI of 3.87, it represents the highest value of the years with a positive RAI. The average of the period is -0.46, which is a dry climatic period according to the classification scale of Freitas (2005) adapted by Araújo et al. (2009). For the second climatic period (1991-2020), it is noted that there were 13 years with a negative value of which 2002 is the year with the highest value (-3.52) and is considered very dry according to the classification table of RAI. The year 2018, classified as extremely wet with an RAI of 5.48 has the largest value of 18 years with a positive RAI of the climatic period 1991-2020. This climatic period is a wet period with an average of 0.32 as RAI value.

Table 3.6: Annual Rainfall index analysis by climatic period (30 years)

30 years	Annual RAI								Mean period	Class period
	Negative				Positive					
	Nber.	Max	Year	Class	Nber.	Max	Year	Class		
1960-1990	17	-4.54	1983	Extremely Dry	14	3.87	1976	Very Humid	-0.46	Dry
1991-2020	13	-3.52	2002	Very Dry	18	5.48	2018	Extremely Humid	0.32	Humid

The following Table 3.7 presents the detailed result of the RAI analysis by decade between 1960 and 2020. The result shows us 3 wet decades (1960-1970, 1991-2000 and 2011-2020) against 3 dry decades (1971-1980, 1981-1990 and 2001-20100). The average RAI of the decades varies between -0.3 and 1.35. The number of positive and negative years varies from decade to decade.

Table 3.7: Analysis of Annual Rainfall Anomaly index by decade

Decade	Annual RAI			
	Number of negative years	Number of Positive years	Mean	Class
1960-1970	3	7	0.63	Humid
1971-1980	5	5	-0.3	Dry
1981-1990	9	1	-1.83	Dry
1991-2000	6	4	0.11	Humid
2001-2010	5	5	-0.26	Dry
2011-2020	1	9	1.35	Humid

3.2.2.3.2 Seasonal variation of Rainfall Anomaly Index

The Figure 3.28 represents the seasonal variation of the March-April-May precipitation anomaly index from 1960 to 2020. The analysis of the result shows 33 years with a negative RAI and 28 with a positive RAI. The year 2015 represents the year with the largest value of negative RAI, i.e. -1.55. The largest value of positive RAI is 5.72 in 1968 and the average for the period (1960-2020) is 0.32.
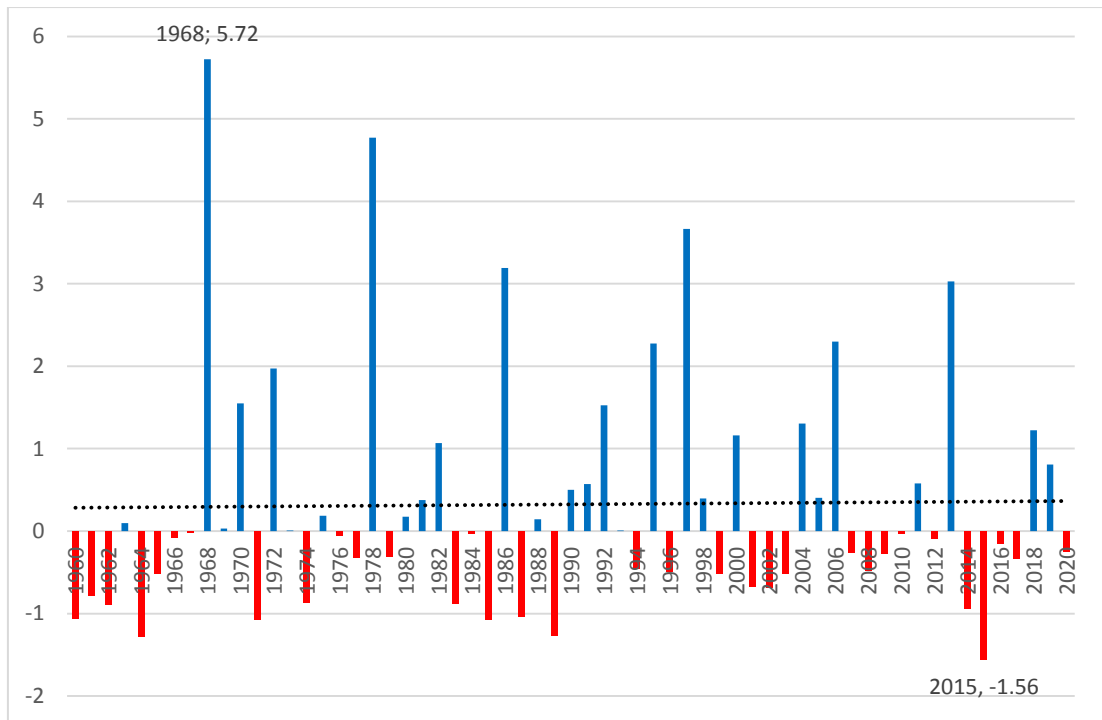
Figure 3.28: Seasonal March-April-May Rainfall Anomaly index

Interpretation of the result of the March-April-May seasonal analysis over the two 30 years (1960-19900 and 1991-2020) in the Table 3.8 below shows that both periods were wet with a successive average of 0.26 and 0.38. On the one hand, it is observed that the period 1960-1990 recorded 17 years with a negative RAI value against 16 for the period 1991-2020. The year 1964 with an RAI of -1.27 has the highest value of years with a negative RAI in the period 1960-1990. For the period 1991-2020, 2015 with -1.55 has the highest value of years with RAI of the period 1991-2020. On the other hand, the table shows that both climate periods (1960-1990 and 1991-2020) have all 14 years with a positive RAI value. 1968 was an extremely humid year with 5.72 RAI while 1997 was a very humid year with 3.66 for the 1960-1990 and 1991-2020 climatic periods respectively.

Table 3.8: Seasonal March-April-May Rainfall Anomaly index by period
climatic (30 years)

30 years	Seasonal March-April-May Rainfall Anomaly Index								Mean period	Class period
	Negative				Positive					
	Nber	Max	Year	Class	Nber	Max	Year	Class		
1960-1990	17	-1.27	1964	Dry	14	5.72	1968	Extremely Humid	0.26	Humid
1991-2020	16	-1.55	2015	Dry	14	3.66	1997	Very Humid	0.38	Humid

The analysis of RAI by decade between 1960 and 2020 in the table below tells us that all decades (1960-1970, 1981-1990, 1991-2000, 2001-2010 and 2011-2020) were wet, with average RAI values ranging from 0.1 to 0.81. The number of positive and negative years varies from decade to decade.

Table 3.9: Analysis of Seasonal March-April-May Rainfall Anomaly index by
decade

Decade	Seasonal March-April-May RAI			
	Number of negative years	Number of positive years	Mean	Class
1960-1970	7	3	0.25	Humid
1971-1980	5	5	0.44	Humid
1981-1990	5	5	0.1	Humid
1991-2000	3	7	0.81	Humid
2001-2010	7	3	1.1	Humid
2011-2020	6	4	0.23	Humid

The following Figure 3.29 represents the seasonal variation of the June-July-August precipitation anomaly index from 1960 to 2020. There are 29 years with a negative precipitation anomaly index and 32 years with a positive precipitation anomaly index. The average for the period is -0.007 RAI, with -4.48 RAI, 1983 was the driest year and 4.97 RAI, 2016 was the wettest year of the period.
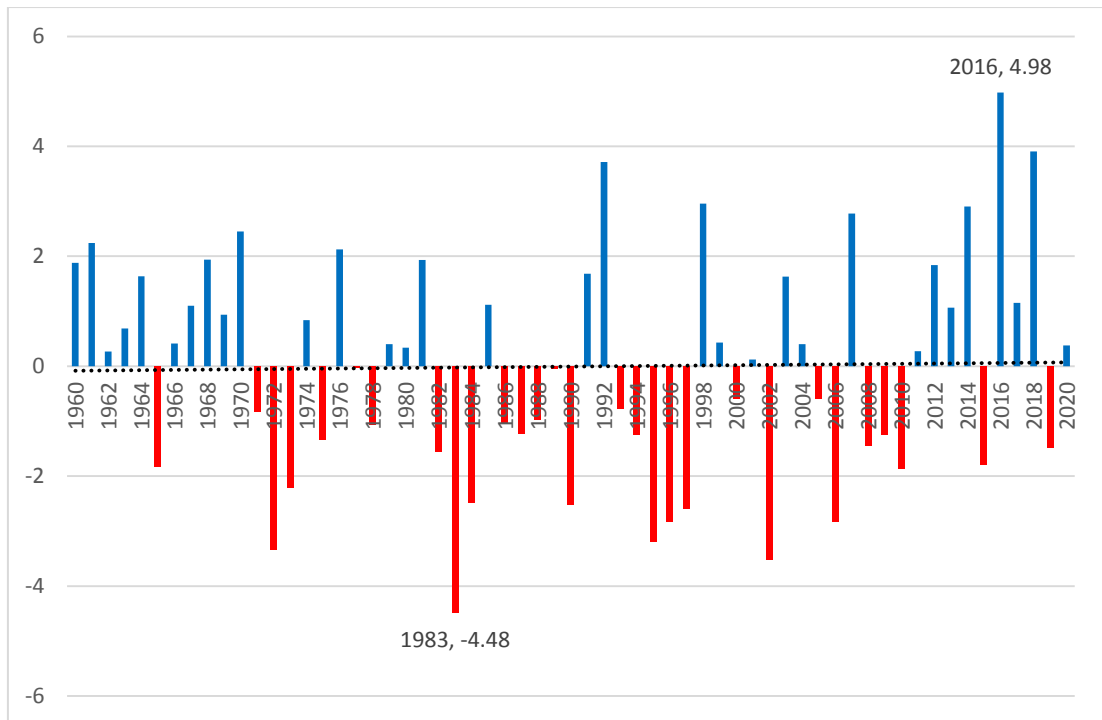
Figure 3.29: Seasonal June-July-August Rainfall Anomaly index

The Table 3.10 illustrates the situation of the June-July-August seasonal precipitation anomaly index between 1960 and 2020 by 30-year climate period. The period 1960-1990 was a dry period with -0.15 of average precipitation anomaly index; while, the period 1991-2020 was wet with 0.15 of average precipitation anomaly index. During the period 1991-2020, there were 14 years with negative RAI value and 16 years with positive RAI, while there were 15 years with negative RAI and 16 years with positive RAI for the period 1960-1990. It is also noted that 1983 (-4.48 RAI) was the driest year of the 1960-1990 period and 2002 (-3.51 RAI), considered very dry, was the driest year of the second climatic period. For the wet years of each climatic period, we observe 1970 with 2.45 RAI (Very humid) and 2016 with 4.97 RAI (Extremely Humid) for the period 1960-1990 and 1991-2020 respectively.

Table 3.10: Seasonal June-July-August Rainfall Anomaly index by period climatic (30 years)

30years	Seasonal June-July-August RAI							
	Negative			Positive			Mean period	Class period
	Nber.	Max	Year	Class	Nber.	Max	Year	Class	
1960-1990	15	-4,48	1983	Extremely Dry	16	2,45	1970	Very Humid	-0,15	Dry
1991-2020	14	-3,51	2002	Very Dry	16	4,97	2016	Extremely Humid	0,15	Humid

Table 3.11 shows the status of the June-July-August seasonal precipitation anomaly index (RAI) by decade from 1960 to 2020 in southern Mali. The situation of seasonal RAI shows, in general, a strong variability in the number of years with a negative and positive RAI depending on the decade. The averages range from -0.64 to 1.32. Finally, the table shows that the 1960-1970 and 2011-2020 decades were wet and the others were dry.

Table 3.11: Analysis of Seasonal June-July-August Rainfall Anomaly index by decade

Decade	Seasonal June-July-August RAI			
	Number of negative years	Number of positive years	Mean	Class
1960-1970	1	9	1,06	Humid
1971-1980	6	4	-0,5	Dry
1981-1990	8	2	-1,13	Dry
1991-2000	6	4	-0,24	Dry
2001-2010	6	4	-0,64	Dry
2011-2020	2	8	1,32	Humid

The Figure 3.30 illustrates the result of the analysis of the September-October-November seasonal precipitation anomaly index between 1960 and 2020 for the Sikasso district of southern Mali. During the period there is a significant number of years with a negative RAI (33 years) compared to 28 years with a positive RAI. 1973 was the driest year of the period with a precipitation anomaly index of -5.90 (extremely dry) while 1976 was the extremely humid year of the period with a precipitation anomaly index of 4.69.
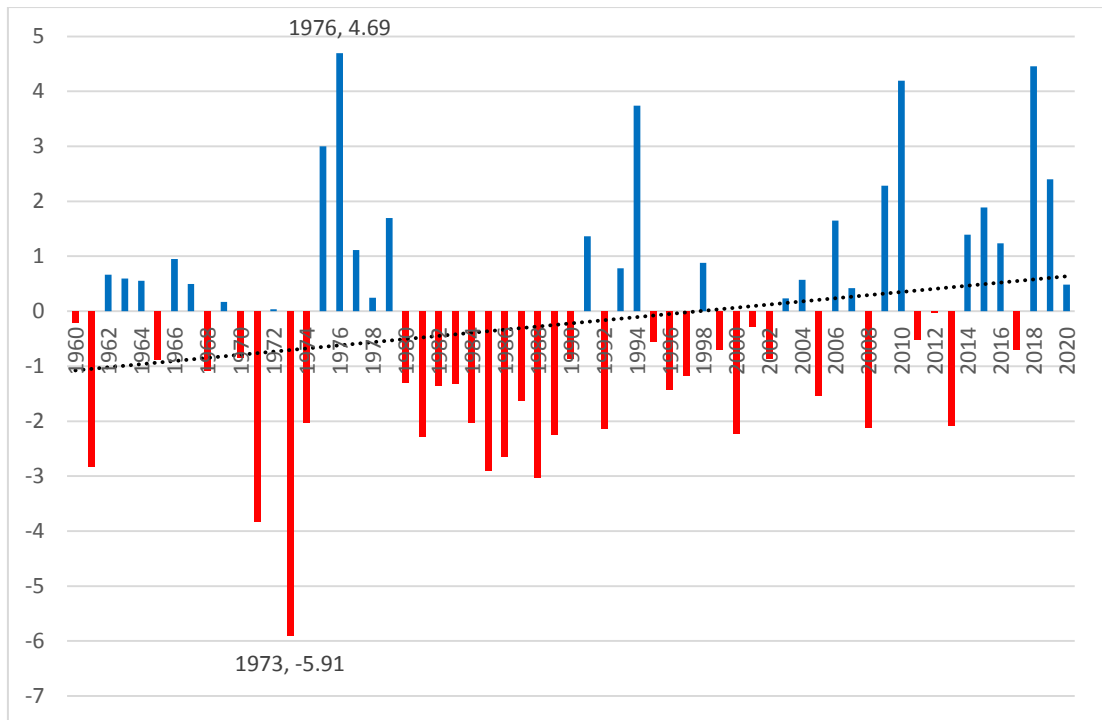
Figure 3.30: Seasonal September-October-November Rainfall Anomaly Index

The Table 3.12 illustrates the result of the analysis of the index of seasonal precipitation anomaly September-October-November of the study area between 1960 and 2020 by two climatic periods of 30 years. The interpretation of the result of the first climatic period (1960-1990), allows us to highlight that it was dry with an index of the average precipitation anomaly of -0.80, unlike the second period (1991-2020), with an index of the average precipitation anomaly of 0.38 is wet. The period 1991-2020 has more years with a positive RAI (16) than the period 1960-1990 (12). Both had 1976 with an RAI of 4.69 and 2018 with an RAI of 4.45 as the wettest year for the period 1960-1990 and 1991-2020. 1973 considered as an extremely dry year with a precipitation anomaly index of -5.90, was the driest year of the 1960-1990 climatic period; while 2000 classed as very dry with a precipitation anomaly index of -2.22 was the driest of the 1991-2000 period. The climatic period 1991-2020 recorded fewer years with a negative precipitation anomaly index (14) than the period 1960-1990 with 19 years.

Table 3.12: Seasonal September-October-November Rainfall Anomaly index by period climatic (30 years)

30years	Seasonal September-October-November RAI							
	Negative			Positive			Mean period	Class period
	Nber.	Max	Year	Class	Nber.	Max	Year	Class		
1960-1990	19	-5,90	1973	Extremely Dry	12	4,69	1976	Extremely Humid	-0,80	Dry
1991-2020	14	-2,22	2000	Very Dry	16	4,45	2018	Extremely Humid	0,38	Humid

The Table 3.13 below shows the situation of seasonal precipitation anomaly index September-October-November by decade from 1960 to 2020 of the study area. The analysis of the result presented in the table, shows us that the decades 1960-1970, 1971-18980 and 1991-2000 were dry with successively an average of the precipitation anomaly index of -0.21, -0.22 and -0.14. Decades 2001-2010 and 2011-2020 were wet with respectively 0.45 and 0.85 of the average precipitation anomaly indices, contrary to the decade 1981-1990 which was very dry with an average RAI of -2.02. There is a total domination of negative precipitation anomaly index during the 1981-1990 decade, while for the other decades there is a fluctuation between negative and positive precipitation anomaly index from one decade to another.

Table 3.13: Analysis of Seasonal September-October-November Rainfall Anomaly index by decade

Decade	Seasonal September-October-November RAI			
	Number of negative years	Number of positive years	Mean	Class
1960-1970	5	6	-0,21	Dry
1971-1980	4	6	-0,22	Dry
1981-1990	10	0	-2,02	Very Dry
1991-2000	6	4	-0,14	Dry
2001-2010	4	6	0,45	Humid
2011-2020	4	6	0,85	Humid

The Figure 3.31 illustrates the result of the analysis of the December-January-February seasonal precipitation anomaly index between 1960 and 2020 for the Sikasso district of southern Mali. During the period there is a significant number of years with a negative RAI (39 years) compared to 22 years with a positive RAI. 2014 was the extremely wet year of the period with a precipitation anomaly index of 5.38.
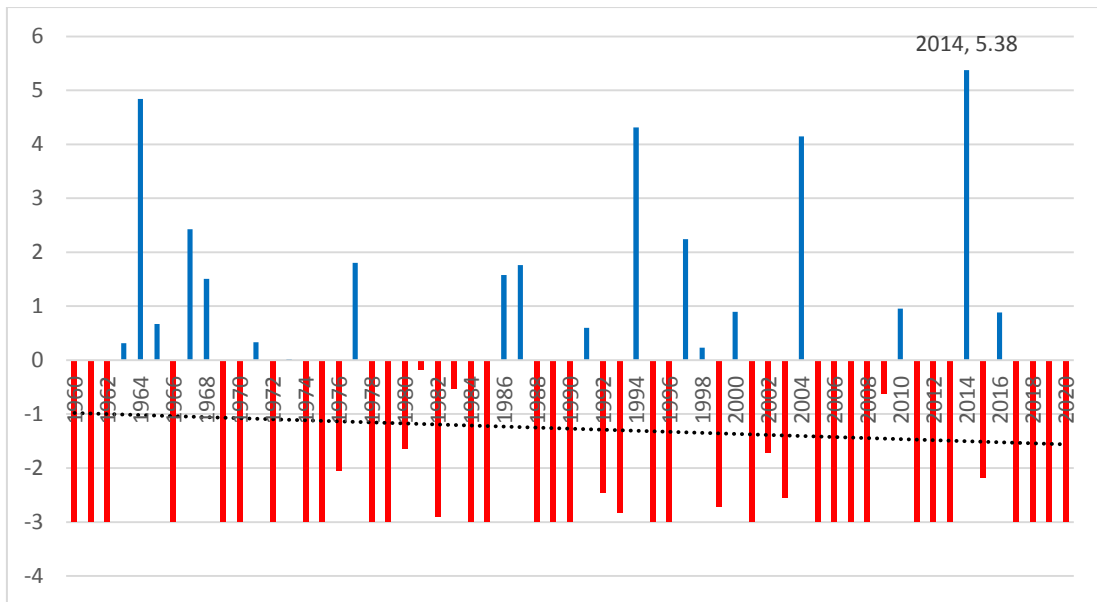
Figure 3.31: Seasonal December-January-February Rainfall Anomaly Index

The Table 3.14 represents the results of the analysis of the December-January-February seasonal precipitation anomaly index over a period of 61 years (1960 and 2020) of the Sikasso district in southern Mali by climatic period of 30 years. The observation of the results indicates that both 1960-1990 and 1991-2020 were dry with successively a period average of -1.29 and -1.24 RAI. The 1960-1990 period had 21 years with a negative precipitation anomaly index and 10 years with a positive RAI while the 1991-2020 period had 20 years with a negative RAI and 10 with a positive RAI. Both periods had -3 highest negative RAI value.

Table 3.14: Seasonal December-January-February Rainfall Anomaly index by period climatic (30 years)

30 years	Seasonal December-January-February RAI									
	Negative				Positive				Mean period	Class period
	Number	Max	Year	Class	Number	Max	Year	Class		
1960-1990	21	-3	1960,1961, 1962, 1966, 1969, 1970, 1972, 1974, 1975, 1978, 1979,1984, 1985, 1988, 1989,1990	Very Dry	10	4,83	1964	Extremely Humid	-1,29	Dry
1991-2020	20	-3	1995,1996, 2001, 2005, 2006, 2007, 2008, 2011, 2012, 2013, 2017,2018, 2019, 2020	Very Dry	10	5,37	2014	Extremely Humid	-1,24	Dry

82

The Table 3.15 shows the December-January-February seasonal precipitation anomaly index between 1960 and 2020 by decade. It is noted that all decades are dry with average values ranging from -1.69 to -1.47 and that the number of years with negative and positive precipitation anomaly index is variable from one decade to another.

Table 3.15: Analysis of Seasonal December-January-February Rainfall Anomaly index by decade

Decade	Seasonal December-January-February RAI			
	Number of negative years	Number of positive years	Mean	Class
1960-1970	6	5	-0.74	Dry
1971-1980	7	3	-1.65	Dry
1981-1990	8	2	-1.52	Dry
1991-2000	5	5	-0.57	Dry
2001-2010	8	2	-1.47	Dry
2011-2020	8	2	-1.69	Dry

3.2.2.3.3 Annual and seasonal Trends of Rainfall Anomaly Index

An analysis was conducted to assess the trends in the Rainfall Anomaly Index (RAI) for both annual and seasonal data from 1960 to 2020. The trend direction (whether increasing or decreasing) was determined using the well-known Mann-Kendall test, while the magnitudes of the trends were estimated using Sen's slope method. These statistical tests were carried out at a significance level of 5%. The results obtained from these tests were then compared with those obtained using the linear trend method. The findings of the trend analysis for RAI based on observed data are presented in Table 3.16. It was observed that the annual RAI and the seasonal RAI for March-April-May and September-October-November exhibited increasing trends. On the other hand, the seasonal RAI for June-July-August and December-January-February showed decreasing trends. Specifically, the linear trend approach revealed a decreasing slope of -0.0097 mm/year for the December-January-February RAI, while the annual RAI and the seasonal RAI for March-April-May, June-July-August, and September-October-November indicated increasing trends.

Table 3.16: Trend of Rainfall Anomaly Index

Time Scale	Rainfall Anomaly Index				
	Mann Kendall Test		Sen's Slope	Linear regression	
	Trend	P-value		Trend	R-square
Annual	Increasing	0,322	0,013	Increasing	0,0228
MAM	Increasing	0,380	0,008	Increasing	0,0003
JJA	Decreasing	0,760	-0,004	Increasing	0,0005
SON	Increasing	0,078	0,026	Increasing	0,0618
DJF	Decreasing	0,533	0,000	Decreasing	0,0052

3.2.2.3.4 Rainfall Anomalies Index Classification

The analysis of the classification of precipitation anomaly indices was done for the years 1960-2020. The classification of whether a year was categorized as dry or wet was done using the classification table developed by Freitas (2005) and adapted by Araújo et al. (2009). To determine the classification for each year, the results were analysed in Microsoft Excel, which provided information on the years classified as dry, very dry, extremely dry, wet, very wet, and extremely wet. The outcomes of the RAI classification analysis based on the observed data can be found in the presented table. For the annual RAI, the years 1973 and 1983 were extremely dry with -4.09 and -4.54 respectively while 2016 and 2018 were extremely wet with successively 0.06 and 5.48 RAI.

Table 3.17: Annual Rainfall Anomaly Index

Years	Annual Rainfall Anomaly Index					
	Dry	Very Dry	Extremely Dry	Humid	Very Humid	Extremely Humid
1960				0.31		
1961	-0.28					
1962	-0.25					
1963				0.85		
1964				0.77		
1965		-2.06				
1966				0.66		
1967				1.19		
1968					3.26	
1969				0.69		
1970				1.9		
1971		-3.07				
1972	-1.65					
1973			-4.09			
1974	-1.04					
1975				0.67		
1976					3.87	
1977				0.45		

Year						
1978				1.19		
1979				0.86		
1980	-0.27					
1981				0.57		
1982	-1.33					
1983			-4.54			
1984		-2.75				
1985	-1.37					
1986	-0.45					
1987		-2.3				
1988	-2					
1989		-2.11				
1990		-2.06				
1991					2.16	
1992					2.26	
1993	-0.2					
1994				1.08		
1995	-1.68					
1996		-3.13				
1997	-0.7					
1998					2.7	
1999	-0.48					
2000	-0.82					
2001	-0.67					
2002		-3.52				
2003				0.79		
2004				1.4		
2005	-0.97					
2006	-0.26					
2007				1.88		
2008		-2.42				
2009				0.12		
2010				0.98		
2011				0.14		
2012				1.13		
2013				1.01		
2014					2.41	
2015	-1.59					
2016						4.06
2017				0.19		
2018						5.48
2019				0.5		
2020				0.25		

The Table 3.18 below shows the seasonal analysis of March-April-May precipitation anomaly index between 1960 and 2020. 2015 and 1964 were dry with while 1978 and 1968 are considered extremely dry, we record successively 4.76 and 5.72, the value of RAI during the study period.

Table 3.18: Seasonal March-April-May Rainfall Anomaly Index

Years	Seasonal March-April-May RAI			
	Dry	Humid	Very Humid	Extremely Humid
1960	-1.07			
1961	-0.78			
1962	-0.89			
1963		0.1		
1964	-1.28			
1965	-0.51			
1966	-0.08			
1967	-0.02			
1968				5.72
1969		0.03		
1970		1.55		
1971	-1.07			
1972		1.97		
1973		0.01		
1974	-0.87			
1975		0.19		
1976	-0.06			
1977	-0.32			
1978				4.77
1979	-0.31			
1980		0.18		
1981		0.38		
1982		1.07		
1983	-0.88			
1984	-0.03			
1985	-1.07			
1986			3.19	
1987	-1.04			
1988		0.14		
1989	-1.26			
1990		0.5		
1991		0.57		
1992		1.52		
1993		0.01		
1994	-0.46			
1995			2.28	
1996	-0.5			
1997			3.66	
1998		0.4		
1999	-0.52			

Year						
2000				1.16		
2001	-0.67					
2002	-0.69					
2003	-0.51					
2004				1.3		
2005				0.41		
2006					2.3	
2007	-0.26					
2008	-0.48					
2009	-0.27					
2010	-0.03					
2011				0.58		
2012	-0.09					
2013					3.03	
2014	-0.93					
2015	-1.56					
2016	-0.15					
2017	-0.33					
2018				1.22		
2019				0.81		
2020	-0.25					

The result of the June-July-August seasonal analysis from 1960-2020 is presented in the table below (Table 3.19). According to the classification table of the precipitation anomaly index, the year 1983 is identified as an extremely dry year with a value of -4.48, while the year 2002 is classified as a very dry year with a value of -3.51. According to the same classification 2016 is considered as Extremely wet with 4.97 RAI while the year 2018 with 3.90 has been reported as very dry.

Table 3.19: Seasonal June-July-August Rainfall Anomaly Index

Years	Seasonal June-July-August Rainfall Anomaly Index					
	Dry	Very Dry	Extremely Dry	Humid	Very Humid	Extremely Humid
1960				1.88		
1961					2.24	
1962				0.27		
1963				0.69		
1964				1.63		
1965	-1.83					
1966				0.42		
1967				1.1		
1968				1.94		
1969				0.94		
1970					2.45	
1971	-0.82					
1972		-3.33				
1973		-2.21				
1974				0.84		

Year					
1975	-1.34				
1976				2.13	
1977	-0.02				
1978	-1.06				
1979			0.4		
1980			0.34		
1981			1.93		
1982	-1.56				
1983		-4.48			
1984		-2.49			
1985			1.12		
1986	-1.05				
1987	-1.23				
1988	-0.98				
1989	-0.05				
1990		-2.53			
1991			1.68		
1992				3.72	
1993	-0.78				
1994	-1.25				
1995		-3.19			
1996		-2.83			
1997		-2.6			
1998				2.96	
1999			0.43		
2000	-0.59				
2001			0.12		
2002		-3.51			
2003			1.63		
2004			0.4		
2005	-0.58				
2006		-2.83			
2007				2.78	
2008	-1.45				
2009	-1.24				
2010	-1.87				
2011			0.27		
2012			1.84		
2013			1.06		
2014				2.9	
2015	-1.8				
2016					4.98
2017			1.15		
2018				3.91	
2019	-1.48				
2020			0.38		

The following Table 3.20 contains the result of the seasonal analysis September-October-November of the precipitation anomaly index between 1960 and 2020 of southern Mali. The interpretation indicates that 1973 (-5.90) was an extremely dry year, 1971 (-3.81) very dry on one side and the years 2010 (4.19), 2018 (4.45) and 1976 (4.69) are extremely wet.

Table 3.20: Seasonal September-October-November Rainfall Anomaly Index

Years	Seasonal September-October-November Rainfall Anomaly Index					
	Dry	Very Dry	Extremely Dry	Humid	Very Humid	Extremely Humid
1960	-0.2					
1961		-2.83				
1962				0.67		
1963				0.6		
1964				0.55		
1965	-0.87					
1966				0.95		
1967				0.49		
1968	-1.09					
1969				0.17		
1970	-0.84					
1971		-3.82				
1972				0.04		
1973			-5.91			
1974		-2.03				
1975					3	
1976						4.69
1977				1.11		
1978				0.25		
1979				1.69		
1980	-1.31					
1981		-2.27				
1982	-1.35					
1983	-1.33					
1984		-2.02				
1985		-2.89				
1986		-2.65				
1987	-1.63					
1988		-3.02				
1989		-2.25				
1990	-0.86					
1991				1.36		
1992		-2.13				
1993				0.78		
1994					3.74	

Years	Dry	Very Dry	Humid	Very Humid	Extremely Humid
1995	-0.55				
1996	-1.43				
1997	-1.17				
1998			0.88		
1999	-0.71				
2000		-2.22			
2001	-0.29				
2002	-0.86				
2003			0.23		
2004			0.57		
2005	-1.53				
2006			1.65		
2007			0.42		
2008		-2.13			
2009				2.28	
2010					4.2
2011	-0.52				
2012	-0.03				
2013		-2.08			
2014			1.39		
2015			1.89		
2016			1.24		
2017	-0.7				
2018					4.45
2019				2.4	
2020			0.48		

The table 3.21 below is the result of the analysis of the precipitation anomaly based on the observation data of the southern district of Mali between 1960 and 2020. It is noted that 1983 is considered dry with -0.54 and 1984 is classified as very dry with -3. It is also noted that the year 1964 was classified as extremely wet with 4.84 while 1977 is classified as very wet with 2.24.

Table 3.21: Seasonal December-January-February Rainfall Anomaly Index

Years	Seasonal December-January-February Rainfall Anomaly Index				
	Dry	Very Dry	Humid	Very Humid	Extremely Humid
1960		-3			
1961		-3			
1962		-3			
1963			0.32		
1964					4.84
1965			0.67		
1966		-3			
1967				2.43	

Year					
1968			1.51		
1969		-3			
1970		-3			
1971			0.33		
1972		-3			
1973			0.02		
1974		-3			
1975		-3			
1976		-2.04			
1977			1.8		
1978		-3			
1979		-3			
1980	-1.63				
1981	-0.17				
1982		-2.91			
1983	-0.54				
1984		-3			
1985		-3			
1986			1.58		
1987			1.76		
1988		-3			
1989		-3			
1990		-3			
1991			0.6		
1992		-2.45			
1993		-2.82			
1994					4.31
1995		-3			
1996		-3			
1997				2.24	
1998			0.23		
1999		-2.73			
2000			0.9		
2001		-3			
2002	-1.72				
2003		-2.54			
2004					4.14
2005		-3			
2006		-3			
2007		-3			
2008		-3			
2009	-0.63				
2010			0.95		
2011		-3			
2012		-3			
2013		-3			
2014					5.38
2015		-2.18			
2016			0.88		
2017		-3			
2018		-3			
2019		-3			
2020		-3			

3.2.2.3.5 Maximum intensity droughts with durations for the rainfall

The (Table 3.22) presents the maximum intensity drought events for the annual Rainfall Anomaly Index (RAI) in southern Mali from 1960 to 2020. Based on the analysis of the annual RAI, a total of 29 drought events were identified. Among these events, the most severe drought had a maximum intensity of -4.54 and lasted for 9 years, spanning from 1982 to 1990.

Table 3.22: Intensity and duration of droughts

RAI	Start	End	Duration	Intensity
	71	74	4	-4.08
Annual	82	90	9	-4.54
	95	97	3	-3.13
	2000	2002	3	-3.51

3.3.3 Discussion

In this study, we examined the potential effects of climate change on the long-term trends of the rainfall anomaly index in the Sikasso district of southern Mali using 61 years of monthly records. We assessed both long-term and short-term trends in rainfall using various statistical measures, including monotonic linear regression trend analysis, the Mann-Kendall trend test, and the Mann-Kendall seasonal trend. We also considered the serial correlation fed by Sen's slope to capture the trends and variability of the annual and seasonal precipitation anomaly index. To analyze the data comprehensively, we divided it into six aggregated periods.

It is important to note that when a clear trend was identified, the linear regression analysis and the Sen slope derived from the Mann-Kendall test were in agreement. This suggests that simple linear regression can be as effective as other tests in trend analysis, despite the prevailing preference for non-parametric tests in assessing climate data trends.

Overall, our findings indicate that the trend of the annual rainfall anomaly index in the South Mali district has been showing a return of wet periods for approximately two decades, starting in 2003. Similarly, the seasonal rainfall anomaly index for March-April-May and September-October-November also exhibited a dominance of wet periods. This finding is particularly significant as the September-October-November

period is crucial for crop maturity and quality. However, the analysis of the June-July-August seasonal precipitation anomaly index revealed a slight decrease in peak precipitation over the past two decades. This persistent change in the occurrence of precipitation peaks necessitates further analysis of potential climate change issues and risks in the region.

Analysing the average climate periods revealed that rainfall patterns in the Sikasso District are characterized by extended periods of drought interspersed with episodes of intense rainfall occurring at short intervals. Decadal analysis indicated alternating wet and dry decades, with variations in the number of years displaying negative and positive RAI.

3.3.4 Conclusion

In summary, the long-term analysis of rainfall in the Sikasso District demonstrates a trend towards the recovery of rainfall. Based on the current evidence, we recommend implementing strategies for preparing, developing, and managing water resources to adapt to a changing climate and promote sustainability. It is also essential to incorporate flood risk management into Mali's strategic plans for climate change adaptation and mitigation. Furthermore, we strongly recommend conducting more comprehensive research and analysis to investigate the impact of climate change in Mali using a broader range of temporal and spatial climate data.

CHAPTER 3.4: MODELING THE HISTORICAL AND PROSPECTIVE DYNAMICS OF LAND USE AND LAND COVER (LULC) IN THE LOTIO RIVER BASIN, IN WEST AFRICA

3.4.1 Introduction

The process of land use and land cover (LULC) dynamics refers to the changes in the Earth's land cover that occur over different temporal and spatial scales (Hassen *et al.* 2021). These changes have become a growing global concern due to their impacts on both terrestrial and aquatic ecosystems (Sibanda and Ahmed 2021). It is projected that more than 75% of the Earth's already degraded land could reach 90% by 2050 (Cherlet *et al.* 2018). Over the period from 1960 to 2019, approximately one-third of the Earth's land underwent significant changes (Winkler *et al.* 2021). The authors also highlighted a worldwide net loss of forest area totalling 0.8 million km2, while global agriculture expanded by 1.0 million km2. However, it is important to note that these trends vary across different regions.

In Africa, there has been a conversion of natural vegetation in many areas to human-made land uses (Barnieh *et al.* 2020; Bull-ock *et al.* 2021; Findell *et al.* 2017). From 2012 to 2017, there was a substantial reduction in the extent of natural vegetation areas across the continent, with a corresponding increase in impervious areas (Nowak and Greenfield 2020). This phenomenon can be attributed to the increase in population and the gradual desiccation of soils caused by climate change (PNUE 2004).

In West Africa, the conversion of extensive savannah, open forest, and woodland into agricultural fields and urban settlements has been observed from 1975 to 2013 (Barnieh *et al.*, 2020; CILSS, 2016). The data indicate a significant reduction in forest cover, with approximately one-third of the forests disappearing, while there has been a 47% increase in bare land areas over a span of 40 years (CILSS, 2016).

In Mali, the 40-year trends indicate according to (Ruelland *et al.*, 2010) in the Sahelian region, there has been a continuous expansion of croplands and areas with sparse vegetation prone to erosion, leading to a significant decline in the presence of woody covers. In the Sudano-Sahelian area, there has been a notable increase in croplands, accompanied by a moderate decrease in woody covers. In the Sudanian region, agricultural expansion, deforestation, as well as reforestation and land

rehabilitation, have been observed due to alternating periods of exploitation and natural vegetation recolonization.

The swift changes in land use and land cover (LULCC) pose a significant challenge to sustainable development as they have adverse effects on various aspects such as agriculture, the occurrence of floods and droughts, urban planning, and the availability of forests and water resources (Akinyemi 2021; Akpoti *et al.* 2016; Bessah *et al.* 2020; Dimobe *et al.* 2017; Nut *et al.* 2021). Conducting an evaluation of LULCC can offer enhanced insight into the relationships between natural vegetation and human activities. (Floreano and de Moraes 2021; Gupta and Sharma 2020).

the *Lotio* River Basin (LRB) is part of the Sudanian region where agricultural extension, deforestation is a major issue (Ruelland *et al.*, 2010). It occupies about 35% of the area of Mali, and covers 135 villages with 725 494 inhabitants.

Several studies in the Lotio River Basin (LRB) have highlighted an increase cropland areas and decrease in water and vegetation these last decades (Bengaly *et al.*, 2021; Traoré, 2020). However, only limited studies have been conducted to evaluate the changes in past and future LULC across the entire Lotio River Basin. Additionally, most of these studies have relied on the maximum likelihood classification method, which assumes a normal distribution of data and uses pixel resemblance as a basis. While this method can yield satisfactory results, it has certain parametric limitations (Shetty 2019). However, alternative non-parametric machine learning algorithms, such as Random Forest (RF), Support Vector Machines (SVM), Classification and Regression Trees (CART), K-Nearest Neighbour (KNN), Learning Vector Quantization (LVQ), and Stochastic Gradient Boosting (SGB), have been developed and employed in LULC assessments (Dimobe *et al.* 2017; Forkuor *et al.* 2017; Gislason *et al.* 2006; Hackman *et al.* 2017; Nery *et al.* 2016; Shetty 2019; Zoungrana *et al.* 2015). Among these non-parametric classifiers, SVM has gained consensus as an effective method (Orieschnig *et al.*, 2021). Furthermore, various techniques have been developed to project future LULC, including the Cellular Automata-Markov Chain (CA-MC), Markov Chain Model (MCM), Stochastic Markov Chain (STMC), Multi-Layer Perceptron (MLP) Neural Network and Markov Chain Model, and Combined Markov-FLUS Model (Bozkaya *et al.* 2015; Dey *et al.* 2021; Girma *et al.* 2022; Sinha *et al.* 2020; Yang *et al.* 2022). However, the most reliable technique for

such projections is the Multi-Layer Perceptron Neural Network and Markov Chain Model, known for its robustness in machine learning (Eastman 2020; Hussien et al. 2022). In this particular study, the historical dynamics of LULC were assessed using the SVM algorithm, while the Land Change Modeler incorporated the Multi-Layer Perceptron Neural Network and Markov Chain Model to forcast future LULCC in the Lotio River Basin.

3.4.2 Approach and Methods

3.4.2.1 Data Collection

The utilized dataset comprises Landsat 5 TM (1990), Landsat 7 ETM+ (2000 & 2010), and Landsat 8 OLI (2020) images obtained from the Google Earth Engine (GEE) data catalogue. These images, covering the period from January 1 to December 31, were acquired and utilized as inputs for the LULC analysis.

Physical factors such as geography and climate are thought to be the most influential in motivating human behaviour (Muhammad *et al*., 2022). The proximity of roadways helps determine the driving forces behind landscape design. The digital elevation model (DEM) utilized in this study had a spatial resolution of 30 m and was derived from SRTM elevation data available in the Google Earth Engine (GEE) data catalogue. The estimation of slope was performed using the DEM, while proximity factors like distance to roads were determined using the Euclidean distance method in ArcGIS 10.4 (Table 3.23).

Table 3.23: Data sources

Satellite	Spatial resolution	Temporal range
Landsat 5 TM	30m	01/01/1990 to 31/12/1990
Landsat 7 ETM+	30m	01/01/2000 to 31/12/2000
Landsat 8 OLI	30m	01/01/2010 to 31/12/2010
		01/01/2020 to 31/12/2020
Data	**Source**	
DEM	https://asf.alaska.edu/data-sets/derived-data-sets/alos-palsar-rtc/alos-palsar-radiometric-terrain-correction/	
Slope	Calculated from DEM	
Roads	https://www.diva-gis.org/gdata	
Distance from roads	Calculated from road network	

TM: Thematic mapper*, ETM+:* Enhanced Thematic Mapper Plus*, OLI:* Operational land imager

Five main LULC classes were identified: water, forest, shrubland, cropland and bare land (Table 3.24). Each class's samples were gathered from three different sources. Samples from 1990, 2000, and 2010 were obtained using high-resolution historical Google Earth images, while samples from 2020 were collected by a field survey. To classify the 1990, 2000, 2010, and 2020 photos, 325, 265, 205, and 144 disproportional stratified random samples of the five LULC classes were employed, accordingly Table 3.25.

Table 3.24: Land use and land cover classes description

LULC Class	Description
Bare land	Area with no vegetation cover, built-up areas, roads, infrastructures
Cropland	Agriculture lands, area under cultivation, farmland
Forest	An area dominated by trees, community and public forest reserves
Shrubs	Fallow vegetation, trees, grassland
Water	Lakes, streams, reservoirs, rivers

Source: FAO, 2009

Table 3.25: Sample sizes of LULC units for 1990, 2000, 2010 and 2020

LULC Units	Sample seizes				
	1990	2000	2010	2020	**Total**
Bare land	40	34	30	23	**127**
Cropland	98	78	67	44	**287**
Forest	50	40	32	26	**148**
Shrubs	67	50	41	31	**189**
Water	70	63	35	20	**188**
Total	**325**	**265**	**205**	**144**	**939**

3.4.2.2 Methods

Pre-processing

The pre-processing processes included scaling, cloud masking, and additional band computation. To achieve the true surface reflectance values, the images were scaled using the necessary scale factors and offsets. Cloud masking involved the identification and exclusion of pixels containing clouds and shadows to ensure they did not affect subsequent analysis. A median filter was then applied to the captured images of each year to create a composite that was free from cloud interference. Alongside the five original surface reflectance bands, two additional indices, namely the Normalized Difference Vegetation Index (NDVI) and the Normalized Difference

Built-up Index (NDBI), were calculated and utilized as supplementary attributes. The NDVI helped differentiate between vegetated and non-vegetated areas, while the NDBI assisted in distinguishing built-up and bare land regions from other land uses (Barnieh *et al*., 2020; Feng *et al*., 2016; Hackman *et al*., 2017; Yangouliba *et al*., 2022).

LULC Classification

The training samples listed in (Table 3.3. 1) were utilized to classify the pre-processed images. 70% of the samples from each year were allocated for training the classification algorithm, while the remaining 30% were reserved for testing purposes. (Yangouliba *et al*., 2022). The classification method was based on 4 supervised classifications techniques: Classification and Regression Tree (CART), Support Vector Machine (SVM), Random Forest (RF) and Gradient Tree Boosting (GTB) in Google Earth Engine (GEE). The SVM algorithm, initially developed by Vapnik and his team in the late 1970s, has gained significant popularity as a kernel-based learning algorithm in a wide range of machine learning applications. Due to its exceptional performance and output quality, it was selected for the image classification task (Mountrakis *et al*., 2011). In other, according to (Nery *et al*., 2016) when detecting land use and land cover changes in time series imagery, it is advisable to give priority to SVM as the preferred classification method.

Change Detection Analysis

To estimate spatiotemporal changes and calculate land use and land cover (LULC) changes between specific time intervals (1990–2000, 2000–2010, 2010–2020, and 1990–2020), we employed the Semi-Automatic Classification Plugin (SPC) modules within the QGIS software. Four LULC change maps were generated using this approach. Percentage change was computed using the following equation (Hussien *et al*. 2022):

$$P = \frac{(A_{1-}A_e)}{A_e} * 100$$

where p is the percent change, A_1 is the area of a class in the later LULC map (ha), and A_e is the area of a class in the earlier LULC map (ha).

The CA-ANN multilayer perceptron technique was utilized to forecast forthcoming changes in land use and land cover (LULC). Various factors, including the digital elevation model (DEM), slope, and proximity to highways, were used as explanatory variables in the prediction model (Table 3.3.1). These variables are commonly employed in LULC change analysis due to their ability to provide consistent data on the physical and human-induced factors influencing LULC dynamics. (Muhammad *et al*., 2022).

Prediction and Model Validation

Many research suggests that the CA-ANN approach is more efficient than linear regression (El-Tantawi *et al*., 2019), so we used it in the MOLUSCE plugin to model transition potentials and simulate future land use and land cover dynamics in the Lotio Basin. The MOLUSCE plugin computes land use change analyses efficiently (Gismondi, 2013) and is well suited for assessing spatiotemporal forest and land use changes, forecasting transition prospects, and simulating future scenarios.

Based on previous studies indicating the superior efficiency of the CA-ANN approach over linear regression (El-Tantawi *et al*., 2019), we applied this method within the MOLUSCE plugin to model transition potentials and simulate future land use and land cover dynamics in the Lotio Basin. The MOLUSCE plugin is known for its efficient computation of land use change analyses (Gismondi, 2013) and is particularly suitable for assessing spatiotemporal forest and land use changes, forecasting transition prospects, and simulating future scenarios.. To predict the land use and land cover (LULC) for the year 2020, we utilized LULC data from 2000, 2010, explanatory variables, and transition matrices. The accuracy of our model and predictions were assessed using the kappa validation technique and by comparing the actual and projected LULC images. The forecasting process for the CA-ANN model involved 1000 iterations, with a neighborhood size of 3x3 pixels. We set the learning rate at 0.001 and utilized 12 hidden layers, along with a momentum of 0.05. With promising validation results, we proceeded to project the LULC for the year 2030 using the LULC data from 2010 and 2020 (Muhammad *et al*., 2022).
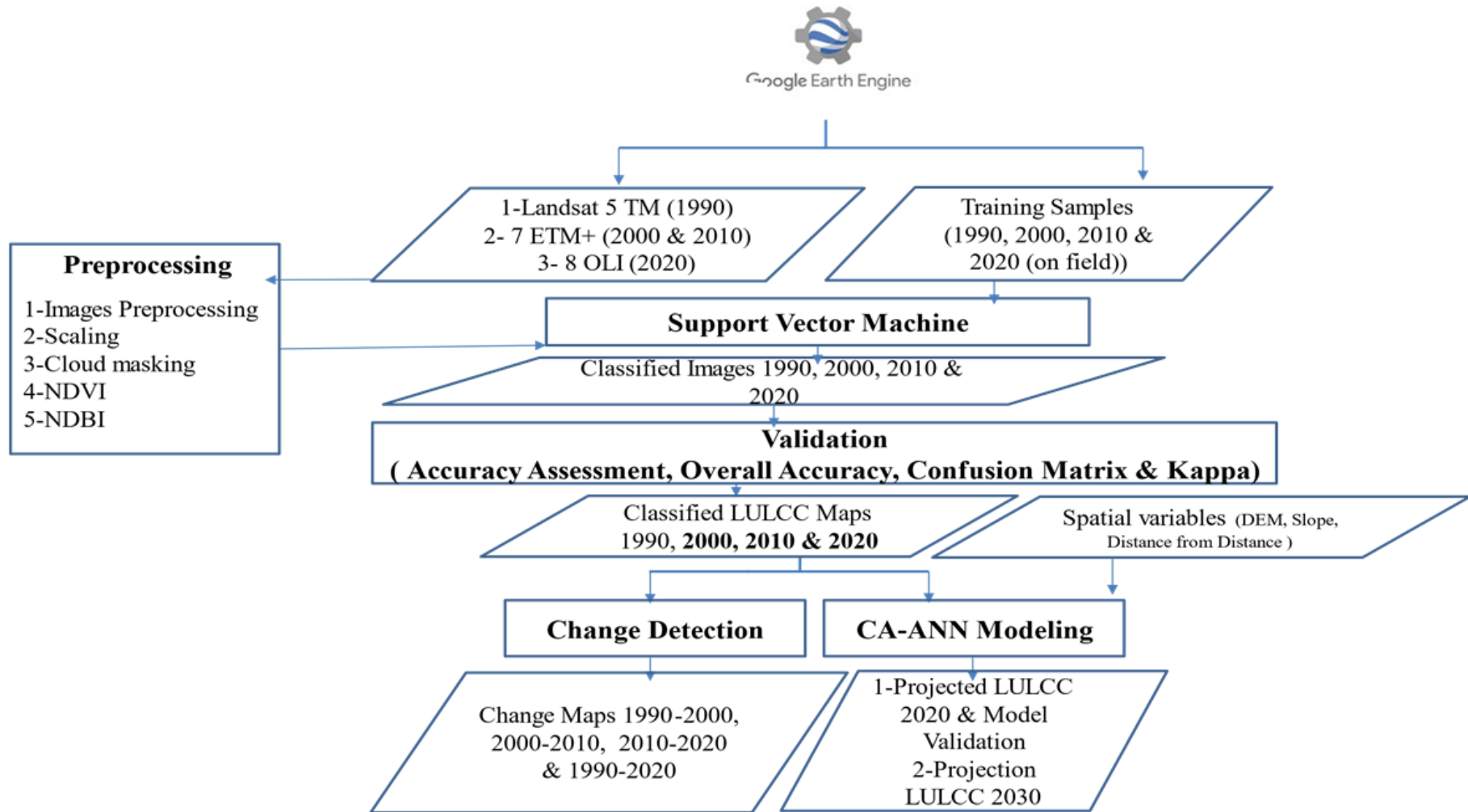
Figure 3.32: Methodology flow chart

3.4.3 Results and interpretation

3.4.3.1 Past Land Use and Land Cover Dynamic

For the purpose of determining changes in land use and land cover in the Southern Mali, notably Lotio River Basin, four images classified were clipped at the study area level, making fours maps. Confusion matrix, user, producer accuracy were used to assess the map accuracy (See Appendix) of land use and land cover maps from 1990 to 2020 are shown in Figure 3.33.
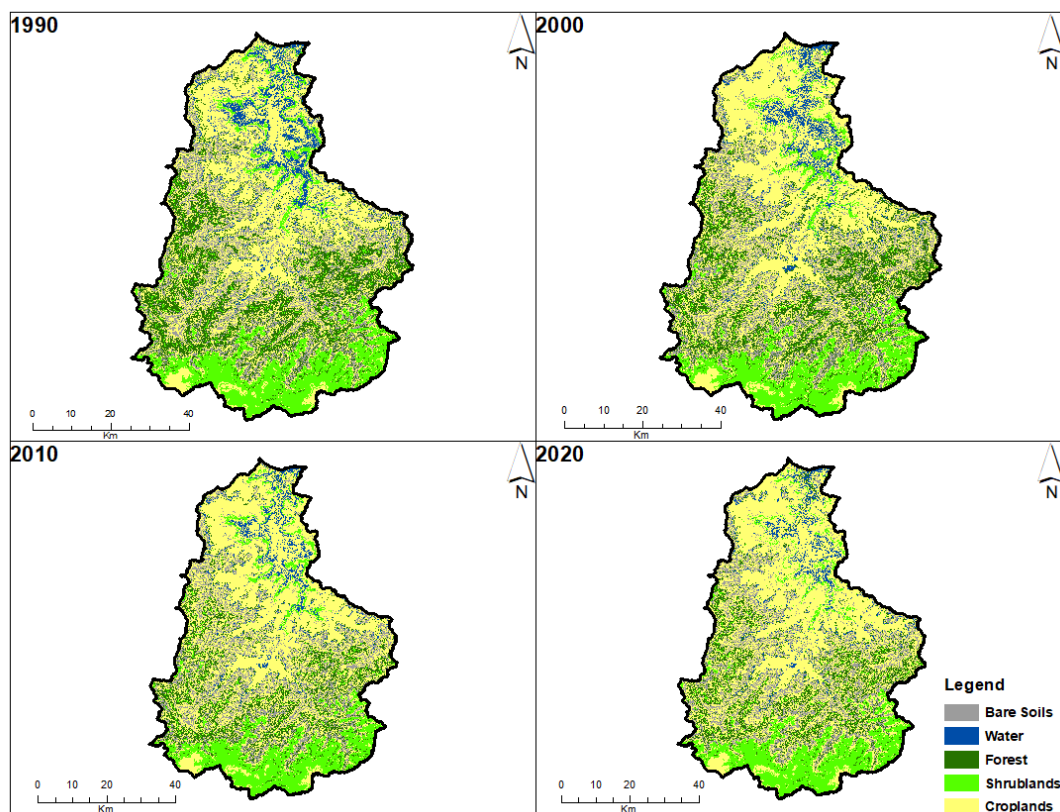
Figure 3.33: Land Use and land cover map from 1990 to 2020

In 1990, farmland (44%) and forest (20%) dominated the Lotio River Basin (LRB) (Table 3.26). These were followed by shrublands, bare soils, and aquatic bodies, which received 16%, 14%, and 6% coverage, respectively. However, the order was confirmed in the year 2000. Cropland and forest covered 48% and 18% of the land area, respectively. As in 1990, the least represented LULC were barren soils and aquatic bodies. In 2010, farmland dominated the basin's land cover, followed by shrubland and forest (51% 16% 15% and 53% 15% 14%, respectively). Natural vegetation has lost way to artificial land uses (cropland) between 1990 and 2020.

Table 3.26: Land Use and Land Cover statistics from 1990 to 2020

LULC Units	1990		2000		2010		2020	
	Area (ha)	Area (%)	Area (ha)	Area (%)	Area (ha)	Area (%)	Area (ha)	Area (%)
Bare soil	61994	14	62049	14	60891	14	59576	14
Water	24177	6	18870	4	17705	4	16611	4
Forest	85615	20	78286	18	62923	15	59841	14
Shrub	69621	16	65696	15	69209	16	66964	16
Crop	188240	44	204746	48	218920	51	226654	53
Total	429647	100	429647	100	429647	100	429647	100

3.4.3.2 Land Use and Land Cover Changes between 1990-2000, 2000-2010, 2010-2020, and 1990 and 2020

The results of the analysis of changes in land use and occupancy between 1990-2000, 2000-2010, 2010-2020 and between 19990-2020 indicate a wide variation in conversion between the different land use units in general (Figure 3.34). However, the result between 1990-2000 and between 2000-2010 highlights areas that have not changed use, whereas between 2010-2020 and between 1990-2020, the entire study area has undergone changes in use.
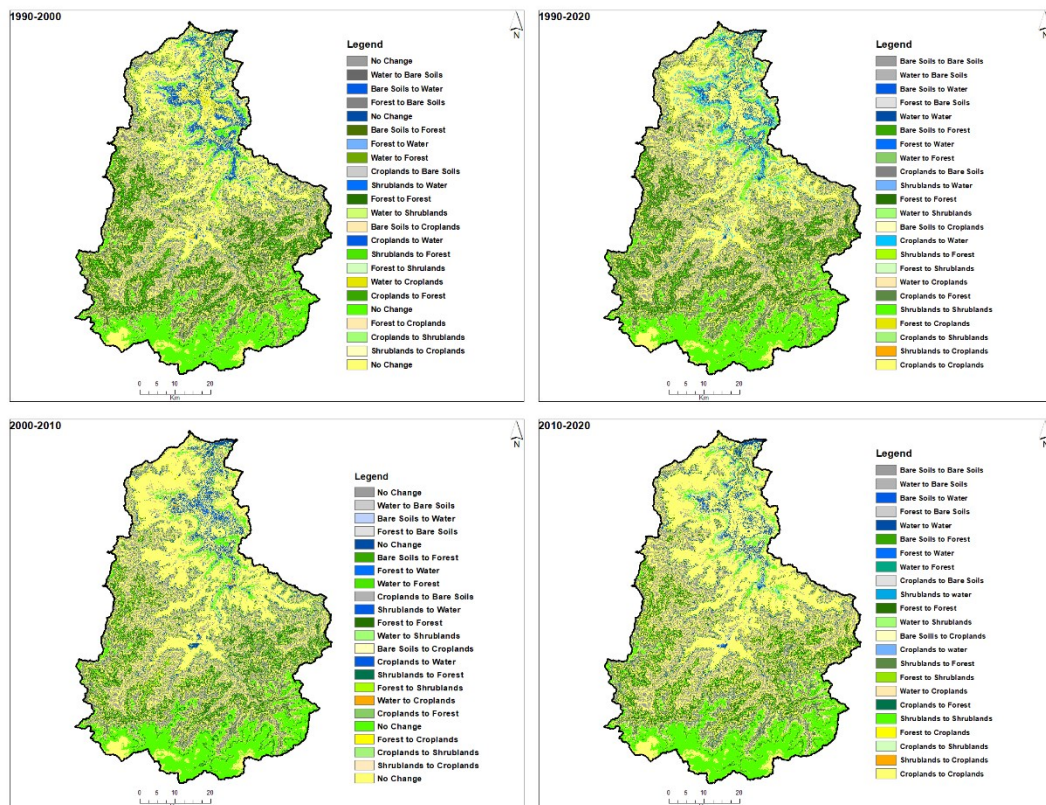
Figure 3.34: Change map

Table 3.27 shows LULC statistics between 1990-2000, 2000-2010, 2010-2020 and between the study period 1990-2020. This table shows the temporal variation between LULC units and the reasons for the variation. The interpretation confirms the results of the change map, i.e. a significant variation between units, but also and above all that the main reason for conversion of the other LULC units is agriculture.

Table 3.27: Land Use Land Cover Change Statistics

		2000				
		Bare Soil	Water	Forest	Shrubland	Cropland
1990	Bare Soil	55401	34	3155	0	3404
	Water	50	13846	346	1492	8442
	Forest	4393	428	64348	872	15573
	Shrubland	0	419	2530	62025	4647
	Cropland	2204	4143	7907	1306	172680
		2010				
	Bare Soil	57047	318	1700	0	2984
	Water	5	14208	58	428	4171
2000	Forest	3168	287	55579	2537	16715
	Shrubland	0	1152	644	61742	2157
	Cropland	671	1739	4943	4502	192892
		2020				
	Bare Soil	56105	467	1485	0	2833
	Water	46	14542	237	645	2235
2010	Forest	1522	41	52978	1072	7309
	Shrubland	0	35	188	64206	4779
	Cropland	1903	1526	4953	1041	209497
		2020				
	Bare Soil	54381	704	1497	0	5412
	Water	18	13660	280	383	9836
1990	Forest	4055	441	53392	1541	26187
	Shrubland	0	115	307	63655	5544
	Cropland	1122	1692	4366	1384	179676

Losses and gains in LULC units were noted between 1990 and 2020. Water (-22%) forest (-9%), and shrubland (-6%) decreased during the first teen years (1990-2000) whereas farmland rise by 9% Table 3.28. From 2000 through 2010, the same dynamics were observed, with some variations. Bare land, water, and forest all fell by -2%, -6%, and -20%, respectively, while shrubland and farmland increased by 5% and 7%, respectively. The reduction in water body area could be attributed to the exploitation of minor beds for rice production in the zone's full growth. Overall, farmland increased by 20% in the LRB over the last 30 years. Between 1990 and

2020, it is probable that the increase occurred by sacrificing forests and water resources, which experienced a decline of approximately 30% and 31% respectively.

Table 3.28: Area of change from 1990 to 2020

LULCC	1990-2000		2000-2010		2010-2020		1990-2020	
Units	Area (ha)	Area (%)	Area (ha)	Area (%)	Area (ha)	Area (%)	Area (ha)	%
Bare soils	55	0	-1159	-2	-1314	-2	-2418	-4
Water	-5307	-22	-1165	-6	-1093	-6	-7565	-31
Forest	-7328	-9	-15363	-20	-3082	-5	-25773	-30
Shrubland	-3925	-6	3514	5	-2245	-3	-2657	-4
Cropland	16506	9	14174	7	7734	4	38414	20

Degree of Dynamics Land

Land use and land cover dynamics showed similar results in the whole study area. Bare soil, Water, Forest and shrubs recorded a negative dynamic degree per annum. While cropland showed a positive dynamic degree per annum.

In the entire study area (Figure 3.35), slight positive dynamic was observed in shrubs area from 2000 to 2010. The most important negative dynamic in water (-31%), forest land (-30%) was recorded from 1990 to 2020, while the most important positive dynamic in cropland (20%) was registered from 1990 to 2020. For bare soil, the highest negative dynamic was -4% (1999-2020).

	Bare soils	Water	Forest	Shrublands	Croplands
■ 1990-2000	0	-22	-9	-6	9
■ 2000-2010	-2	-6	-20	5	7
■ 2010-2020	-2	-6	-5	-3	4
■ 1990-2020	-4	-31	-30	-4	20

■ 1990-2000　■ 2000-2010　■ 2010-2020　■ 1990-2020
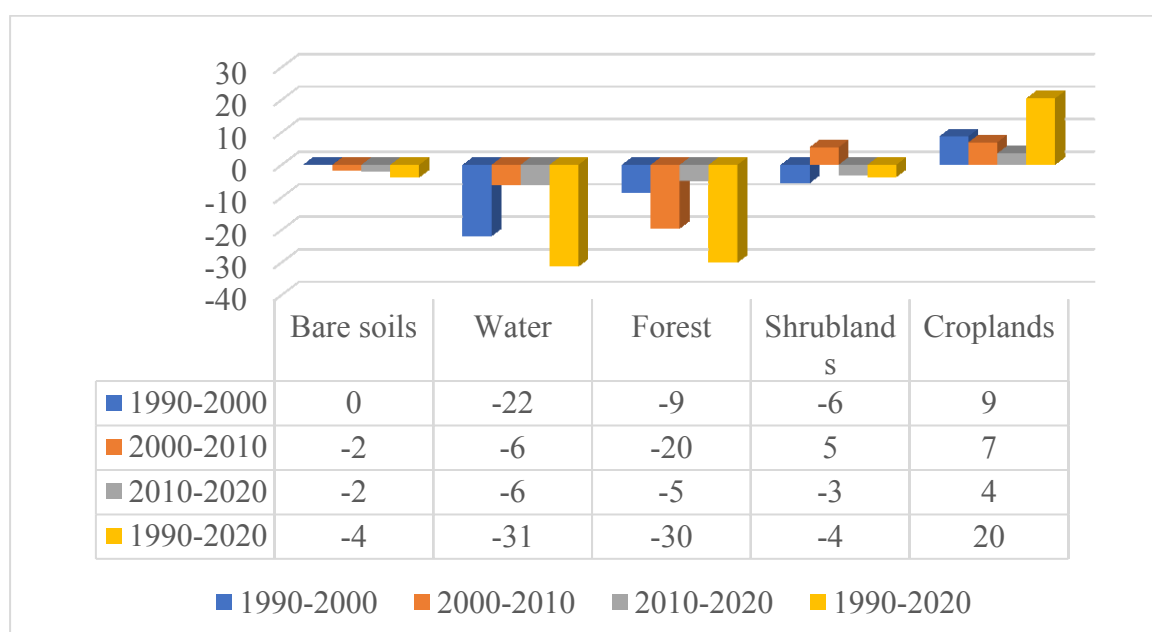
Figure 3.35: Land use and land cover dynamics in Lotio River Basin from 1990 to 2020

3.4.3.3 Land use and land cover matrix of Change

The matrix of change analysis enables an understanding of the nature of changes from one LULC class to another between years. Overall, there was a predominant conversion of forest land into shrub/grassland and a transformation of shrub/grassland into cropland. From 1990 to 2000 (Table 3.29), the foremost conversion was noticed in water with 27%, followed by forest (18%) and cropland 16%). From 2000 to 2010, the greatest rate of conversion occurred in water (19%), followed by cropland (13%) and shrubland (11%). On the other hand, from 2010 to 2020, the most substantial loss was registered in water with 11%, followed by forest (9%), and cropland with 8%. Furthermore, from 1990 to 2020, the highest rate of change was observed in cropland with 23%, followed by water (16%), bare soil and forest (8%).

Table 3.29: Land use and land cover change matrix in Lotio River Basin from 1990 to 2020

		2000				
		Bare Soil	**Water**	**Forest**	**Shrubland**	**Cropland**
1990	**Bare Soil**	89	0	4	0	2
	Water	0	73	0	2	4
	Forest	7	2	82	1	8
	Shrubland	0	2	3	94	2
	Cropland	4	22	10	2	84
	Total change	**11**	**27**	**18**	**6**	**16**
		2010				
2000	**Bare Soil**	92	2	2	0	1
	Water	0	75	0	1	2
	Forest	5	2	71	4	8
	Shrubland	0	6	1	94	1
	Cropland	1	9	6	7	94
	Total change	**6**	**19**	**9**	**11**	**13**
		2020				
2010	**Bare Soil**	90	2	2	0	1
	Water	0	77	0	1	1
	Forest	2	0	68	2	4
	Shrubland	0	0	0	98	2
	Cropland	3	8	6	2	102
	Total change	**6**	**11**	**9**	**4**	**8**
		2020				
1990	**Bare Soil**	88	4	2	0	3
	Water	0	72	0	1	5
	Forest	7	2	68	2	13
	Shrubland	0	1	0	97	3
	Cropland	2	9	6	2	88
	Total change	**8**	**16**	**8**	**5**	**23**

3.4.3.4 Future Land Use and Land Cover Dynamic

Selection of spatial variables

The choice of spatial variables is justified by the fact that many studies use mainly these spatial factors to study the dynamics of LULCC and all transitions observed are essentially between water and forest to cropland. These transitions were influenced by a combination of physical and socioeconomic factors. The statistical significance of the Pearson correlation values suggests that the chosen variables are appropriate for modelling transition potential. The correlation values indicate that incorporating physical and socioeconomic explanatory variables, such as DEM (0.63), slope (0.32), and distance from roads (0.09), is more advantageous in comprehending and forecasting the observed changes in land use and land cover (Table 3.30).

Table 3.30: Person Correlation value of spatial variables

Spatial Variables	Person Correlation
DEM	0.63
Slope	0.32
Distance from roads	0.09

3.4.3.5 Transition Potential Modeling and Model Validation

The MOLUSCE plugin incorporates a range of established methodologies, such as ANN (multilayer perceptron), weights of evidence, multicriteria evaluation, logistic regression, and CA algorithm, to model transition potential. This amalgamation of techniques enables comprehensive and robust analysis, facilitating the simulation of future scenarios and projections regarding land use and land cover (LULC) changes. Geographical variables with significant correlations to LULC were selected for model calibration using Person's coefficient. The CA-ANN approach was employed for transition potential modelling and prediction. To forecast the LULC for 2020, LULC data from 2000 to 2010, along with spatial variables, were utilized. The validation process yielded a high accuracy level with a kappa value of 0.98. Comparison between the projected and actual LULC data for 2020 resulted in an overall accuracy of 97.92% and a kappa value of 0.93. Figure 3.36 visually presents the actual LULC map, while (Table 3.31) provides a detailed comparison between the forecasted and actual LULC maps.
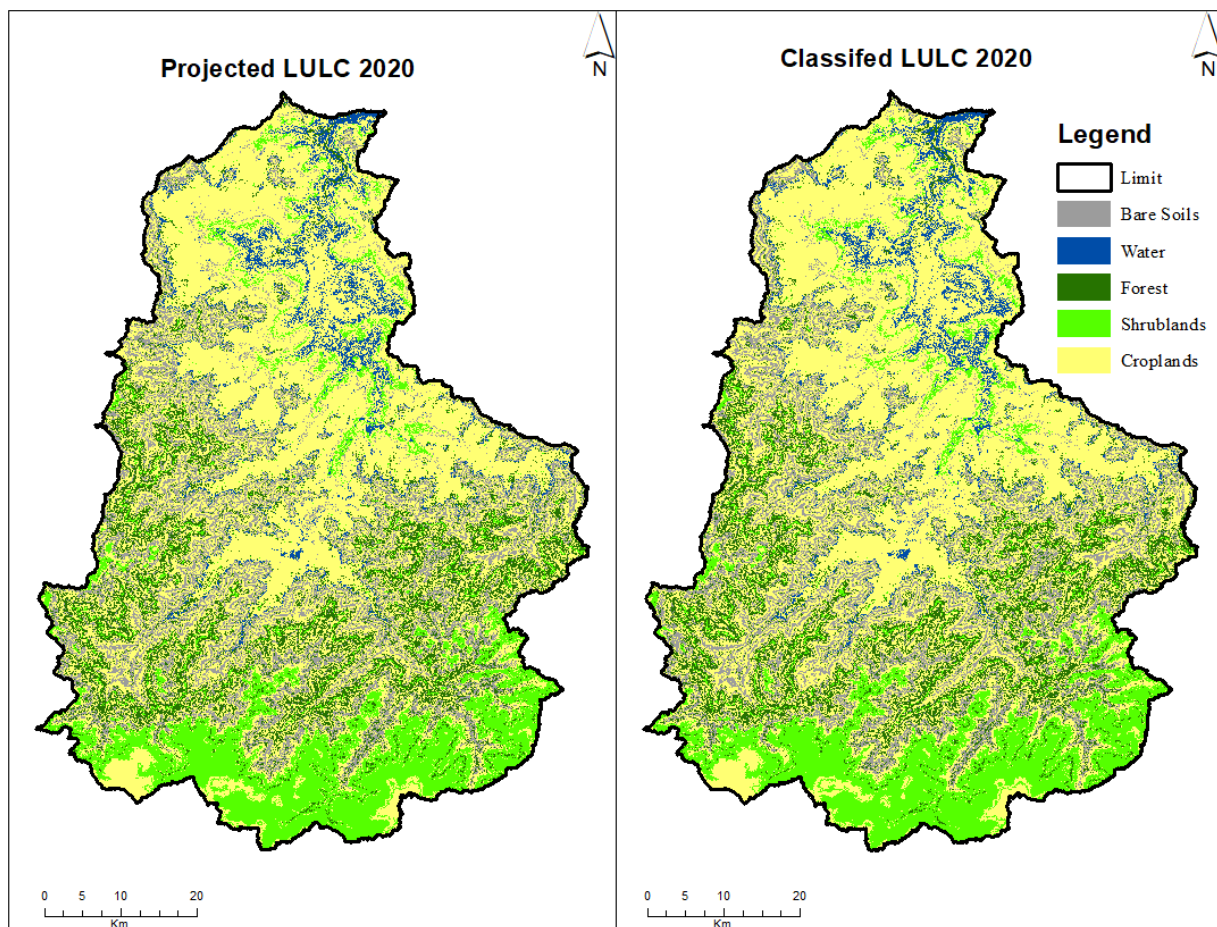
Figure 3.36: Actual and projected LULC 2020.

Table 3.31: Actual and projected LULC of 2020

	Classified		Projected		Accuracy	Kappa Value	
	Ha	%	Ha	%		ANN	Validation
Bare soils	59576	13,866	59570	13,866			
Water	16611	3,866	16612	3,867			
Forest	59841	13,928	59842	13,929	97.92	0.98	0.93
Shrublands	66964	15,586	66956	15,585			
Croplands	226654	52,754	226638	52,753			

3.4.3.6 Prediction of LULC

Following the successful validation of our model, we proceeded to forecast the LULC for the year 2030 Figure 3.37. To make this prediction, we utilised the temporal LULC data from 2010 and 2020 in conjunction with spatial variables. The forecasted LULC for 2030 was then evaluated, yielding a kappa value of 0.94, indicating a high level of accuracy in our predictions.

The statistical results of the LULC projection (Table 3.32), which show that cropland would dominate the basin area in 2030 (48%), followed by forest and shrubland (18% and 15%, respectively). However, in comparison to 2020, cropland will decrease by 5%, while forest land will increase by 4%.
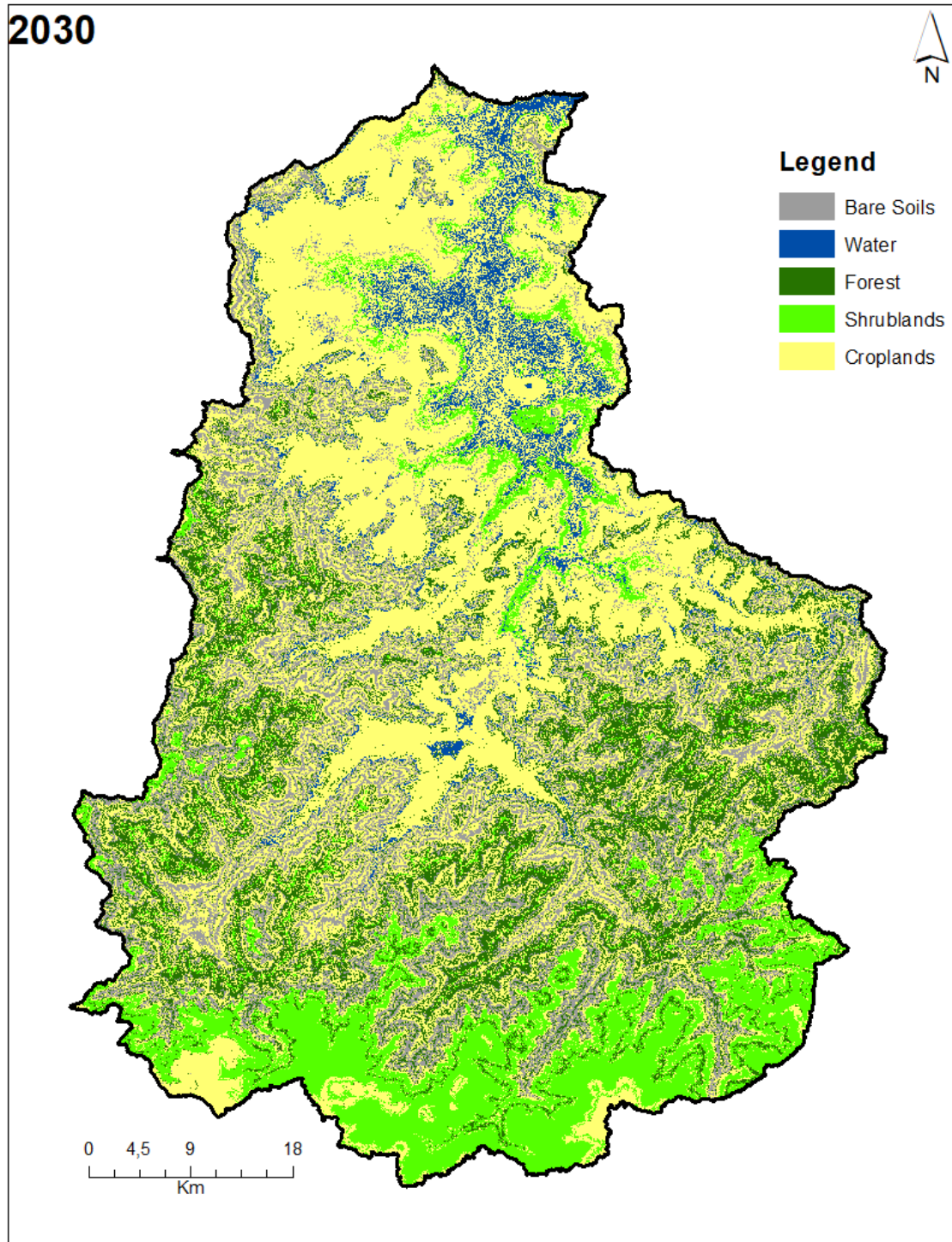
Figure 3.37: LULC prediction 2030

Table 3.32: Predicted area statistics for 2030

LULCC Units	2030				
	Ha	%	Accuracy	Kappa Value	
				ANN	Validation
Bare soils	62440	15			
Water	18764	4			
Forest	75806	18	97	0.94	89
Shrublands	65609	15			
Croplands	207028	48			

3.4.3.7 Prediction of Change

The analysis of land use and land cover (LULC) change explores the spatial fluctuations of the LULC model throughout the study period. The results of the LULC changes between 2020 and 2030 forecast a significant reconfiguration of land use and land cover dynamics in southern Mali's Lioto River Basin (Figure 3.3).

Temporal change statistics between 2020 and 2030 predict a -9% decrease in cropland and a -2% decrease in shrubland by 2030. At the same time, the area of bare soil, water, and forest will increase by 5, 13, and 27%, respectively (Table 3.3).
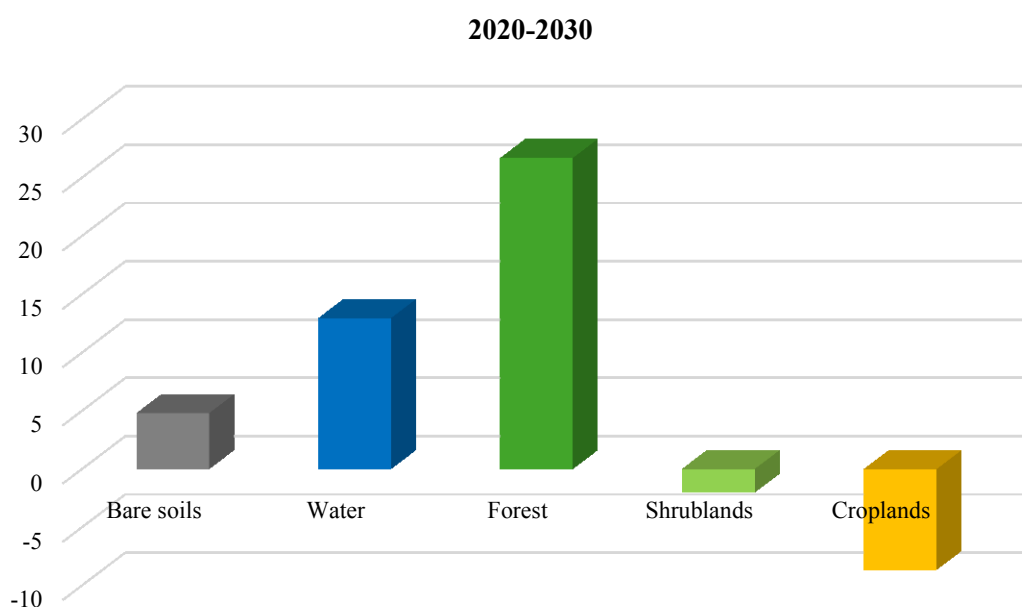
2020-2030

Figure 3.38:Change 2020-2030

3.4.3.8 Future Land use and land cover matrix of Change

LULC matrix change were computed for 2030 to understand the nature and reasons for changes from one LULC class to another in the future. In the Lotio River Basin, from 2020 to 2030 (Table 3.31), the foremost conversion was noticed in the forest (33%), followed by water (29%), and bare soil (13%). In general, most of the cropland will be converted to water and forest, while most of the bare land will be forest.

Table 3.33: Land use and land cover dynamics in Lotio River Basin from 2020 to 2030

Land class	2030				
	Bare Soil	Water	Forest	Shrubland	Cropland
Bare Soil	88	0	4	0	1
Water	1	71	0	1	1
Forest	3	2	64	1	3
Shrubland	0	1	4	92	2
Cropland	8	26	25	7	94
Total change	**13**	**29**	**33**	**8**	**7**

(Row group label "2020" appears vertically to the left of the data rows.)

3.4.4 Discussion

On a global scale, significant advancements in living conditions, particularly in the 21st century, have brought about extensive transformations in natural habitats and landscape configurations. The improvement of living conditions has emerged as a primary driver behind deforestation, propelled by a range of physical and socio-economic factors including geography, demography, and economic expansion, among others. Notably, socio-economic development exerts a more significant influence on the expansion of deforestation and the fragmentation of landscapes, raising apprehensions regarding climate change, food security, and the depletion of natural resources.

The transformation of land use and land cover is intricately linked to geographical factors and development policies. Following the introduction of democracy in Mali in March 1992, economic reforms triggered significant displacements, migrations, and urbanization. Our study examined the changes in land use and land cover from 1990 to 2020 by analyzing spatiotemporal data alongside physical and socioeconomic variables. We employed the MOLUSCE plugin within the QGIS software to generate

transition probability matrices for each time interval. Additionally, utilizing the CA-ANN multilayer perceptron technique integrated into the MOLUSCE plugin, we made projections for land use and land cover (LULC) in 2030.

The results of our study highlight the substantial influence of both physical and socioeconomic factors on landscape patterns throughout the research timeframe. Generally, lower elevations exhibit more pronounced changes in land use and land cover (LULC) due to their geographical suitability for human activities. The most notable transformations have been observed in forested areas and along river systems.

Mali's vision as a landlocked country with a primary-sector-based economy has broader reform goals centred on agricultural development and food security. Many studies have shown that population growth and economic development are the primary causes of forest loss (Li *et al*., 2016; Zhe & Shashi, 2017). The expansion of cropland has adverse effects on the environment, aquatic habitat, and biodiversity. Based on our research findings, significant changes in land use and land cover (LULCC) have occurred within the Lotio River Basin during the past 30 years. These changes primarily stem from the extensive expansion of cultivated land, which has resulted in the rapid conversion of forests and water bodies, particularly within the last decade. Cropland increased from 44% to 53% between 1990 and 2020, with forest contributing 12%, water contributing 4%, and bare soil and shrub contributing 2%. Furthermore, the results of the future simulation show that forests will increase by 27% from 2020 to 2030, while water will increase by 12%. However, cropland will decrease by -9% and shrubland will decrease by -2% during the same time period.

Finally, dramatic changes in LULCC, particularly the expansion of agricultural land and the decline of forests, may endanger natural resources, the environment, and food security. Consequently, the outcomes of our spatial-temporal analysis and future-oriented simulations of land use and land cover change (LULCC) will provide valuable insights to policymakers. These insights will aid in analysing the evolving patterns of LULCC, identifying the socioeconomic factors that contribute to these changes, and facilitating the formulation of policies that promote environmental conservation and sustainable development. It is important to note that our modelling and prediction of LULCC solely relied on physical and socioeconomic characteristics.

111

Future research, on the other hand, could incorporate development policies and climate variables.

3.4.5 Conclusion

The findings indicate a rapid change in the past (1990-2020) Land Use and Land Cover (LULC) in the study area, dominated by an increase in agricultural land at the expense of primarily forest and water. The majority of agricultural land is being converted to forest, and there is a shift in all land use and cover classes except shrubland and bare soil. Agricultural areas will continue to dominate LULC dynamics in 2030. In comparison to 2020, agricultural land will decrease by 5%, while forest land will increase by 4%.

CHAPTER 4 :GENERAL DISCUSSION

4.1 Delineation and distribution of Lowlands in the Lotio Catchment

The study estimated the area of the lowlands at 71,479 ha with a compliance rate of 58.48%. This means that the area has a significant potential in lowlands. The same result was found on a national scale by (Dembele, 2019), who indicated detected areas with agricultural potential in the rural commune of *Bougaribaya*. At the international level, Benin which within the framework of the implementation of the Atlas of the lowlands of the North-West of the country in 2015-2016, the total area of the lowlands surveyed is estimated at 46,264 ha for the department of *Atacora-Donga* (Souberou *et al*., 2017). The multi-criteria approach adopted showed the importance of GIS and remote sensing and the degree of reliability of the results in the identification, estimation and mapping of the lowlands as it had been highlighted by several previous studies (Chabi *et al*., 2010; Demblele, 2019; Kindjinou, 2013; O loukoi, 2016; Souberou *et al*., 2017).

4.2 Variation and trend of Annual and seasonal of Rainfall and temperature

The result of the existence of significant variation and positive trend in annual and seasonal rainfall on the one hand and the significant increase with a positive trend in the south of Mali in mean annual and seasonal temperatures on the other hand, confirms previous work (Barry *et al*., 2018; Bichet & Diedhiou, 2018b, 2018a; Cook & Vizy, 2015; Dosio, 2017; Gutiérrez *et al*., 2021; Kennedy *et al*., 2016; Lelieveld *et al*., 2016; Moron *et al*., 2016; Nicholson *et al*., 2018; Nikiema *et al*., 2017; Ranasinghe *et* ail., 2021; Sanogo *et al*., 2015; Sylla *et al*., 2016; Thomas & Nigam, 2018). These studies show a positive trend, accompanied by an increase in precipitation and temperature variability in Africa's Saharan and Sahelian countries, caused by a combination of anthropogenic aerosols and GHG.

4.3 Farmer's Perception and Adaptation strategies of climate variability changes

Based on the survey conducted, the study area predominantly consisted of lowland producers aged above 20, with the majority having 10 to 50 years of farming experience. Consequently, they possess valuable knowledge regarding climate change and its impacts in the study area. However, it should be noted that the educational level of these farmers was generally low. The ability of farmers to understand climate patterns and adapt to them is influenced by their level of education. Farmers with

primary and secondary education in the lowland areas exhibit a more positive perception of climate change, likely attributed to their frequent interaction with the outside world through migration and easier access to information sources like the media (Kabore *et al*., 2019; Koné *et al*., 2022; Sanogo *et al*., 2016; Assoumana *et al*., 2016). Hence, the educational background of farmers positively influences their ability to adapt to varying temperature and precipitation patterns. Educated farmers exhibit greater awareness of accessing, understanding, accepting, and adapting to climate change information and advancements in technology, leading to enhanced productivity. The level of education among farmers was found to be strongly associated with their extensive understanding of climate change (Jha & Gupta, 2021; Sanogo *et al*., 2016; Assoumana *et al*., 2016).

Globally, significant efforts have been made to enhance living conditions, leading to profound transformations in natural habitats and landscape configurations, particularly in the 21st century. These improvements, driven by physical and socio-economic factors such as geography, demography, and economic expansion, have notably contributed to deforestation. However, it is the socio-economic development that has exerted the most substantial impact on the expansion of deforestation and the fragmentation of landscapes, thereby raising concerns regarding climate change, food security, and the scarcity of natural resources.

The correlation between land use and cover changes and geography, as well as development policies, is tightly intertwined. Following the establishment of democracy in Mali in March 1992, economic reforms triggered significant population displacements, immigration, and urbanization. In order to analyze the transformations in land use and land cover between 1990 and 2020, we employed spatiotemporal data in conjunction with physical and socioeconomic variables. The MOLUSCE plugin, integrated into the QGIS software, was utilized to generate transition probability matrices for each time period. Additionally, the CA-ANN multilayer perceptron technique was employed to forecast land use and land cover (LULC) for the year 2030.

Our research findings underscore the substantial influence of physical and socioeconomic factors on landscape patterns throughout the study period. Generally, lower elevations undergo more rapid changes in LULC due to their inherent

suitability for human activities. Notably, forests and rivers have experienced the most significant transformations.

Mali, as a landlocked country with an economy primarily dependent on the primary sector, has outlined broader reform goals centered around agricultural development and food security. Numerous studies have indicated that population growth and economic development are the primary drivers of forest loss (Li *et al.*, 2016; Zhe & Shashi, 2017). The expansion of cropland has detrimental effects on the environment, aquatic habitats, and biodiversity.

Our findings reveal the remarkable transformation of the Lotio River Basin's LULCC over the past three decades, driven by the rapid expansion of cultivated land and the subsequent conversion of forests and water bodies. Cropland has increased from 44% to 53% between 1990 and 2020, with forests contributing to 12%, water contributing to 4%, and bare soil and shrubland contributing to 2%. Additionally, the future simulation results indicate a projected increase of 27% in forests and 12% in water from 2020 to 2030. Conversely, cropland is expected to decrease by -9%, and shrubland by -2% during the same period.

The significant shifts observed in land use and land cover change (LULCC), specifically the expansion of agricultural land and the reduction of forests, pose considerable risks to natural resources, the environment, and food security. As a result, the spatiotemporal analysis and forward-looking simulations of LULCC offer invaluable insights for policymakers to examine the changing patterns and socioeconomic drivers of LULCC. Moreover, these findings can contribute to the formulation of policies that promote environmental conservation and sustainable development. It is important to note that our modeling and prediction of LULCC focused solely on physical and socioeconomic factors. Future research endeavors could explore the integration of development policies and climate variables into the analysis.

4.4 Modelling Land Use Land Cover Change in the Lotio Catchment
The results of this study reveal the spatiotemporal dynamics of land use and land cover (LULC) in the Lotio River basin, utilizing temporal Landsat data and projecting future scenarios based on driving factors. The findings highlight the significant

challenges posed by rapid agricultural land expansion and forest fragmentation, leading to environmental degradation and depletion of water quality in the Lotio region. These issues further complicate the task of achieving sustainable regional development and preserving the environment.

While acknowledging that development policies, migration, immigration, and climatic conditions can all contribute to shaping landscape patterns, our modeling and prediction focused solely on incorporating physical and socioeconomic factors. By limiting our analysis to these specific elements, we aimed to capture the essential aspects influencing LULC changes in the Lotio River basin.

In light of the findings, it is crucial to establish a strong connection between agricultural and development policies to promote sustainable land management practices. This integrated approach can effectively address the challenges posed by rapid changes in LULC and ensure the preservation of the environment while fostering regional development. use. It is suggested that future studies examine the effects of more factors and data on landscape patterns.

CHAPTER 5: CONCLUSIONS AND RECOMMENDATIONS

5.1 Conclusions

Based on the formulated objectives, the methodology employed, data collected and the analysis, the following conclusions are drawn:

The southern zone of Mali has a rich potential in lowlands with a good spatial distribution. The multi-criteria approach is a recognized and recommendable method for the identification, area estimation, geophysical and geomorphological characterization of lowlands. Precipitation and temperature in the Sikasso District exhibit considerable variability throughout the year. There is a slight upward trend in both annual and seasonal rainfall, particularly during the AMA (April to May) and SON (September to November) seasons. However, there is no statistically significant trend observed for the JJA (June to August) season, which shows a decrease in rainfall. The average annual temperature in the study area ranges from 26.6 to 28.5 degrees Celsius, with a noticeable increase over time. The rise in mean annual and seasonal temperatures is statistically significant. While there are intermittent shifts in average annual and seasonal precipitation, no breaks are observed in the temporal variation of average annual and seasonal temperatures. Farmers in the research area possess a comprehensive understanding of climate variations and have developed numerous strategies to adapt to these changes.

In the present study, the potential impacts of climate change on the long-term trends of the rainfall anomaly index over Sikasso district in southern Mali were examined using 61 years of monthly records. The analysis examines both long-term and short-term trends in rainfall using various statistical measures, including parametric and non-parametric methods. These measures include monotonic linear regression trend analysis, the Mann-Kendall trend test, and the Mann-Kendall seasonal trend. The assessment considers both the presence and absence of serial correlation, utilizing Sen's slope to account for the serial correlation. To fully capture the trends and variability of the annual, seasonal precipitation anomaly index, the data were divided into six aggregated periods. It is worth mentioning that when a clear trend emerges, the linear regression analysis and the Sen slope corresponding to the Mann-Kendall test are in perfect agreement. In other words, the results showed that despite the prevailing preference of non-parametric tests for assessing trends in climate data, simple linear regression can still give as good a trend analysis as other tests.

117

In general, it was found that the trend of the annual rainfall anomaly index over the South Mali district has been in a phase of return of wet periods for about two decades (2003). The seasonal rainfall anomaly index for March-April-May and September-October-November is also dominated by the return of wet periods. This result is important because the period (September-October-November) corresponds to the end of season period and the end of season precipitation is important for a good crop maturity and also especially the quality of the crops. Furthermore, the examination of anomaly indices for seasonal precipitation in June, July, and August revealed a slight reduction in peak precipitation levels over the past two decades. This consistent and significant long-term alteration in the occurrence of precipitation peaks emphasizes the need for additional investigation into potential climate change concerns and risks in the southern region.

Analysis of the climate period average highlights the fact that rainfall patterns are characterized by long periods of drought that are interspersed with episodes of extreme heavy rainfall with short recurrence intervals. The decadal analysis potentially indicates a succession of wet and dry decades with a variation in the number of years with a negative and positive RAI. In summary, the long-term rainfall analysis in Sikasso District shows a trend towards a recovery in rainfall and, in light of the current evidence, strategies for preparing, developing and managing water resources in a changing climate are recommended as a way forward for sustainability. Flood risk management should also be designed as an integral part of Mali's strategic plans for climate change adaptation and mitigation. In addition, it is strongly recommended that a more comprehensive research and analysis of the impact of climate change in Mali be conducted using a broader spectrum of temporal and especially spatial climate data.

The findings of this study demonstrate the spatiotemporal variations in land use and land cover (LULC) in the Lotio River basin, utilizing temporal Landsat data and projecting future scenarios based on driving factors. The rapid expansion of agricultural land and the fragmentation of forests in the Lotio area have resulted in environmental degradation and the depletion of water quality. These factors further complicate the challenges associated with sustaining regional development and preserving the environment. While acknowledging that development policies,

migration, immigration, and climatic conditions can all contribute to shaping landscape patterns, our analysis focused solely on the incorporation of physical and socioeconomic factors for modelling and prediction. However, it is important to recognize that a comprehensive understanding of landscape patterns may require the consideration of additional factors and data in future studies. Moreover, the integration of agricultural and development policies can play a crucial role in promoting sustainable land use practices. By aligning these policies, we can effectively address the challenges posed by rapid LULC changes and work towards achieving both regional development and environmental preservation objectives.

5.2 Limitations of the Study

Like all human works this study has some limitations. They are

Sample size

The number of units of analysis used in this study was determined by the type of research question being investigated. Thus, we took the household as the unit, surveying 395 households in 25 villages, which is quite large, but the number of households per village was still quite low, at less than 25. The future researchers should modify the specific approach to data collection.

Lack of available or reliable data

A lack of observed daily climatic data in the study area was a limiting factor in the choice of the type of analysis of certain climatic parameters on the one hand, and on the other, the existence of gaps in the monthly data collected reduced the study period initially desired.

5.3 Recommendations

5.3.1 Recommendations for further research

Based on the research, the possible future researches are as follows;

The approaches used in this study showed usefulness and applicability, but require further validation and refinement, and ideally the inclusion of both good observation or gridded data,

- Earth observation can considerably contribute to monitoring vegetation conditions over time,

- Prediction results highlighted hotspots of significant change that need subsequent detailed investigation on the ground

5.3.2 Recommendations for Policy

The following recommendations are articulated to assist policy and decision-making for better planning, management and sustainability of the available natural resources in the LRB.

- Farmers should be encouraged to leave more trees on their farmland to compensate for the forest loss
- The rapid land use and cover change could be reduced by reforestation and afforestation
- Raising awareness of the threats posed by forest and water transformations to the preservation, availability, sustainable and efficient management

5.4 Contribution to Knowledge

The findings from this work will contribute to the knowledge gap with regards to lowlands distribution, land use and land cover dynamics and its predictions, variability, trends, farmers' perceptions and adaptations strategies of temperature and rainfall in the Southern Mali.

- The results from the first objective which focused on inventory and map the spatial distribution of lowland indicated that there is 71 479 Ha and it is mostly concentred in the north of the study are for agriculture. And GIS and remote sensing methods and technics are reliable and give very good results within lowlands identifications.
- Annual and seasonal precipitation and temperature are highly variable and the temperature present a positive trend between 1960 to 2020 in southern Mali. The producers of southern Mali have a good knowledge about climate variability and have adopted lot of measures to face of this problem. The observation data of rainfall and temperature are importance for climate variability analysis and the filled gap in data with the median is better appropriate than mean. Mann Kendall Test, Sen's Slope analysis, Pettit test for change point detection, seasonal trend analysis and Rainfall Anomaly Index

used in this work are adequate to capture climate variability over the time series.

- Google Earth Engine is a sophisticated cloud-based geospatial analysis platform that combines a massive collection of satellite imagery and geographic datasets with a suite of analysis tools and processing capabilities, allowing for advanced geospatial research at any scale. Among Classification and Regression Tree (CART), Support Vector Machine (SVM), Random Forest (RF) and Gradient Tree Boosting (GTB) classification technics used in this study the SVM technic is the mostly used because of the quality of its final result within LULC detection. The result of the study demonstrates, the domination of cropland compares to others LULC classes and the fast change in the past LULC in this zone.

- Through this work, future LULC have been ass and it will be dominated by cropland. The dynamic in 2030 compare to 2020, indicates the decreasing by 5%, while forest will be increasing by 4%. These are important for the environment and human activities in the study site.

REFERENCES

Ahmadi, Traore, F. B., Simpara, & B., M. (1994). Mise en valeur des bas-fonds au Mali. *Agriculture et Développement*, *2*(33), 1–69. https://agritrop.cirad.fr/387 065/1/document_387065.pdf

Ahouandjinou, N. (2004). *Pression urbaine sur les milieux humides : cas des vallons de Zounvi et de Boué à Porto-Novo* [FLASH/UAC, Bénin]. https://www. memoireonline.com/11/07/715/pression-urbaine-milieux-humides-vallons-zounvi-boue-porto-novo.html

Albereel, J., & Claude, J. (1988). *Fonctionnement hydrologique des bas-fonds en Afrique de l'Ouest*.

Albergel, J., Gadelle, F., Lamachère, J.-M., Lidon, B., Mokadem, A. I., Ran, A.-M., Van driel, W., & Al., E. (1993). Mise en valeur agricole des bas-fonds au Sahel. Typologie, fonctionnement hydrologique, potentialités agricoles. *Rapport Final d'un Projet CORAF-R3S*, 335. https://core.ac.uk/download /pdf/39857847.pdf

Bank Word, I. (2018). *Place de l'agriculture malien dans l'economie*.

Barnieh, B. A., Jia, L., Menenti, M., Zhou, J., & Zeng, Y. (2020). *Mapping Land Use Land Cover Transitions at Different Spatiotemporal Scales in West Africa*. 1–52. https://doi.org/10.3390/su12208565

Barry, A. A., Caesar, J., Klein Tank, A. M. G., Aguilar, E., McSweeney, C., Cyrille, A. M., Nikiema, M. P., Narcisse, K. B., Sima, F., Stafford, G., Touray, L. M., Ayilari-Naa, J. A., Mendes, C. L., Tounkara, M., Gar-Glahn, E. V. S., Coulibaly, M. S., Dieh, M. F., Mouhaimouni, M., Oyegade, J. A., … Laogbessi, E. T. (2018). West Africa climate extremes and climate change indices. *International Journal of Climatology*, *38*, e921–e938. https://doi.org/ 10.1002/joc.5420

Benestad, R. E. (2013). Association between trends in daily rainfall percentiles and the global mean temperature. *Journal of Geophysical Research Atmospheres*, *118*(19), 10,802-10,810. https://doi.org/10.1002/jgrd.50814

Bengaly, S., Youssouf, C., & Guindo, A. M. (2021). *Dynamique des signatures spectrales des formations paysagiques dans le bassin versant de Lotio de 1990-2019. August*.

Bichet, A., & Diedhiou, A. (2018a). Less frequent and more intense rainfall along the coast of the Gulf of Guinea in West and Central Africa (1981-2014). *Climate Research*, *76*(3), 191–201. https://doi.org/10.3354/cr01537

Bichet, A., & Diedhiou, A. (2018b). West African Sahel has become wetter during the last 30 years , but dry spells are shorter and more frequent. *Climate Research*, *August*. https://doi.org/10.3354/cr01515

Brown, M. E., Antle, J. M., Backlund, P., Carr, E. R., Easterling, W. E., Walsh, M. K., Ammann, C., Attavanich, W., Barrett, C. B., Bellemare, M. F., Dancheck, V., Funk, C., Grace, K., Ingram, J. S. I., Jiang, H., Maletta, H., Mata, T., Murray, A., Ngugi, M., … Tebaldi, C. (2015). *Climate Change, Global Food Security, and the U.S. Food System*. https://doi.org/10.7930/J0862DC7

Canadell, J. G., Le Quéré, C., Raupach, M. R., Field, C. B., Buitenhuis, E. T., Ciais, P., Conway, T. J., Gillett, N. P., Houghton, R. A., & Marland, G. (2007). Contributions to accelerating atmospheric CO2 growth from economic activity, carbon intensity, and efficiency of natural sinks. *Proceedings of the National Academy of Sciences of the United States of America*, *104*(47), 18866–18870. https://doi.org/10.1073/pnas.0702737104

Chabi, A., Oloukoi, J., Mama, V. J., & Kiepe, P. (2010). Inventaire par télédétection des agro-écosystèmes de bas-fonds dans le centre du Bénin. *Cahiers Agricultures*, *19*(6), 446–453. https://doi.org/10.1684/agr.2010.0434

Chahal, M., Singh, O., Bhardwaj, P., & Ganapuram, S. (2021). Exploring spatial and temporal drought over the semi-arid Sahibi river basin in Rajasthan, India. *Environmental Monitoring and Assessment Volume*, . *Environ*(193). https://doi.org/10.1007/s10661-021-09539-4

Ciesla, W. M. (1995). *Climate change, forests and forest management - an overview*.

Commod Africa. (2018, October). La Libye veut raviver Malibya Agriculture au Mali. *Commodafrica*. http://www.commodafrica.com/04-10-2018-la-libye-veut-raviver-malibya-agriculture-au-mali

Cook, K. H., & Vizy, E. K. (2015). Detection and Analysis of an Amplified Warming of the Sahara Desert. *Journal of Climate*, 6560–6580. https://doi.org/10.1175/JCLI-D-14-00230.1

Cooper, R., McCarthy, J., & Metz, B. (2002). Climate Change 2001: The Scientific Basis. In *Foreign Affairs* (Vol. 81, Issue 1). https://doi.org/10.2307/20033020

DEMBELE, A. . B. (2019). *Detection des zones a potentiel agricole dans la commune rurale de bougaribaya (cercle de kita)*.

Donat, M. G., Peterson, T. C., Brunet, M., King, A. D., Almazroui, M., Kolli, R. K., Boucherf, D., Al-Mulla, A. Y., Nour, A. Y., Aly, A. A., Nada, T. A. A., Semawi, M. M., Al Dashti, H. A., Salhab, T. G., El Fadli, K. I., Muftah, M. K., Dah Eida, S., Badi, W., Driouech, F., … Al Shekaili, M. N. (2014). Changes in extreme temperature and precipitation in the Arab region: Long-term trends and variability related to ENSO and NAO. *International Journal of Climatology*, *34*(3), 581–592. https://doi.org/10.1002/joc.3707

Dosio, A. (2017). Projection of temperature and heat waves for Africa with an ensemble of CORDEX Regional Climate Models. *Climate Dynamics*, *49*(1), 493–519. https://doi.org/10.1007/s00382-016-3355-5

Doukoro, D., Abbey, G. A., & Kalifa, T. (2022). *Drought Monitoring and Assessment of Climate Parameters Variability in Koutiala and San Districts , Mali*. 230–249. https://doi.org/10.4236/ajcc.2022.113011

Easterling, D. R., Meehl, G. A., Parmesan, C., Changnon, S. A., Karl, T. R., & Mearns, L. O. (2012). Climate Extremes: Observations, Modeling, and Impacts. *Science NAAAS*, *2068*(2000). https://doi.org/10.1126/science.289.5487.2068

El-Tantawi, A. M., Bao, A., Chang, C., & Liu, Y. (2019). Monitoring and predicting land use/cover changes in the Aksu-Tarim River Basin, Xinjiang-China (1990–2030). *Environmental Monitoring and Assessment*, *191*(8), 1–18. https://doi.org/10.1007/s10661-019-7478-0

Facult, K. (2013). *CARTOGRAPHIE DES BAS-FONDS A L ' AIDE DE LA TELEDETECTION ET DES DONNEES SECONDAIRES ET Présenté par : Faculté des Sciences et Techniques (FAST) INTENSIFICATION CULTURALE AU TOGO Mémoire de Master*.

Fao. (2013). Les forêts et le changement climatique. *Vi Semana Cientifica Del Catie*, 20p.

Feng, D., Zhao, Y., Yu, L., Li, C., Wang, J., Clinton, N., Bai, Y., Belward, A., Zhu, Z., & Gong, P. (2016). Circa 2014 African land-cover maps compatible with FROM-GLC and GLC2000 classification schemes based on multi-seasonal Landsat data. *International Journal of Remote Sensing*, *1161*(August). https://doi.org/10.1080/01431161.2016.1218090

Gismondi, M. (2013). *MOLUSCE – An Open Source Land Use Change Analyst*. 1–2. http://2013.foss4g.org/conf/programme/presentations/107/

Goswami, A. (2018). *Identifying the Frequency and Intensity of Dry and Wet Years over Sub-Himalayan West Bengal , India using Rainfall Anomaly Index*. *3085*(11), 461–465.

Gutiérrez, J. M., Jones, R. G., Narisma, G. T., Alves, L. M., Amjad, M. J., Gorodetskaya, I. V., Grose, M., Krakovska, N. A. B., S., K., J, L., Martínez-Castro, D., Mearns, L. O., Mernild, S. H., Ngo-Duc, T., Hurk, B. van den, & Yoon, J.-H. (2021). *Atlas. In Climate Change 2021: The Physical Science Basis. Contribution of Working Group I to the Sixth Assessment Report of the Intergovernmental Panel on Climate Change*. Cambridge University Press, Cambridge, United Kingdom and New York, NY, USA. https://doi.org/10.1017/9781009157896.021.1928

Hackman, K. O., Gong, P., & Wang, J. (2017). New land-cover maps of Ghana for 2015 using Landsat 8 and three popular classifiers for biodiversity assessment. *International Journal of Remote Sensing*, *38*(14), 4008–4021. https://doi.org/10.1080/01431161.2017.1312619

IPCC. (2011). Climate change science - the status of climate change science today. *United Nations Framework Convention on Climate Change, February 2011*, 1–7. https://doi.org/10.1111/j.1467-9388.1992.tb00046.x

IPCC. (2013). Climate Change 2013: The Physical Science Basis. Contribution of Working Group I to the Fifth Assessment Report of the Intergovernmental Panel on Climate Change. *Cambridge University Press, Cambridge, United Kingdom and New York, NY, USA.*, *32*(2), 127–133.

Jha, C. K., & Gupta, V. (2021). Farmer's perception and factors determining the adaptation decisions to cope with climate change: An evidence from rural India. *Environmental and Sustainability Indicators*, *10*(May 2020), 100112. https://doi.org/10.1016/j.indic.2021.100112

Jones, J. R., Schwartz, J. S., Ellis, K. N., Hathaway, J. M., & Jawdy, C. M. (2015). Temporal variability of precipitation in the Upper Tennessee Valley. *Journal of Hydrology: Regional Studies*, *3*, 125–138. https://doi.org/10.1016/j.ejrh.2014.10.006

Kabore, P. N., Barbier, B., Ouoba, P., Kiema, A., Some, L., & Ouedraogo, A. (2019). Perceptions du changement climatique, impacts environnementaux et stratégies endogènes d'adaptation par les producteurs du Centre-nord du Burkina Faso. *VertigO*, *19*(Volume 19 Numéro 1), 1–29. https://doi.org/10.4000/vertigo.24637

Kendall, M. G. (1975). *Rank correlation methods (4th ed. 2d impression). Griffin.* (Oxford Uni). Charles Griffin.

Kennedy, J., Dunn, R., Mccarthy, M., Titchner, H., & Morice, C. (2016). Global and regional climate in 2016. *Royal Meteorological Society*, *0*(c), 219–225.

Khalil, A. (2022). Space-time characterization of droughts in the Mae Klong River Basin, Thailand, using rainfall anomaly index. *Water Supply*, *22*(9), 7352–7374. https://doi.org/10.2166/ws.2022.306

Kindjinou, A. (2013). *CARTOGRAPHIE DES BAS-FONDS A L ' AIDE DE LA TELEDETECTION ET DES DONNEES SECONDAIRES ET INTENSIFICATION CULTURALE AU TOGO*. Université d'Abomey-Calavi (UAC).

Koné, I., Agyare, W. A., Gaiser, T., Owusu-prempeh, N., & Kouadio, K. H. (2022). Local Cotton Farmers ' Perceptions of Climate Change Events and Adaptations Strategies in Cotton Basin of Cote d ' Ivoire. *Journal of Sustainable Development*, *15*(3), 108–124. https://doi.org/10.5539/jsd.v15n3p108

Lelieveld, J., Proestos, Y., & Hadjinicolaou, P. (2016). Strongly increasing heat extremes in the Middle East and North Africa (MENA) in the 21st century. *Climatic Change*, 245–260. https://doi.org/10.1007/s10584-016-1665-6

Li, S., Dragicevic, S., Antón, F., Sester, M., Winter, S., Coltekin, A., Pettit, C., Jiang, B., Haworth, J., Stein, A., & Cheng, T. (2016). Geospatial big data handling theory and methods : A review and research challenges. *ISPRS Journal of Photogrammetry and Remote Sensing*, *115*, 119–133. https://doi.org/10.1016/j.isprsjprs.2015.10.012

Liebmann, B., Dole, R. M., Jones, C., Bladé, I., & Allured, D. (2010). Influence of choice of time period on global surface temperature trend estimates. *Bulletin of the American Meteorological Society*, *91*(11), 1485–1491. https://doi.org/10.1175/2010BAMS3030.1

Malmgren, B. A., Hulugalla, R., Hayashi, Y., & Mikami, T. (2003). Precipitatioon trends in Sri Lanka since the 1870s and relationships to El Niño-southern oscillation. *International Journal of Climatology*, *23*(10), 1235–1252. https://doi.org/10.1002/joc.921

Mann, H. B. (1945). Non-Parametric Test Against Trend. *Econometrica*, *13*(3), 245–259. http://www.economist.com/node/18330371?story%7B_%7Did=18330371

Manning, A. C., & Keeling, R. F. (2006). Global oceanic and land biotic carbon sinks from the scripps atmospheric oxygen flask sampling network. *Tellus, Series B: Chemical and Physical Meteorology*, *58*(2), 95–116. https://doi.org/10.1111/j.1600-0889.2006.00175.x

MANTON, M. J., DELLA-MARTA, P. M., HAYLOCK, M. R., HENNESSY, K. J., NICHOLLS, N., CHAMBERS, L. E., COLLINS, D. A., DAW, G., FINET, A., GUNAWAN, D., INAPE, K., ISOBE, H., KESTIN, T. S., LEFALE, P., LEYU, C. H., LWIN, T., MAITREPIERRE, L., OUPRASITWONG, N., PAGE, C. M., … YEE, D. (2007). TRENDS IN EXTREME DAILY RAINFALL AND TEMPERATURE IN SOUTHEAST ASIA AND THE SOUTH PACIFIC: 1961–1998. *INTERNATIONAL JOURNAL OF CLIMATOLOGY*, *284*, 269–284. https://doi.org/10.1002/joc/610

Meehl, G. A., Arblaster, J. M., & Tebaldi, C. (2007). Contributions of natural and anthropogenic forcing to changes in temperature extremes over the United States. *Geophysical Research Letters*, *34*(19), 1–5. https://doi.org/10.1029/2007GL030948

Merabtene, T., Siddique, M., & Shanableh, A. (2016). Assessment of Seasonal and Annual Rainfall Trends and Variability in Sharjah City, UAE. *Advances in Meteorology*, *2016*. https://doi.org/10.1155/2016/6206238

Moron, V., Oueslati, B., Pohl, B., Rome, S., & Janicot, S. (2016). Trends of mean temperatures and warm extremes in northern tropical Africa (1961–2014) from observed and PPCA-reconstructed time series. *Journal of Geophysical Research : Atmospheres*, 5298–5319. https://doi.org/10.1002/2015JD024303. Received.

Mountrakis, G., Im, J., & Ogole, C. (2011). Support vector machines in remote sensing: A review. *ISPRS Journal of Photogrammetry and Remote Sensing*, *66*(3), 247–259. https://doi.org/10.1016/j.isprsjprs.2010.11.001

Muhammad, R., Zhang, W., Abbas, Z., Guo, F., & Gwiazdzinski, L. (2022). Spatiotemporal Change Analysis and Prediction of Future Land Use and Land Cover Changes Using QGIS MOLUSCE Plugin. *MDPI*. https://doi.org/https://doi.org/10.3390/land11030419

Nasher, N. M. R. (2021). *Maximum and Minimum Temperature Trends Variation over Northern and Southern Part of Bangladesh Maximum and Minimum Temperature Trends Variation over Northern and Southern Part of Bangladesh*. *January*. https://doi.org/10.3329/jesnr.v6i2.22101

Ndlovu, M. S., & Demlie, M. (2020). Assessment of meteorological drought and wet conditions using two drought indices across Kwazulu-Natal province, South Africa. *Atmosphere*, *11*(6), 1–20. https://doi.org/10.3390/atmos11060623

Nery, T., Sadler, R., Solis-Aulestia, M., White, B., Polyakov, M., & Chalak, M. (2016). Comparing supervised algorithms in Land Use and Land Cover classification of a Landsat time-series. *International Geoscience and Remote Sensing Symposium (IGARSS)*, *2016-Novem*, 5165–5168. https://doi.org/10.1109/IGARSS.2016.7730346

Neville, A., Herniou, C., Fontaine, G., Marnat, E., & Petitprez, S. (1998). Les amenagements de bas-fonds en Guinee forestiere: l'experience de l'Afvp dans le cadre du projet riz. *Agriculture et Developpement*, *19*, 54–61. https://agritrop.cirad.fr/401300/1/document_401300.pdf

Nicholson, S. E., Funk, C., & Fink, A. H. (2018). Rainfall over the African continent from the 19th through the 21st century. *Global and Planetary Change*, *165*(May 2017), 114–127. https://doi.org/10.1016/j.gloplacha.2017.12.014

Nikiema, P. M., Sylla, B., Ogunjobi, K., Kebe, I., & Giorgi, F. (2017). Multi-model CMIP5 and CORDEX simulations of historical summer temperature and precipitation variabilities over West Africa. *Royal Meteorological Society*, *2450*(August 2016), 2438–2450. https://doi.org/10.1002/joc.4856

Olivry, J. ., Diallo, M. I., & Bricquet, I. P. (1994). *Changement climatique et tendance a la desertification*.

Oloukoi, J. (2016). *Detection et inventaire des basfonds et zones humides par teledetection au Benin View project Land cover dynamics and impacts on inland valleys in the Centre of Benin republic View project*. https://www.researchgate.net/publication/315005084

OLOUKOI, J. (2016). CARTOGRAPHIE DU POTENTIEL EN BAS-FONDS AMENAGEABLES DE LA COMMUNE DE MATERI AU BENIN SOUBEROU. *Revue de Géographie de l'Université Ouaga I Pr Joseph KI-ZERBO*, *2*(005). https://www.researchgate.net/publication/315005084_

CARTOGRAPHIE_DU_POTENTIEL_EN_BAS-FONDS_AMENAGEABLES
_DE_LA_COMMUNE_DE_MATERI_AU_BENIN

OLOUKOI J, A. E. S. K. (2016). CARTOGRAPHIE DU POTENTIEL EN BAS-FONDS AMENAGEABLES DE LA COMMUNE DE MATERI AU BENIN. *Revue de Géographie de l'Université Ouaga I Pr Joseph KI-ZERBO, 2*(005). https://www.researchgate.net/publication/315005084_CARTOGRAPHIE_DU_POTENTIEL_EN_BAS-FONDS_AMENAGEABLES_DE_LA_COMMUNE_DE_MATERI_AU_BENIN

Ouma, Y., Nkwae, B., Moalafhi, D., Odirile, P., Parida, B., Anderson, G., & Qi, J. (2022). COMPARISON OF MACHINE LEARNING CLASSIFIERS FOR MULTITEMPORAL AND MULTISENSOR MAPPING OF URBAN LULC FEATURES. *The International Archives of the Photogrammetry, Remote Sensing and Spatial Information Sciences, XLIII*(June), 6–11.

Praveen, B., Talukdar, S., Shahfahad, Mahato, S., Mondal, J., Sharma, P., Islam, A. R. M. T., & Rahman, A. (2020). Analyzing trend and forecasting of rainfall changes in India using non-parametrical and machine learning approaches. In *Scientific Reports* (Vol. 10, Issue 1). https://doi.org/10.1038/s41598-020-67228-7

Ranasinghe, R., Ruane, A. C., Vautard, R., Arnell, N., Coppola, E., Cruz, F. A., Dessai, S., Islam, A. S., Rahimi, M., Carrascal, D. R., Sillmann, J., Sylla, M. B., Tebaldi, C., Wang, W., & Zaaboul, R. (2021). *Climate Change Information for Regional Impact and for Risk Assessment*. https://doi.org/10.1017/9781009157896.014.1768

Raunet, M. (1985). *Les bas-fonds en Afrique et à Madagascar* . 431453.

Ruelland, D., Levavasseur, F., & Tribotte, A. (2010). Patterns and dynamics of land-cover changes since the 1960s over three experimental areas in Mali. *International Journal of Applied Earth Observation and Geoinformation*. https://doi.org/10.1016/j.jag.2009.10.006

Samake, A., Jean-François, B., Pierre-Marie, B., & Ousmane, S. (2007). *Les implications structurelles de la libéralisation sur l'agriculture et le développement rurale. Première Phase: Synthèse nationale*. http://web.worldbank.org/WBSITE/EXTERNAL/COUNTRIES/AFRICAEXT/0,,menuPK:311690~page

Sanogo, K., Binam, J., Bayala, J., Villamor, G. B., Kalinganire, A., & Dodiomon, S. (2016). Farmers' perceptions of climate change impacts on ecosystem services delivery of parklands in southern Mali. *Agroforestry Systems, 91*(2), 345–361. https://doi.org/10.1007/s10457-016-9933-z

Sanogo, S., Fink, A. H., Omotosho, J. A., & Ba, A. (2015). Spatio-temporal characteristics of the recent rainfall recovery in West Africa. *Royal Meteorological Society*. https://doi.org/10.1002/joc.4309

Sillmann, J., & Roeckner, E. (2008). Indices for extreme events in projections of anthropogenic climate change. *Climatic Change*, *86*(1–2), 83–104. https://doi.org/10.1007/s10584-007-9308-6

Sonia, P., & Joël, H. (2010). *Valorisation du potentiel agricole des bas-fonds au Sud-Bénin*. 932. https://agritrop.cirad.fr/562168/1/document_562168.pdf

Souberou, K. T., Agbossou, K. E., & Ogouwale, E. (2017). Inventaire et caractérisation des bas-fonds dans le bassin versant de l'Oti au Bénin à l'aide des images Landsat et ASTER DEM. *International Journal of Environment, Agriculture and Biotechnology*, *2*(4), 1601–1623. https://doi.org/10.22161/ijeab/2.4.20

Sudre, X. (2015). *Développer une méthode pour spatialiser les bas-fonds en zone subsaharienne. Cas des bas fonds de la commune de Sagabary du cercle de Kita (région de Kayes, Mali)*. Université PAUL-VAlERY MONTPELLIER 3.

Sylla, M. B., Nikiema, P. M., Gibba, P., Kebe, I., Ama, N., & Klutse, B. (2016). Climate Change over West Africa : Recent Trends and Future Projections. *Springer International Publishing Switzerland 2016*, 25–40. https://doi.org/10.1007/978-3-319-31499-0

Thomas, N., & Nigam, S. (2018). Twentieth-Century Climate Change over Africa : Seasonal Hydroclimate Trends and Sahara Desert Expansion. *Journal of Climate*, 3349–3370. https://doi.org/10.1175/JCLI-D-17-0187.1

Toukal Assoumana, B., Ndiaye, M., Der Puije, G. Van, Diourte, M., & Gaiser, T. (2016). Comparative Assessment of Local Farmers' Perceptions of Meteorological Events and Adaptations Strategies: Two Case Studies in Niger Republic. *Journal of Sustainable Development*, *9*(3), 118. https://doi.org/10.5539/jsd.v9n3p118

Traoré, S. M. (2020). *Fonctionnement hydroclimatique et dynamique des états de surface du bassin versant du Lotio*. UNIVERSITE DES SCIENCES SOCIALES ET DE GESTION DE BAMAKO (USSGB).

Unite State Environmental Protection Agency. (2015). Climate Impacts on Agriculture and Food Supply | Climate Change Impacts | US EPA. In *US Environmental Protection agency* (pp. 1–10). https://www.epa.gov/climate-impacts/climate-impacts-agriculture-and-food-supply

United Nations. (2013). World population prospects: The 2012 revision. In *Population Division of the Department of Economic and …*. http://scholar.google.com/scholar?hl=en&btnG=Search&q=intitle:World+Population+Prospects+The+2012+Revision#1

World Bank. (2021). *Annexure 20-2 Methodology for transect walk, from Study on Environmental and Social Aspects of Pradhan Mantri Gram Sadak Yojana*. 4.

Yangouliba, G. I., Jean, B., Zoungrana, B., Oppong, K., Hagen, H., Yabré, S., Bonkoungou, B., Sougué, M., Gadiaga, A., & Koffi, B. (2022). Modelling past and future land use and land cover dynamics in the Nakambe River Basin , West Africa. *Modeling Earth Systems and Environment, 0123456789.* https://doi.org/10.1007/s40808-022-01569-2

Zhe, J., & Shashi, S. (2017). *Spatial Big Data Science*. Springer International Publishing AG. https://sci-hub.hkvisa.net/10.1007/978-3-319-60195-3

Survey on the Perceptions and Adaptations of Farmers in Southern Mali to Climate Change

Geographical coordinates:

Latitude :…..………………. Longitude : ….……………. Date of survey: …………….

QUESTIONNAIRE ADDRESSED TO THE HEAD OF THE HOUSEHOLD (please write in lower case, do not capitalize the form)

		codes
Region		
District		
Commune		
Town/Village		

IDENTIFICATION	
First and last Name of interviewer:	
First and last Name of respondent	

I. HOUSEHOLD SOCIO-DEMOGRAPHIC CHARACTERISTICS		
Gender of respondent	Male	1
	Female	2
Age of respondent (age absolutely, do not enter year)	0-25	
	25-35	2
	35-45	3
	45-50	4
	Plus 50	5
What is your marital status?	Married/in Couple	1
	Single	2
	Veuf (Ve)	3
	Divorced	4
What is your level of education	Any	1
	Primairy	2
	Secondairy	3
	Higher	4
	Quranic school	5
Ethnic group		
What's your status in the zone?	Indigenous	1
	Allochthonous	2
	Allogenic	3
Household size	1. Number of women (if male and married)	1:
	2. Nomber of children	2:
	3. Other family members	3:
Relationship with head of household (if respondent is not head of household)	Head of household	1
	Wife	2
	Child	3
	Brother	4
	Nephew	5
	Other to specify	6
Are you a member of a producer cooperative?	Yes	1
	No	2
If yes, name of cooperative		

II. HOUSEHOLD ECONOMIC CHARACTERISTICS		
How many years have you been growing cotton?	………………………………………..	
How do you access land?	Heritage	1
	Donation	2
	Purchase	3
	Rental	4
	Loan	5
	Land metayage	6
	Pledge	7
Do you use a workforce?	Yes	1
	No	2
If so, what type of manpower do you use?	Family	1
	Employee	2
	Entraide	3
If so, what is the number of this workforce by type?	Family Employee Entraide	………………..
What are your main crops? In order of importance?	Cotton	1
	cashew nuts	2
	Rice	3
	Corn	4
	Orchard	5
	Yam	6
	Sorghum	7
	Millet	8
Justify your answer	……………………………………	
Give the area of your main crops	Cotton	……
	Groundnut	………..
	Rice	……
	Corn	………
	Swede	……..
	Sesame	…….
	Sorghum	…….
	Millet	……

Economic information about your cotton farm over the last 5 years					
Years	Area (ha)	Production (t)	**Yield (t/ha)**	Coast of production	Imput charges
2016					
2017					
2018					
2019					
2020					

IMPORTANCE OF COTTON GROWING (Name and rank the varieties of cotton grown in the region in order of importance for production, marketing or consumption in the locality.)			
Number	Variety Name	Importance of production	Importance of commercialization
1			
2			
3			

[1]Production: High yield, early cycle, adapted to regional soil, cultivation habit

[2]Commercialization: strong market demand, high selling price, profitability

III. PERCEPTION OF CLIMATE DYNAMICS		
How do you rate the length of the rainy season in your area over the past decade, compared with the two or three years ago?	Longer	1
	Shorter	2
	No change	3
How do you feel about the arrival of the rainy season in recent years compared with the two or three years ago?	Early	1
	Normal	2
	Late	3
What elements in nature indicate the arrival of rain or the dry season? Justify your answer?		
How do you rate the number of rainy days in recent years?	Increase	1
	Decrease	2
	No change	3
If changes (increase or decrease), when do they occur?	Period of increasing rainfall	
	Period of reduced rainfall	
How do you rate the weather in your area in recent years?	Increase	1
	Decrease	2
	No change	3
If changes (increase or decrease), when do they occur?	Period of rising temperature (1 Dry, 2 Wet)	1
	Period of falling temperature (1 Dry, 2 Wet)	2
In your locality, winds tend to be?	Stronger	1
	Less strong	2
	No change	3
If changes, when do they occur?	Period of strong winds	1
	Period of lighter winds	2
With the observations you've just made, can we talk about climate change in your area?	Yes	1
	No	2
Justiy your response		
In your opinion, what are the causes of climate change in your area?	Deforestation	1
	Bush fires	2
	Violation of traditional prohibitions	3
	Others to be specified......................	4
If the climate changes (rainy season, temperature), do you think the men in the village are responsible?	Yes	1
	No	2
Justify youre response		
Have you noticed any impact of climate change on production in your area?	Yes	1
	No	2
If so, how?	Decrease in production	1
	Disruption of cropping calendar	2
	Soil impoverishment	3
	Proliferation of insect pests	4
	Increase in weeds	5
	Others to be specified	6
If the cultivation calendar is disrupted, at what time of year do you carry out these different cotton cultivation operations?	Soil preparation	1
	Pre-emergence herbicide	2
	Reseeding	3
	Disbudding	4

	Post-emergence herbicide	5
	First weeding	6
	Second weeding	7
	Application of NPK fertilizer	8
	Urea application	9
	Insecticide treatments	10
	Harvest	11
If the cultivation calendar has been disrupted, at what time of year do you now carry out these different cotton cultivation operations?	Soil preparation	1
	Pre-emergence herbicide	2
	Reseeding	3
	Disbudding	4
	Post-emergence herbicide	5
	First weeding	6
	Second weeding	7
	Application of NPK fertilizer	8
	Urea application	9
	Insecticide treatments	10
	Harvest	11
If production is down, what are you doing to increase it?		
If soil decline, impoverishment, what are you doing to improve it?		

V. PERCEPTION OF LAND USE		
How has vegetation cover changed in your region over the past 20 years?	Increase	1
	Intact	2
	Decrease	3
How do you feel about the level of deterioration over the past 20 years?	Low	1
	Medium	2
	High	3
How land use affects soil fertility	Through chemical fertilizers	1
	Through water erosion	2
	Unsuitable cultivation practices	3
	Others to be specified	4
Justify your response		
How do you weed your plot?	Cattle plough	1
	Tractor	2
	Daba	3
	Machete	4
	Herbicides	5
Do you combine cotton with other crops in your field?	Yes	1
	No	2
If so, which crops	Food crops	1
	Other to be specified …...	2
Why do you make the association?		
If food crops, does this association have any impact on cotton?	Yes	1
	No	2
Justify your response		

VI. IDENTIFYING ADAPTATION MEASURES		
What tools do you no longer use?		
What new tools do you use now?		
In the face of climate change, have you changed your cotton varieties?	Yes	1
	No	2
If so, do these varieties give good yields?	Yes	1
	No	2
If yes, do these new varieties adapt to the climate?	Yes	1
	No	2
If yes, with these new varieties, how many tons do you produce per hectare?		
With climate change, which cotton varieties do you prefer?	Early	1
	Medium	2
	Late	3
Why?		
Faced with climate variability, have you increased or reduced your acreage?	Yes	1
	No	2
Have you changed your technical itinerary by :	Choice of plot	1
	Cultivation technique	2
	Other	3
Why?		
With climatic variability, have you changed your semi-period?	Yes	1
	No	2
Justify response		
If so, in which decade do you currently sow cotton?	D1	1
	D2	2
	D3	3
	D4	4
With climate change, do you practice semi-drying?	Yes	1
	No	2
Justify your response		
Do you use plant protection products	Yes	1
	No	2
If so, which ones and why?		
Did this climatic context push you towards other crops?	Yes	1
	No	2
Do you grow other crops in association or rotation with cotton?	Yes	1
	No	2
If so, why?		
In your opinion, are there other adaptation strategies?	Yes	1
	No	2
If so, which ones?		
In the face of climate change, what would you like to see done to improve your cotton production?		

Thank you for your availability and participation

Confusion matrices of 1990 image classification

Class	Bare Soils	Water	Forest	Shrub	Crop	Total	Prod Acc.	User Acc.
Bare Soils	31	3	7	0	12	53	0,58	0,79
Water	1	44	4	2	12	63	0,70	0,62
Forest	1	4	11	8	24	48	0,23	0,4 1
Shrub	0	4	0	63	2	69	0,91	0,79
Croplands	6	16	5	7	64	98	0,65	0,56
OA							0,64	
Accuracy statistics(kappa)							0,54	

Confusion matrices of 2000 image classification

Class	Bare Soils	Water	Forest	Shrub	Crop	Total	Prod Acc.	User Acc.
Bare Soils	28	1	10	0	14	53	0,53	0,82
Water	1	46	5	4	7	63	0,73	0,70
Forest	0	4	23	6	15	48	0,48	0,56
Shrub	0	2	0	65	2	69	0,94	0,78
Croplands	5	13	3	8	69	98	0,70	0,64
OA							0,70	
Accuracy statistics(kappa)							0,61	

Confusion matrices of 2010 image classification

Class	Bare Soils	Water	Forest	Shrub	Crop	Total	Prod Acc.	User Acc.
Bare Soils	52	0	0	0	1	53	0,981	0,98
Water	0	61	0	0	2	63	0,968	1,00
Forest	1	0	47	0	0	48	0,979	1,00
Shrub	0	0	0	67	2	69	0,971	0,99
Crop	5	0	0	0	1	97	0,052	0,95
OA							0,979	
Accuracy statistics(kappa)							0,973	

Confusion matrices of 2020 image classification

Class	Bare Soils	Water	Forest	Shrub	Crop	Total	Prod Acc.	User Acc.
Bare Soils	53	0	0	0	0	53	1,000	1,000
Water	0	63	0	0	0	63	1,000	0,969
Forest	0	0	47	0	1	48	0,979	1,000
Shrub	0	2	0	67	0	69	0,971	0,985
Crop	0	0	0	1	97	98	0,000	0,990
OA							0,988	
Accuracy statistics(kappa)							0,985	

Seasonal (DJF) Rainfall Variation
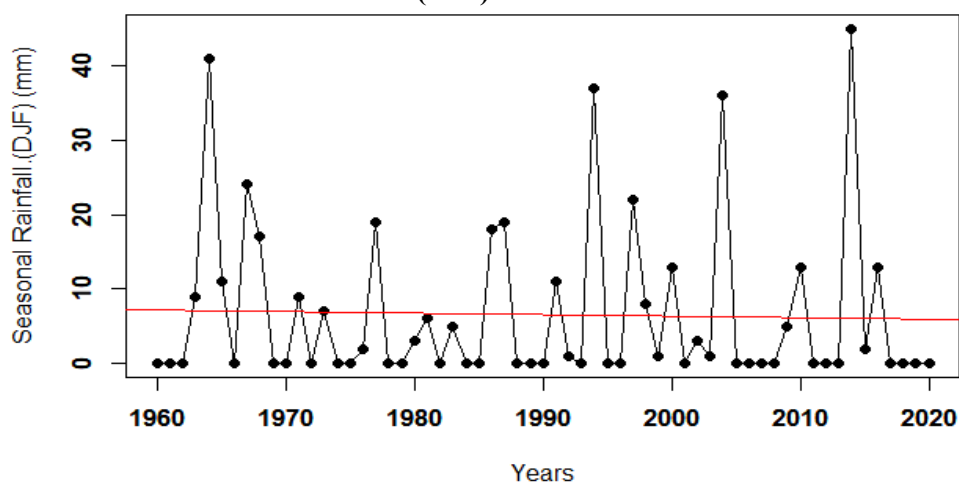
Seasonal (DJF) Rainfall Break
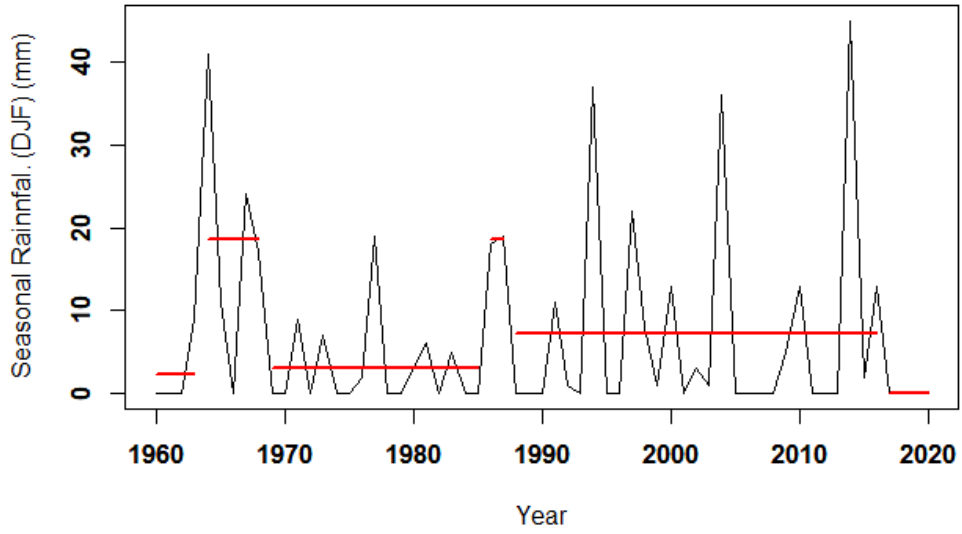
Seasonal (DJF) Temperature Variation

Seasonal (DJF) Temperature Break